

REPORT NO.  
UCB/EERC-85/10  
JUNE 1986

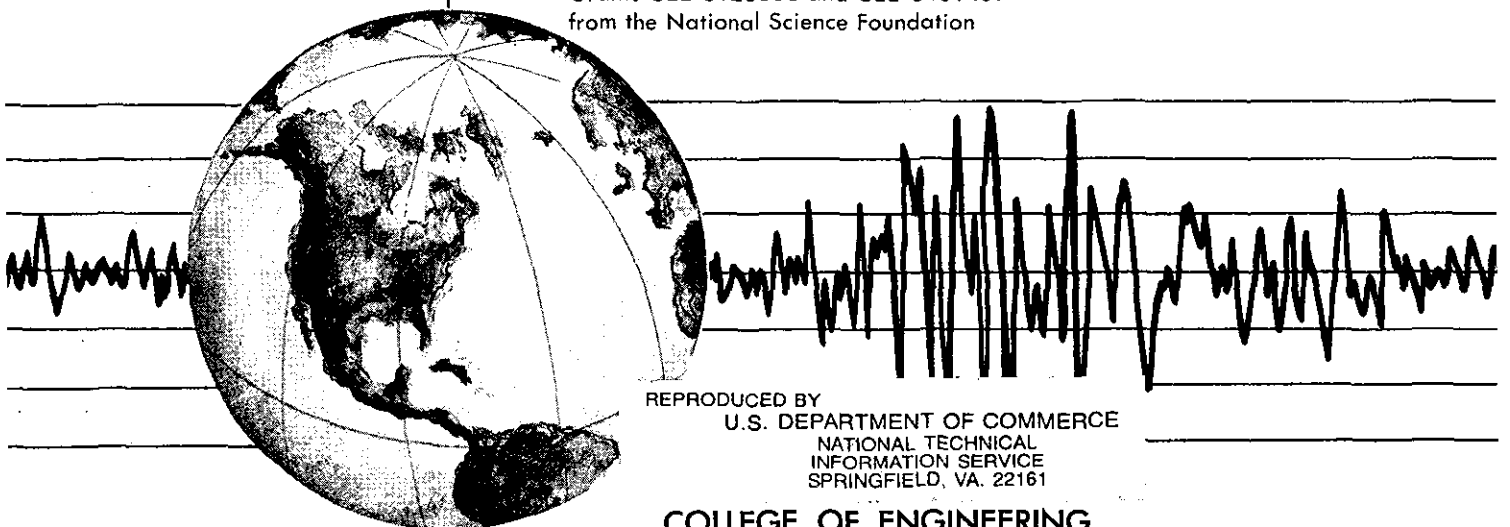
EARTHQUAKE ENGINEERING RESEARCH CENTER

# SIMPLIFIED ANALYSIS FOR EARTHQUAKE RESISTANT DESIGN OF CONCRETE GRAVITY DAMS

by

GREGORY FENVES  
ANIL K. CHOPRA

A Report on Research Conducted Under  
Grants CEE-8120308 and CEE-8401439  
from the National Science Foundation



REPRODUCED BY  
U.S. DEPARTMENT OF COMMERCE  
NATIONAL TECHNICAL  
INFORMATION SERVICE  
SPRINGFIELD, VA. 22161

COLLEGE OF ENGINEERING

UNIVERSITY OF CALIFORNIA • Berkeley, California

For sale by the National Technical Information Service, U.S. Department of Commerce, Springfield, Virginia 22161.

See back of report for up to date listing of EERC reports.

**DISCLAIMER**

Any opinions, findings, and conclusions or recommendations expressed in this publication are those of the authors and do not necessarily reflect the views of the National Science Foundation or the Earthquake Engineering Research Center, University of California, Berkeley

<b>REPORT DOCUMENTATION PAGE</b>		<b>1. REPORT NO.</b> NSF/ENG 85066	<b>2.</b>	<b>3. Recipient's Accession No.</b> PB87 124160/AS	
<b>4. Title and Subtitle</b> Simplified Analysis for Earthquake Resistant Design of Concrete Gravity Dams				<b>5. Report Date</b> June, 1986	
<b>7. Author(s)</b> Gregory Fenves and Anil K. Chopra				<b>8. Performing Organization Rept. No.</b> UCB/EERC-85/10	
<b>9. Performing Organization Name and Address</b> Earthquake Engineering Research Center University of California, Berkeley 1301 South 46th Street Richmond, California 94804				<b>10. Project/Task/Work Unit No.</b>	
<b>12. Sponsoring Organization Name and Address</b> National Science Foundation 1800 G. Street, N.W. Washington, D.C. 20050				<b>11. Contract(C) or Grant(G) No.</b> XXXXXX (C) NSF No. CEE-8120308 (G) And No. CEE-8401439	
<b>15. Supplementary Notes</b>				<b>13. Type of Report &amp; Period Covered</b>	
<b>16. Abstract (Limit: 200 words)</b> <p>A two-stage procedure was proposed in 1978 for the analysis phase of elastic design and safety evaluation of concrete gravity dams: (1) a simplified analysis procedure in which the response due only to the fundamental vibration mode is estimated directly from the earthquake design spectrum; and (2) a refined response history analysis procedure for finite element idealizations of the dam monolith. The former was recommended for the preliminary design and safety evaluation of dams, and the latter for accurately computing the dynamic response and checking the adequacy of the preliminary evaluation. In this report, the simplified analysis procedure has been extended to include the effects of dam-foundation rock interaction and of reservoir bottom sediments, in addition to the effects of dam-water interaction and water compressibility included in the earlier procedure. Also included now in the simplified procedure is a "static correction" method to consider the response contributions of the higher vibration modes. Thus, the design procedure proposed in 1978, which is still conceptually valid, should utilize the new simplified analysis procedure.</p>				<b>14.</b>	
<b>17. Document Analysis a. Descriptors</b> gravity dams earthquake finite element interaction					
<b>b. Identifiers/Open-Ended Terms</b>					
<b>c. COSATI Field/Group</b>					
<b>18. Availability Statement</b>  Release Unlimited			<b>19. Security Class (This Report)</b> Unclassified		<b>21. No. of Pages</b> 154
			<b>20. Security Class (This Page)</b> Unclassified		<b>22. Price</b>

# DO NOT PRINT THESE INSTRUCTIONS AS A PAGE IN A REPORT

## INSTRUCTIONS

Optional Form 272, Report Documentation Page is based on Guidelines for Format and Production of Scientific and Technical Reports, ANSI Z39.18-1974 available from American National Standards Institute, 1430 Broadway, New York, New York 10018. Each separately bound report—for example, each volume in a multivolume set—shall have its unique Report Documentation Page.

1. Report Number. Each individually bound report shall carry a unique alphanumeric designation assigned by the performing organization or provided by the sponsoring organization in accordance with American National Standard ANSI Z39.23-1974, Technical Report Number (STRN). For registration of report code, contact NTIS Report Number Clearinghouse, Springfield, VA 22161. Use uppercase letters, Arabic numerals, slashes, and hyphens only, as in the following examples: FASEB/NS-75/87 and FAA/RD-75/09.
2. Leave blank.
3. Recipient's Accession Number. Reserved for use by each report recipient.
4. Title and Subtitle. Title should indicate clearly and briefly the subject coverage of the report, subordinate subtitle to the main title. When a report is prepared in more than one volume, repeat the primary title, add volume number and include subtitle for the specific volume.
5. Report Date. Each report shall carry a date indicating at least month and year. Indicate the basis on which it was selected (e.g., date of issue, date of approval, date of preparation, date published).
6. Sponsoring Agency Code. Leave blank.
7. Author(s). Give name(s) in conventional order (e.g., John R. Doe, or J. Robert Doe). List author's affiliation if it differs from the performing organization.
8. Performing Organization Report Number. Insert if performing organization wishes to assign this number.
9. Performing Organization Name and Mailing Address. Give name, street, city, state, and ZIP code. List no more than two levels of an organizational hierarchy. Display the name of the organization exactly as it should appear in Government indexes such as Government Reports Announcements & Index (GRA & I).
10. Project/Task/Work Unit Number. Use the project, task and work unit numbers under which the report was prepared.
11. Contract/Grant Number. Insert contract or grant number under which report was prepared.
12. Sponsoring Agency Name and Mailing Address. Include ZIP code. Cite main sponsors.
13. Type of Report and Period Covered. State interim, final, etc., and, if applicable, inclusive dates.
14. Performing Organization Code. Leave blank.
15. Supplementary Notes. Enter information not included elsewhere but useful, such as: Prepared in cooperation with . . . Translation of . . . Presented at conference of . . . To be published in . . . When a report is revised, include a statement whether the new report supersedes or supplements the older report.
16. Abstract. Include a brief (200 words or less) factual summary of the most significant information contained in the report. If the report contains a significant bibliography or literature survey, mention it here.
17. Document Analysis. (a). Descriptors. Select from the Thesaurus of Engineering and Scientific Terms the proper authorized terms that identify the major concept of the research and are sufficiently specific and precise to be used as index entries for cataloging.  
(b). Identifiers and Open-Ended Terms. Use identifiers for project names, code names, equipment designators, etc. Use open-ended terms written in descriptor form for those subjects for which no descriptor exists.  
(c). COSATI Field/Group. Field and Group assignments are to be taken from the 1964 COSATI Subject Category List. Since the majority of documents are multidisciplinary in nature, the primary Field/Group assignment(s) will be the specific discipline, area of human endeavor, or type of physical object. The application(s) will be cross-referenced with secondary Field/Group assignments that will follow the primary posting(s).
18. Distribution Statement. Denote public releasability, for example "Release unlimited", or limitation for reasons other than security. Cite any availability to the public, with address, order number and price, if known.
19. & 20. Security Classification. Enter U.S. Security Classification in accordance with U.S. Security Regulations (i.e., UNCLASSIFIED).
21. Number of pages. Insert the total number of pages, including introductory pages, but excluding distribution list, if any.
22. Price. Enter price in paper copy (PC) and/or microfiche (MF) if known.

**SIMPLIFIED ANALYSIS FOR EARTHQUAKE RESISTANT DESIGN  
OF CONCRETE GRAVITY DAMS**

by

Gregory Fennes

Anil K. Chopra

A Report on Research Conducted under  
Grants CEE-8120308 and CEE-8401439  
from the National Science Foundation

Report No. UCB/EERC-85/10  
Earthquake Engineering Research Center  
University of California  
Berkeley, California

June 1986



## ABSTRACT

A two-stage procedure was proposed in 1978 for the analysis phase of elastic design and safety evaluation of concrete gravity dams: (1) a simplified analysis procedure in which the response due only to the fundamental vibration mode is estimated directly from the earthquake design spectrum; and (2) a refined response history analysis procedure for finite element idealizations of the dam monolith. The former was recommended for the preliminary design and safety evaluation of dams, and the latter for accurately computing the dynamic response and checking the adequacy of the preliminary evaluation. In this report, the simplified analysis procedure has been extended to include the effects of dam-foundation rock interaction and of reservoir bottom sediments, in addition to the effects of dam-water interaction and water compressibility included in the earlier procedure. Also included now in the simplified procedure is a "static correction" method to consider the response contributions of the higher vibration modes. Thus, the design procedure proposed in 1978, which is still conceptually valid, should utilize the new simplified analysis procedure.

## ACKNOWLEDGEMENTS

This research investigation was supported by Grants CEE-8120308 and CEE-8401439 from the National Science Foundation to the University of California, Berkeley, for which the writers are grateful. This work was started while the first writer was a graduate student at Berkeley but was completed subsequent to the submission of his doctoral dissertation in May 1984. The first writer wishes to acknowledge The University of Texas at Austin for support in completing this work.

Both writers are grateful to Hanchen Tan, graduate student at the University of California at Berkeley, for his contributions that led to Appendix A, and completion of the standard data presented in this report.



## TABLE OF CONTENTS

ABSTRACT .....	i
ACKNOWLEDGEMENTS .....	ii
TABLE OF CONTENTS .....	iii
INTRODUCTION .....	1
SIMPLIFIED ANALYSIS OF FUNDAMENTAL MODE RESPONSE .....	2
Equivalent Lateral Forces .....	3
One-Dimensional Approximation of Lateral Forces .....	6
Approximation of Hydrodynamic Pressure .....	7
STANDARD PROPERTIES FOR FUNDAMENTAL MODE RESPONSE .....	8
Vibration Properties of the Dam .....	8
Modification of Period and Damping: Dam-Water Interaction .....	9
Modification of Period and Damping: Dam-Foundation Rock Interaction .....	9
Hydrodynamic Pressure .....	10
Generalized Mass and Earthquake Force Coefficient .....	11
STATIC CORRECTION FOR HIGHER MODE RESPONSE .....	11
Dams on Rigid Foundation Rock with Empty Reservoir .....	12
Dams on Flexible Foundation Rock with Empty Reservoir .....	12
Dams on Flexible Foundation Rock with Impounded Water .....	13
RESPONSE COMBINATION .....	14
Dynamic Response .....	14
Total Response .....	15
SIMPLIFIED ANALYSIS PROCEDURE .....	15
Selection of System Parameters .....	16
Design Earthquake Spectrum .....	17
Computational Steps .....	17
Use of Metric Units .....	20
EVALUATION OF SIMPLIFIED ANALYSIS PROCEDURE .....	21
System and Ground Motion .....	21
Computation of Earthquake Forces .....	22
Computation of Stresses .....	23
Comparison with Refined Analysis Procedure .....	24
CONCLUSIONS .....	26
REFERENCES .....	28
NOTATION .....	29
TABLES .....	33
FIGURES .....	55
APPENDIX A: LIMITATIONS OF THE SIMPLIFIED ANALYSIS PROCEDURE FOR DAM-WATER SYSTEMS .....	91
Limitations of the Equivalent SDF System .....	91

Limitations of the Approximate Expression for $R_r$ .....	92
Comments on Added Hydrodynamic Damping .....	93
Figures .....	95
APPENDIX B: RESPONSE CONTRIBUTIONS OF HIGHER VIBRATION MODES .....	105
Dams with Empty Reservoir .....	105
Dams with Impounded Water .....	107
APPENDIX C: DETAILED CALCULATIONS FOR PINE FLAT DAM .....	109
Simplified Model of Monolith .....	109
Equivalent Lateral Forces -- Fundamental Mode .....	109
Stress Computation -- Fundamental Mode .....	110
Equivalent Lateral Forces -- Higher Vibration Modes .....	111
Stress Computation -- Higher Vibration Modes .....	111
Initial Static Stresses .....	112
Response Combination: Maximum Principal Stresses .....	112
Tables .....	114
APPENDIX D: COMPUTER PROGRAM FOR STRESS COMPUTATION .....	123
Simplified Model of Dam Monolith .....	123
Program Input .....	123
Computed Response .....	125
Example .....	126
Program Listing .....	131

## INTRODUCTION

The earthquake analysis of concrete gravity dams has come a long way, progressing from traditional "static" methods for computing design forces to dynamic analysis procedures. With the aid of dynamic response analysis, considering the effects of interaction between the dam and impounded water and of water compressibility, it has been demonstrated that the traditional design procedures have serious limitations because they are based on unrealistic assumptions: rigid dam and incompressible water (3). In order to improve dam design procedures, a simplified version of the general dynamic analysis procedure was developed (3).

A two-stage procedure was proposed for the analysis phase of elastic design and safety evaluation of dams: the simplified analysis procedure in which the maximum response is estimated directly from the earthquake design spectrum; and a refined response history analysis procedure for finite element idealizations of the dam monolith. The former is recommended for the preliminary phase of design and safety evaluation of dams and the latter for accurately computing the dynamic response and checking the adequacy of the preliminary evaluation (3). Both procedures have been utilized in practical applications. At the time (1978) the design procedure was presented, both of these analysis procedures included the effects of dam-water interaction and compressibility of water.

More recently, the response history analysis procedure for two-dimensional finite element idealizations of gravity dam monoliths has been extended to also consider the absorption of hydrodynamic pressure waves into the alluvium and sediments deposited at the bottom of reservoirs, and the interaction between the dam and underlying flexible foundation rock. With the aid of response analysis utilizing EAGD-84 (9), the computer program that implements the extended procedure, these effects have been demonstrated to be significant (6, 7). Thus, this procedure and computer program supersede the earlier procedure for the final design and safety evaluation of dams.

The objective of this report is to extend the simplified analysis procedure (3) to include the effects of dam-foundation rock interaction and reservoir bottom materials so that these important effects can be considered also in the preliminary design phase. The simplified procedure involves computation of the lateral earthquake forces associated with the fundamental vibration mode of the dam. Utilizing the analytical development underlying the procedure (4, 5), this paper is concerned with implementation of the procedure. Recognizing that the cross-sectional geometry of concrete gravity dams does not vary widely, standard data for the vibration properties of dams and the quantities that depend on them are presented to minimize the computations. Also included now in the simplified procedure is a "static correction" method to consider the response contributions of the higher vibration modes, and a rule for combining the modal responses. The use of the simplified procedure is illustrated by examples and is shown to be sufficiently accurate for the preliminary phase of design and safety evaluation of dams.

### **SIMPLIFIED ANALYSIS OF FUNDAMENTAL MODE RESPONSE**

The dynamic response of short-vibration-period structures, such as concrete gravity dams, to earthquake ground motion is primarily due to the fundamental mode of vibration. Thus, this is the most important vibration mode that need be considered in a simplified analysis procedure. The dam response to the vertical ground motion is less significant relative to the horizontal ground motion (7), and is therefore not included in the simplified procedure.

Even the analysis of the fundamental mode response of a dam is very complicated because dam water-foundation rock interaction introduces frequency-dependent, complex-valued hydrodynamic and foundation terms in the governing equations. However, frequency-independent values for these terms can be defined and an equivalent single-degree-of-freedom (SDF) system developed to represent approximately the fundamental mode response of concrete gravity dams (5).

For computing the response of the dam to intense earthquake ground motion it is appropriate to consider the two-dimensional vibration of individual monoliths. Each monolith is assumed to be supported on a viscoelastic half plane and impounding a reservoir of water, possibly with alluvium and sediments at the bottom (Fig. 1). Although the equivalent SDF system representation is valid for dams of any cross-section, the upstream face of the dam was assumed to be vertical (4,5) only for the purpose of evaluating the hydrodynamic terms in the governing equations. The standard data presented in this report is also based on this assumption, which is reasonable for actual concrete gravity dams because the upstream force is vertical or almost vertical for most of the height, and the hydrodynamic pressure on the dam face is insensitive to small departures of the face slope from vertical, especially if these departures are near the base of the dam, which is usually the case. The dynamic effects of the tail water are neglected because it is usually too shallow to influence dam response. A complete description of the dam-water-foundation rock system is presented in Refs. 4 and 8.

### Equivalent Lateral Forces

Considering only the fundamental mode of vibration of the dam, the maximum effects of the horizontal earthquake ground motion can be represented by equivalent lateral forces acting on the dam (5):

$$f_1(x,y) = \frac{\tilde{L}_1}{\tilde{M}_1} \frac{S_a(\tilde{T}_1, \tilde{\xi}_1)}{g} [w_s(x,y) \phi_1^x(x,y) + g\bar{p}_1(y, \tilde{T}_r) \delta(x)] \quad (1)$$

In Eq. 1, the x-coordinate is along the breadth of the dam monolith, the y-coordinate is measured from the base of the dam along its height,  $w_s(x,y) = gm_s(x,y)$  is the unit weight of the dam,

$$\tilde{M}_1 = M_1 + \text{Re} \left[ \int_0^H \bar{p}_1(y, \tilde{T}_r) \phi_1^x(0,y) dy \right] \quad (2a)$$

$$M_1 = \int \int m_s(x,y) \left\{ [\phi_1^x(x,y)]^2 + [\phi_1^y(x,y)]^2 \right\} dx dy \quad (2b)$$

$$\tilde{L}_1 = L_1 + \int_0^H \bar{p}_1(y, \tilde{T}_r) dy \quad (3a)$$

$$L_1 = \iint m_s(x,y) \phi_1^x(x,y) dx dy \quad (3b)$$

$M_1$  is the generalized mass and  $L_1$  the generalized earthquake force coefficient, with the integrations in Eqs. 2b and 3b extending over the cross-sectional area of the dam monolith;  $\phi_1^x(x,y)$  and  $\phi_1^y(x,y)$  are, respectively, the horizontal and vertical components of displacement in the fundamental vibration mode shape of the dam supported on rigid foundation rock with empty reservoir;  $\bar{p}_1(y, \tilde{T}_r)$  is the complex-valued function representing the hydrodynamic pressure on the upstream face due to harmonic acceleration of period  $\tilde{T}_r$  (defined later) in the fundamental vibration mode;  $H$  is the depth of the impounded water;  $\delta(x)$  is the Dirac delta function, which indicates that the hydrodynamic pressure acts at the upstream face of the dam;  $g$  is the acceleration due to gravity; and  $S_a(\tilde{T}_1, \tilde{\xi}_1)$  is the pseudo-acceleration ordinate of the earthquake design spectrum evaluated at the vibration period  $\tilde{T}_1$  and damping ratio  $\tilde{\xi}_1$  of the equivalent SDF system representing the dam-water-foundation rock system.

The natural vibration period of the equivalent SDF system representing the fundamental mode response of the dam on rigid foundation rock with impounded water is (4):

$$\tilde{T}_r = R_r T_1 \quad (4a)$$

in which  $T_1$  is the fundamental vibration period of the dam on rigid foundation rock with empty reservoir. Because of the frequency-dependent, added hydrodynamic mass arising from dam-water interaction, the factor  $R_r > 1$ . It depends on the properties of the dam, the depth of the water, and the absorptiveness of the reservoir bottom materials. The natural vibration period of the equivalent SDF system representing the fundamental mode response of the dam on flexible foundation rock with empty reservoir is (4):

$$\tilde{T}_f = R_f T_1 \quad (4b)$$

Because of the frequency-dependent, added foundation-rock flexibility arising from dam-foundation rock interaction, the factor  $R_f > 1$ . It depends on the properties of the dam and foundation rock.

The natural vibration period of the equivalent SDF system representing the fundamental mode response of the dam on flexible foundation rock with impounded water is approximately given by (5):

$$\tilde{T}_1 = R_r R_f T_1 \quad (4c)$$

The damping ratio of this equivalent SDF system is (5):

$$\tilde{\xi}_1 = \frac{1}{R_r} \frac{1}{(R_f)^3} \xi_1 + \xi_r + \xi_f \quad (5)$$

in which  $\xi_1$  is the damping ratio of the dam on rigid foundation rock with empty reservoir;  $\xi_r$  represents the added damping due to dam-water interaction and reservoir bottom absorption; and  $\xi_f$  represents the added radiation and material damping due to dam-foundation rock interaction. Considering that  $R_r$  and  $R_f > 1$ , Eq. 5 shows that dam-water interaction and dam-foundation rock interaction reduce the effectiveness of structural damping. However, usually this reduction is more than compensated by the added damping due to reservoir bottom absorption and due to dam-foundation rock interaction, which leads to an increase in the overall damping of the dam.

It is important to note that the effects of dam-water interaction and dam-foundation rock interaction on the parameters of the equivalent SDF system -- natural vibration period, damping ratio, generalized mass and earthquake force coefficient -- are computed independently of each other and applied sequentially to give values for the parameters that include the simultaneous interaction effects. The ability to separate the interaction effects in the computation of the natural vibration period and generalized mass is a consequence of the fact that dam-foundation rock interaction has little influence on the added hydrodynamic mass, and dam-water interaction does not substantially alter the effects of foundation rock flexibility. Such separation of the interaction effects is less accurate in the computation of the overall damping ratio and earthquake force coefficient by the simplified expressions of Eqs. 5 and 3a, but the results are acceptable for the preliminary phase of design and safety evaluation of dams. The separate consideration of dam-water interaction effects and dam-foundation rock interaction effects is an important feature of the simplified analysis procedure in that it greatly simplifies the evaluation of the fundamental vibration mode response of dams on flexible foundation rock with impounded water.

The quantities  $R_r$ ,  $R_f$ ,  $\xi_r$ ,  $\xi_f$ ,  $\bar{p}_1(\nu, \tilde{T}_r)$ ,  $\tilde{L}_1$ , and  $\tilde{M}_1$ , which are required to evaluate the equivalent lateral forces, Eq. 1, contain all the modifications of the vibration properties of the

equivalent SDF system and of the generalized earthquake force coefficient necessary to account for the effects of dam-water interaction, reservoir bottom absorption, and dam-foundation rock interaction. Even after the considerable simplification necessary to arrive at Eq. 1, its evaluation is still too complicated for practical applications because the afore-mentioned quantities are complicated functions of the hydrodynamic and foundation-rock flexibility terms (5). Fortunately, as will be seen in a later section, the computation of lateral forces can be considerably simplified by recognizing that the cross-sectional geometry of concrete gravity dams does not vary widely.

### One-Dimensional Approximation of Lateral Forces

The lateral forces  $f_1(x,y)$  due to the fundamental vibration mode, Eq. 1, are distributed over the cross-section of the dam monolith. Because the variation of the fundamental vibration mode shape  $\phi_1^x(x,y)$  across the dam breadth is small, i.e.  $\phi_1^x(x,y) \approx \phi_1^x(0,y)$ , it would be reasonable in a simplified analysis to integrate  $f_1(x,y)$  over the breadth of the monolith to obtain equivalent lateral forces  $f_1(y)$  per unit height of the dam:

$$f_1(y) = \frac{\tilde{L}_1}{\tilde{M}_1} \frac{S_a(\tilde{T}_1, \tilde{\xi}_1)}{g} [w_s(y) \phi(y) + g\bar{p}_1(y, \tilde{T}_r)] \quad (6)$$

in which  $\phi(y) = \phi_1^x(0,y)$  is the horizontal component of displacement at the upstream face in the fundamental vibration mode shape of the dam;  $w_s(y)$  is the weight of the dam per unit height; and all other quantities are as defined before except that the generalized mass and earthquake force coefficient, Eqs. 2b and 3b, are now represented by one-dimensional integrals:

$$M_1 = \frac{1}{g} \int_0^{H_s} w_s(y) \phi^2(y) dy \quad (7a)$$

$$L_1 = \frac{1}{g} \int_0^{H_s} w_s(y) \phi(y) dy \quad (7b)$$

in which  $H_s$  is the height of the dam. Eq. 6 is an extension of Eq. 9 in Ref. 3 to include the effects of dam-foundation rock interaction and reservoir bottom materials on the lateral forces.



### Approximation of Hydrodynamic Pressure

If the hydrodynamic wave absorption in the alluvium and sediments at the bottom of a reservoir is considered, the hydrodynamic pressure function  $\bar{p}_1(y, \tilde{T}_r)$  is complex-valued at the period  $\tilde{T}_r$ . The distributions of the real- and imaginary-valued components of lateral forces  $f_1(y)$  at the upstream face of a typical concrete dam monolith with nearly full reservoir ( $H/H_s = 0.95$ ) are shown in Fig. 2. The hydrodynamic pressure and hence lateral forces are real-valued for nonabsorptive reservoir bottom materials, i.e.  $\alpha = 1$  (3). Even when reservoir bottom absorption is considered, the imaginary-valued component of lateral forces is small relative to the real-valued component, increasing near the base of the dam, where, because of the large stiffness of the dam, it will have little influence on the stresses in the dam. Consequently, the imaginary-valued component of  $\bar{p}_1(y, \tilde{T}_r)$  may be neglected in the evaluation of the lateral forces  $f_1(y)$ , and Eq. 6 becomes:

$$f_1(y) = \frac{\tilde{L}_1}{\tilde{M}_1} \frac{S_a(\tilde{T}_1, \tilde{\xi}_1)}{g} \left[ w_s(y) \phi(y) + gp(y, \tilde{T}_r) \right] \quad (8)$$

where  $p(y, \tilde{T}_r) \equiv \text{Re}[\bar{p}_1(y, \tilde{T}_r)]$ . Although the imaginary-valued component of  $\bar{p}_1(y, \tilde{T}_r)$  has been dropped in Eq. 8, its more important effect, the contribution to added hydrodynamic damping  $\xi_r$  in Eq. 5, is still considered.

The generalized mass  $\tilde{M}_1$  of the equivalent SDF system, Eq. 2a, only depends on the real-valued component of hydrodynamic pressure:

$$\tilde{M}_1 = M_1 + \int_0^H p(y, \tilde{T}_r) \phi(y) dy \quad (9a)$$

where  $M_1$  is defined in Eq. 7a. However, the generalized earthquake force coefficient  $\tilde{L}_1$ , Eq. 3a, contains both real-valued and imaginary-valued components of the hydrodynamic pressure. Again, dropping the imaginary-valued component gives:

$$\tilde{L}_1 = L_1 + \int_0^H p(y, \tilde{T}_r) dy \quad (9b)$$

where  $L_1$  is defined in Eq. 7b.

## STANDARD PROPERTIES FOR FUNDAMENTAL MODE RESPONSE

Direct evaluation of Eq. 8 would require complicated computation of several quantities:  $p(y, \tilde{T}_r)$  from an infinite series expression; the period lengthening ratios  $R_r$  and  $R_f$  due to dam-water and dam-foundation rock interactions by iterative solution of equations involving frequency-dependent terms; damping ratios  $\xi_f$  and  $\xi_r$  from expressions involving complicated foundation-rock flexibility and hydrodynamic terms; the integrals in Eq. 9; and the fundamental vibration period and mode shape of the dam (4, 5). The required computations would be excessive for purposes of preliminary design of dams. Recognizing that the cross-sectional geometry of concrete gravity dams does not vary widely, standard values for the vibration properties of dams and all quantities in Eq. 8 that depend on them are developed in this section. Tables and curves of the standard values are presented.

### Vibration Properties of the Dam

Computed by the finite element method, the fundamental vibration period, in seconds, of a "standard" cross-section for nonoverflow monoliths of concrete gravity dams on rigid foundation rock with empty reservoir is (3):

$$T_1 = 1.4 \frac{H_s}{\sqrt{E_s}} \quad (10)$$

in which  $H_s$  is the height of the dam, in feet; and  $E_s$  is the Young's modulus of elasticity of concrete, in pounds per square inch. The fundamental vibration mode shape  $\phi(y)$  of the standard cross-section is shown in Fig. 3a, which is compared in Fig. 3b with the mode shape for four idealized cross-sections and two actual dams. Because the fundamental vibration periods and mode shapes for these cross-sections are similar, it is appropriate to use the standard vibration period and mode shape presented in Fig. 3a for the preliminary design and safety evaluation of concrete gravity dams. The ordinates of the standard vibration mode shape are presented in Table 1.

### Modification of Period and Damping: Dam-Water Interaction

Dam-water interaction and reservoir bottom absorption modify the natural vibration period (Eq. 4a) and the damping ratio (Eq. 5) of the equivalent SDF system representing the fundamental vibration mode response of the dam. For the standard dam cross-section, the period lengthening ratio  $R_r$  and added damping  $\xi_r$  depend on several parameters, the more significant of which are: Young's modulus  $E_s$  of the dam concrete, ratio  $H/H_s$  of water depth to dam height, and wave reflection coefficient  $\alpha$ . This coefficient,  $\alpha$ , is the ratio of the amplitude of the reflected hydrodynamic pressure wave to the amplitude of a vertically propagating pressure wave incident on the reservoir bottom (4, 8, 10, 11);  $\alpha = 1$  indicates that pressure waves are completely reflected, and smaller values of  $\alpha$  indicate increasingly absorptive materials.

The results of many analyses of the "standard" dam cross-section, using the procedures developed in Ref. 4 and modified in Appendix A for dams with larger elastic modulus  $E_s$ , are summarized in Figs. 4 and 5 and Table 2. The period lengthening ratio  $R_r$  and added damping  $\xi_r$  are presented as a function of  $H/H_s$  for  $E_s = 5.0, 4.5, 4.0, 3.5, 3.0, 2.5, 2.0,$  and  $1.0$  million psi; and  $\alpha = 1.00, 0.90, 0.75, 0.50, 0.25,$  and  $0$ . Whereas the dependence of  $R_r$  and  $\xi_r$  on  $E_s, H/H_s$  and  $\alpha$ , and the underlying mechanics of dam-water interaction and reservoir bottom absorption are discussed elsewhere in detail (4, 5), it is useful to note that  $R_r$  increases and  $\xi_r$ , generally, but not always, increases with increasing water depth, absorptiveness of reservoir bottom materials, and concrete modulus; also see Appendix A. The effects of dam-water interaction and reservoir bottom absorption may be neglected, and the dam analyzed as if there is no impounded water, if the reservoir depth is not large,  $H/H_s < 0.5$ ; in particular  $R_r \approx 1$  and  $\xi_r \approx 0$ .

### Modification of Period and Damping: Dam-Foundation Rock Interaction

Dam-foundation rock interaction modifies the natural vibration period (Eq. 4b) and added damping ratio (Eq. 5) of the equivalent SDF system representing the fundamental vibration mode response of the dam. For the "standard" dam cross-section, the period lengthening ratio  $R_f$  and the added damping  $\xi_f$  due to dam-foundation rock interaction depend on several parameters, the more

significant of which are: moduli ratio  $E_f/E_s$ , where  $E_s$  and  $E_f$  are the Young's moduli of the dam concrete and foundation rock, respectively; and the constant hysteretic damping factor  $\eta_f$  for the foundation rock. The period ratio  $R_f$  is, however, insensitive to  $\eta_f$ .

The results of many analyses of the "standard" dam cross-section, using the procedures developed in Ref. 4, are summarized in Figs. 6 and 7 and Table 3. The period lengthening ratio  $R_f$  and added damping  $\xi_f$  are presented for many values of  $E_f/E_s$  between 0.2 and 5.0, and  $\eta_f = 0.01, 0.10, 0.25, \text{ and } 0.50$ . Whereas the dependence of  $R_f$  and  $\xi_f$  on  $E_f/E_s$  and  $\eta_f$ , and the underlying mechanics of dam-foundation rock interaction are discussed elsewhere in detail (4, 5), it is useful to note that the period ratio  $R_f$  is essentially independent of  $\eta_f$ , but increases as the moduli ratio  $E_f/E_s$  decreases, which for a fixed value of  $E_s$  implies an increasingly flexible foundation rock. The added damping  $\xi_f$  increases with decreasing  $E_f/E_s$  and increasing hysteretic damping factor  $\eta_f$ . The foundation rock may be considered rigid in the simplified analysis if  $E_f/E_s > 4$  because then the effects of dam-foundation rock interaction are negligible.

### Hydrodynamic Pressure

In order to provide a convenient means for determining  $p(y, \tilde{T}_r)$  in Eqs. 8 and 9, a nondimensional form of this function  $gp(\hat{y})/wH$ , where  $\hat{y} = y/H$ , and  $w$  = the unit weight of water, has been computed from the equations presented in Ref. 4 for  $\alpha = 1.00, 0.90, 0.75, 0.5, 0.25, \text{ and } 0$ , and the necessary range of values of

$$R_w = \frac{T_1^r}{\tilde{T}_r} \quad (11)$$

in which the fundamental vibration period of the impounded water  $T_1^r = 4H/C$ , where  $C$  is the velocity of pressure waves in water. The results presented in Fig. 8 and Table 4 are for full reservoir,  $H/H_s = 1$ . The function  $gp(\hat{y})/wH$  for any other value of  $H/H_s$  is approximately equal to  $(H/H_s)^2$  times the function for  $H/H_s = 1$  (3).

For nonabsorptive reservoir bottom materials ( $\alpha = 1$ ), Fig. 8 shows that the function  $p(\hat{y})$  increases monotonically with increasing period ratio  $R_w$ . Because dam-water interaction always

lengthens the fundamental vibration period  $\tilde{T}_r$  of the dam to a value greater than  $T_1^r$ , the period ratio  $R_w$  cannot exceed unity (10). For  $R_w \leq 0.5$ , the effects of water compressibility are negligible and  $p(\hat{y})$  is essentially independent of  $R_w$ .

Figure 8 shows that  $p(\hat{y})$  decreases because of the absorption of hydrodynamic pressure waves into the reservoir bottom materials ( $\alpha < 1$ ). The period ratio  $R_w$  can exceed unity if  $\alpha < 1$ , but  $p(\hat{y})$  decreases as  $R_w$  increases because of the increasingly stiff dam. The upper limit for  $R_w$  of 1.2 is the largest value that can result from the data presented in Fig. 4 and Table 2.

### Generalized Mass and Earthquake Force Coefficient

The generalized mass  $\tilde{M}_1$  (Eq. 9a) of the equivalent SDF system representing the dam, including hydrodynamic effects, can be conveniently computed from (4):

$$\tilde{M}_1 = (R_r)^2 M_1 \quad (12a)$$

in which  $M_1$  is given by Eq. 7a and standard values are presented later. In order to provide a convenient means to compute the generalized earthquake force coefficient  $\tilde{L}_1$ , Eq. 9b is expressed as:

$$\tilde{L}_1 = L_1 + \frac{1}{g} F_{st} \left[ \frac{H}{H_s} \right]^2 A_p \quad (12b)$$

where  $F_{st} = \frac{1}{2} w H^2$  is the total hydrostatic force on the dam, and  $A_p$  is the integral of the function  $2gp(\hat{y})/wH$  over the depth of the impounded water, for  $H/H_s = 1$ . The hydrodynamic force coefficient  $A_p$  is presented in Table 5 for a range of values for the period ratio  $R_w$  and the wave reflection coefficient  $\alpha$ .

### STATIC CORRECTION FOR HIGHER MODE RESPONSE

Because the earthquake response of short vibration period structures, such as concrete gravity dams, is primarily due to the fundamental mode of vibration, the response contributions of the higher

vibration modes have, so far, been neglected in the simplified analysis procedure presented in the preceding sections. However, the height-wise mass distribution of concrete gravity dams is such that the effective mass (2) in the fundamental vibration mode is small, e.g. it is 35 percent of the total mass for the standard dam section mentioned earlier. Thus, the contributions of the higher vibration modes to the earthquake forces may not be negligible, and a simple method to consider them is presented in this section.

### **Dams on Rigid Foundation Rock with Empty Reservoir**

Because the periods of the higher vibration modes of concrete gravity dams are very short, the corresponding ordinates of the pseudo-acceleration response spectrum for the design earthquake will be essentially equal to the zero-period ordinate or maximum ground acceleration. With little dynamic amplification, the higher vibration modes respond in essentially a static manner to earthquake ground motion, leading to the "static correction" concept (1, 12). The maximum earthquake effects associated with the higher vibration modes can then be represented by the equivalent lateral forces (Appendix B):

$$f_{sc}(y) = \frac{1}{g} w_s(y) \left[ 1 - \frac{L_1}{M_1} \phi(y) \right] a_g \quad (13)$$

in which  $a_g$  is the maximum ground acceleration. The shape of only the fundamental vibration mode enters into Eq. 13 and the shapes of the higher modes are not required, thus simplifying the analysis considerably.

### **Dams on Flexible Foundation Rock with Empty Reservoir**

Just as in the case of multistory buildings (14), soil-structure interaction effects may be neglected in a simplified procedure to compute the contributions of the higher vibration modes to the earthquake response of dams. Thus, Eq. 13 for the equivalent lateral forces is still valid.

To demonstrate the accuracy of Eq. 13, based on the "static correction" method to determine the response contributions of the higher vibration modes, the response of an idealized triangular dam

monolith with empty reservoir to the S69E component of Taft ground motion is presented. Assuming the dam base to be rigid, which is reasonable (4), the earthquake response of the dam was computed as a function of time, considering a variable number of natural vibration modes of the dam on rigid foundation rock, in addition to the two rigid-body modes of the base allowed by foundation-rock flexibility. The height-wise distribution of maximum shear force  $V_{\max}$  and maximum bending moment  $M_{\max}$  for two dam heights and three values of  $E_f/E_s$  is presented in Figs. 9 and 10 from three analyses: (1) using the first eight vibration modes, which essentially gives the exact response; (2) using only the fundamental vibration mode; and (3) using the fundamental vibration mode and the “static correction” for the higher mode response contributions. It is apparent that in some cases the higher mode response contributions may be significant and that they are estimated to a useful degree of accuracy by the “static correction” procedure.

#### Dams on Flexible Foundation Rock with Impounded Water

Dam-water interaction introduces significant damping in the response of the higher vibration modes of concrete gravity dams (6), but it has little effect on the higher vibration periods. Because these periods for concrete gravity dams are very short and the corresponding modes are heavily damped, the “static correction” method would be appropriate to represent the higher mode responses of the dam, even with impounded water. The equivalent lateral earthquake forces associated with the higher vibration modes of dams, including the effects of the impounded water, are given by an extension of Eq. 13 (Appendix B):

$$f_{sc}(y) = \frac{1}{g} \left\{ w_s(y) \left[ 1 - \frac{L_1}{M_1} \phi(y) \right] + \left[ gp_o(y) - \frac{B_1}{M_1} w_s(y) \phi(y) \right] \right\} a_g \quad (14)$$

In Eq. 14,  $p_o(y)$  is a real-valued, frequency-independent function describing the hydrodynamic pressure on a rigid dam undergoing unit acceleration, with water compressibility neglected, both assumptions being consistent with the “static correction” concept; and  $B_1$  provides a measure of the portion of  $p_o(y)$  that acts in the fundamental vibration mode. Standard values for  $p_o(y)$  are presented in Fig. 11 and Table 6. Using the fundamental mode vibration properties of the standard

dam:

$$B_1 = 0.052 \frac{F_{st}}{g} \left[ \frac{H}{H_s} \right]^2 \quad (15)$$

where  $F_{st}$  is the total hydrostatic force on the dam.

## RESPONSE COMBINATION

### Dynamic Response

As shown in the preceding two sections, the maximum effects of earthquake ground motion in the fundamental vibration mode of the dam have been represented by equivalent lateral forces  $f_1(y)$  and those due to all the higher modes by  $f_{sc}(y)$ . Static analysis of the dam for these two sets of forces provide the values  $r_1$  and  $r_{sc}$  for any response quantity  $r$ , e.g., the shear force or bending moment at any horizontal section, or the shear or bending stresses at any point. Because the maximum responses  $r_1$  and  $r_{sc}$  do not occur at the same time during the earthquake, they should be combined to obtain an estimate of the dynamic response  $r_d$  according to the well known modal combination rules: square-root-of-the-sum-of-squares (SRSS) of modal maxima leading to

$$r_d = \sqrt{(r_1)^2 + (r_{sc})^2} \quad (16)$$

or the sum-of-absolute-values (ABSUM) which always provides a conservative result:

$$r_d = |r_1| + |r_{sc}| \quad (17)$$

Because the natural frequencies of lateral vibration of a concrete dam are well separated, it is not necessary to include the correlation of modal responses in Eq. 16. Later in the report when the accuracy of the simplified analysis procedure is evaluated, the SRSS combination rule will be shown to be preferable.

The SRSS and ABSUM combination rules are applicable to the computation of any response quantity that is proportional to the generalized modal coordinate responses. Thus, these combination



rules are generally inappropriate to determine the principal stresses. However, as shown in Appendix C, the principal stresses at the faces of a dam monolith may be determined by the SRSS method if the upstream face is nearly vertical and the effects of tail water at the downstream face are small.

### Total Response

In order to obtain the total value of a response quantity  $r$ , the SRSS estimate of dynamic response  $r_d$  should be combined with the static effects  $r_{st}$ . The latter may be determined by standard analysis procedures to compute the initial stresses in a dam prior to the earthquake, including effects of the self weight of the dam, hydrostatic pressures, and temperature changes. In order to recognize that the direction of lateral earthquake forces is reversible, combinations of static and dynamic stresses should allow for the worst case, leading to the maximum value of total response:

$$r_{\max} = r_{st} \pm \sqrt{(r_1)^2 + (r_{sc})^2} \quad (18)$$

This combination of static and dynamic responses is appropriate if  $r_{st}$ ,  $r_1$  and  $r_{sc}$  are oriented similarly. Such is the case for the shear force or bending moment at any horizontal section, for the shear and bending stresses at any point, but generally not for principal stresses except under the restricted conditions mentioned above.

## SIMPLIFIED ANALYSIS PROCEDURE

The maximum effects of an earthquake on a concrete gravity dam are represented by equivalent lateral forces in the simplified analysis procedure. The lateral forces associated with the fundamental vibration mode are computed to include the effects of dam-water interaction, water compressibility, reservoir bottom absorption, and dam-foundation rock interaction. The response contributions of the higher vibration modes are computed under the assumption that the dynamic amplification of the modes is negligible, the interaction effects between the dam, impounded water, and foundation rock are not significant, and that the effects of water compressibility can be neglected. These

approximations provide a practical method for including the most important factors that affect the earthquake response of concrete gravity dams.

### Selection of System Parameters

The simplified analysis procedure requires only a few parameters to describe the dam-water-foundation rock system:  $E_s$ ,  $\xi_1$ ,  $H_s$ ,  $E_f$ ,  $\eta_f$ ,  $H$  and  $\alpha$ .

The Young's modulus of elasticity  $E_s$  for the dam concrete should be based on the design strength of the concrete or suitable test data, if available. The value of  $E_s$  may be modified to recognize the strain rates representative of those the concrete may experience during earthquake motions of the dam (3). In using the figures and tables presented earlier to conservatively include dam-water interaction effects in the computation of earthquake forces (Eq. 8), the  $E_s$  value should be rounded down to the nearest value for which data are available:  $E_s = 1.0, 2.0, 2.5, 3.0, 3.5, 4.0, 4.5,$  or 5.0 million pounds per square inch. Forced vibration tests on dams indicate that the viscous damping ratio  $\xi_1$  for concrete dams is in the range of 1 to 3 percent. However, for the large motions and high stresses expected in a dam during intense earthquakes,  $\xi_1 = 5$  percent is recommended. The height  $H_s$  of the dam is measured from the base to the crest.

The Young's modulus of elasticity  $E_f$  and constant hysteretic damping coefficient  $\eta_f$  of the foundation rock should be determined from a site investigation and appropriate tests. To be conservative, the value of  $\eta_f$  should be rounded down to the nearest value for which data are available:  $\eta_f = 0.01, 0.10, 0.25,$  or 0.50, and the value of  $E_f/E_s$  should be rounded up to the nearest value for which data are available. In the absence of information on damping properties of the foundation rock, a value of  $\eta_f = 0.10$  is recommended.

The depth  $H$  of the impounded water is measured from the free surface to the reservoir bottom. It is not necessary for the reservoir bottom and dam base to be at the same elevation. The standard values for unit weight of water and velocity of pressure waves in water are  $w = 62.4$  pcf and  $C = 4720$  fps, respectively.

It may be impractical to determine reliably the wave reflection coefficient  $\alpha$  because the reservoir bottom materials may consist of highly variable layers of exposed bedrock, alluvium, silt and other sediments, and appropriate site investigation techniques have not been developed. However, to be conservative, the estimated value of  $\alpha$  should be rounded up to the nearest value for which the figures and tables are presented:  $\alpha = 1.0, 0.90, 0.75, 0.50, 0.25, 0.00$ . For proposed new dams or recent dams where sediment deposits are meager,  $\alpha = 0.90$  or  $1.0$  is recommended and, lacking data,  $\alpha = 0.75$  or  $0.90$  is recommended for older dams where sediment deposits are substantial. In each case, the larger  $\alpha$  value will generally give conservative results which is appropriate at the preliminary design stage.

### Design Earthquake Spectrum

The horizontal earthquake ground motion is specified by a pseudo-acceleration response spectrum in the simplified analysis procedure. This should be a smooth response spectrum -- without the irregularities inherent in response spectra of individual ground motions -- representative of the intensity and frequency characteristics of the design earthquakes which should be established after a thorough seismological and geological investigation; see Ref. 3 for more detail.

### Computational Steps

The computation of earthquake response of the dam is organized in three parts:

**Part I:** The earthquake forces and stresses due to the fundamental vibration mode can be determined approximately for purposes of preliminary design by the following computational steps.

1. Compute  $T_1$ , the fundamental vibration period of the dam, in seconds, on rigid foundation rock with an empty reservoir from Eq. 10 in which  $H_s$  = height of the dam in feet, and  $E_s$  = design value for Young's modulus of elasticity of concrete, in pounds per square inch.
2. Compute  $\tilde{T}_r$ , the fundamental vibration period of the dam, in seconds, including the influence of impounded water from Eq. 4a in which  $T_1$  was computed in Step 1;  $R_r$  = period ratio determined from Fig. 4 or Table 2 for the design values of  $E_s$ , the wave reflection coefficient  $\alpha$ ,

and the depth ratio  $H/H_s$ , where  $H$  is the depth of the impounded water, in feet. If  $H/H_s < 0.5$ , computation of  $R_r$  may be avoided by using  $R_r \approx 1$ .

3. Compute the period ratio  $R_w$  from Eq. 11 in which  $\tilde{T}_r$  was computed in Step 2, and  $T_1' = 4H/C$  where  $C = 4720$  feet per second.
4. Compute  $\tilde{T}_1$ , the fundamental vibration period of the dam in seconds, including the influence of foundation-rock flexibility and of impounded water, from Eq. 4c in which  $R_r$  was determined in Step 2;  $R_f =$  period ratio determined from Fig. 6 or Table 3 for the design value of  $E_f/E_s$ ; and  $E_f$  is the Young's modulus of the foundation rock in pounds per square inch. If  $E_f/E_s > 4$ , use  $R_f \approx 1$ .
5. Compute the damping ratio  $\tilde{\xi}_1$  of the dam from Eq. 5 using the period ratios  $R_r$  and  $R_f$  determined in Steps 2 and 4, respectively;  $\xi_1 =$  viscous damping ratio for the dam on rigid foundation rock with empty reservoir;  $\xi_r =$  added damping ratio due to dam-water interaction and reservoir bottom absorption, obtained from Fig. 5 or Table 2 for the selected values of  $E_s$ ,  $\alpha$  and  $H/H_s$ ; and  $\xi_f =$  added damping ratio due to dam-foundation rock interaction, obtained from Fig. 7 or Table 3 for the selected values of  $E_f/E_s$  and  $\eta_f$ . If  $H/H_s < 0.5$ , use  $\xi_r = 0$ ; if  $E_f/E_s > 4$ , use  $\xi_f = 0$ ; and if the computed value of  $\tilde{\xi}_1 < \xi_1$ , use  $\tilde{\xi}_1 = \xi_1$ .
6. Determine  $gp(y, \tilde{T}_r)$  from Fig. 8 or Table 4 corresponding to the value of  $R_w$  computed in step 3 -- rounded to one of the two nearest available values, the one giving the larger  $p(y)$  -- the design value of  $\alpha$ , and for  $H/H_s = 1$ ; the result is multiplied by  $(H/H_s)^2$ . If  $H/H_s < 0.5$ , computation of  $p(y, \tilde{T}_r)$  may be avoided by using  $p(y, \tilde{T}_r) \approx 0$ .
7. Compute the generalized mass  $\tilde{M}_1$  from Eq. 12a: in which  $R_r$  was computed in Step 2, and  $M_1$  is computed from Eq. 7a, in which  $w_s(y) =$  the weight of the dam per unit height; the fundamental vibration mode shape  $\phi(y)$  is given in Fig. 3 or Table 1; and  $g = 32.2$  feet per squared second. Evaluation of Eq. 7a may be avoided by obtaining an approximate value from  $M_1 = 0.043 W_s/g$ , where  $W_s$  is the total weight of the dam monolith.
8. Compute the generalized earthquake force coefficient  $\tilde{L}_1$  from Eq. 12b in which  $L_1$  is computed from Eq. 7b;  $F_{st} = wH^2/2$ ; and  $A_p$  is given in Table 5 for the values of  $R_w$  and  $\alpha$  used in Step 6.

If  $H/H_s < 0.5$  computation of  $\tilde{L}_1$  may be avoided by using  $\tilde{L}_1 \approx L_1$ . Evaluation of Eq. 7b may be avoided by obtaining an approximate value from  $L_1 = 0.13 W_s/g$ .

*Note:* Computation of Steps 7 and 8 may be avoided by using conservative values:  $\tilde{L}_1/\tilde{M}_1 = 4$  for dams with impounded water, and  $L_1/M_1 = 3$  for dams with empty reservoirs.

9. Compute  $f_1(y)$ , the equivalent lateral earthquake forces associated with the fundamental vibration mode from Eq. 8 in which  $S_a(\tilde{T}_1, \tilde{\xi}_1)$  = the pseudo-acceleration ordinate of the earthquake design spectrum in feet per squared second at period  $\tilde{T}_1$  determined in Step 4 and damping ratio  $\tilde{\xi}_1$  determined in Step 5;  $w_s(y)$  = weight per unit height of the dam;  $\phi(y)$  = fundamental vibration mode shape of the dam from Fig. 3 or Table 1;  $\tilde{M}_1$  and  $\tilde{L}_1$  = generalized mass and earthquake force coefficient determined in Steps 7 and 8, respectively; the hydrodynamic pressure term  $gp(y, \tilde{T}_r)$  was determined in Step 6; and  $g = 32.2$  feet per squared second.
10. Determine by static analysis of the dam subjected to equivalent lateral forces  $f_1(y)$ , from Step 9, applied to the upstream face of the dam, all the response quantities of interest, in particular the stresses throughout the dam. Traditional procedures for design calculations may be used wherein the bending stresses across a horizontal section are computed by elementary formulas for stresses in beams. Alternatively, the finite element method may be used for accurate static stress analysis.

**Part II:** The earthquake forces and stresses due to the higher vibration modes can be determined approximately for purposes of preliminary design by the following computational steps:

11. Compute  $f_{sc}(y)$  the lateral forces associated with the higher vibration modes from Eq. 14 in which  $M_1$  and  $L_1$  were determined in Steps 7 and 8, respectively;  $gp_o(y)$  is determined from Fig. 11 or Table 6;  $B_1$  is computed from Eq. 15; and  $a_g$  is the maximum ground acceleration, in feet per squared second, of the design earthquake. If  $H/H_s < 0.5$  computation of  $p_o(y)$  may be avoided by using  $p_o(y) \approx 0$  and hence  $B_1 \approx 0$ .
12. Determine by static analysis of the dam subjected to the equivalent lateral forces  $f_{sc}(y)$ , from Step 11, applied to the upstream face of the dam, all the response quantities of interest, in

particular the bending stresses throughout the dam. The stress analysis may be carried out by the procedures mentioned in Step 10.

**Part III:** The total earthquake forces and stresses in the dam are determined by the following computational step:

13. Compute the total value of any response quantity by Eq. 18, in which  $r_1$  and  $r_{sc}$  are values of the response quantity determined in Steps 10 and 12 associated with the fundamental and higher vibration modes, respectively, and  $r_{st}$  is its initial value prior to the earthquake due to various loads, including the self weight of the dam, hydrostatic pressure, and thermal effects.

### Use of Metric Units

Because the standard values for most quantities required in the simplified analysis procedure are presented in non-dimensional form, implementation of the procedure in metric units is straightforward. The expressions and data requiring conversion to metric units are noted here:

1. The fundamental vibration period  $T_1$  of the dam on rigid foundation rock with empty reservoir (Step 1), in seconds, is given by:

$$T_1 = 0.38 \frac{H_s}{\sqrt{E_s}} \quad (19)$$

where  $H_s$  is the height of the dam in meters; and  $E_s$  is the Young's modulus of elasticity of the dam concrete in mega-Pascals.

2. The period ratio  $R_r$  and added damping ratio  $\xi_r$  due to dam-water interaction presented in Figs. 4 and 5 and Table 2 is for specified values of  $E_s$  in psi which should be converted to mega-Pascals as follows: 1 million psi = 7 thousand mega-Pascals.
3. Where required in the calculations, the unit weight of water  $w = 9.81$  kilo-Newtons per cubic meter; the acceleration due to gravity  $g = 9.81$  meters per squared second; and velocity of pressure waves in water  $C = 1440$  meters per second.

## EVALUATION OF SIMPLIFIED ANALYSIS PROCEDURE

As mentioned earlier (4, 5) and in the preceding sections, various approximations were introduced to develop the simplified analysis procedure and these were individually checked to ensure that they would lead to acceptable results. In order to provide an overall evaluation of the simplified analysis procedure, it is used to determine the earthquake-induced stresses in Pine Flat Dam, and the results are compared with those obtained from a refined response history analysis -- rigorously including dam-water-foundation rock interaction and reservoir bottom absorption effects -- in which the dam is idealized as a finite element system.

### System and Ground Motion

The system properties for the simplified analysis are taken to be the same as those assumed for the complete response history analysis: the tallest, nonoverflow monolith of the dam is shown in Fig. 12; height of the dam,  $H_s = 400$  ft, modulus of elasticity of concrete,  $E_s = 3.25 \times 10^6$  psi; unit weight of concrete = 155 pcf; damping ratio  $\xi_1 = 5\%$ ; modulus of elasticity of foundation rock  $E_f = 3.25 \times 10^6$  psi; constant hysteretic damping coefficient of foundation rock,  $\eta_f = 0.10$ ; depth of water,  $H = 381$  ft; and, at the reservoir bottom, the wave reflection coefficient  $\alpha = 0.5$ .

The ground motion for which the dam is analyzed is the S69E component of the ground motion recorded at the Taft Lincoln School Tunnel during the Kern County, California, earthquake of July 21, 1952. The response spectrum for this ground motion is shown in Fig. 13. Such an irregular spectrum of an individual ground motion is inappropriate in conjunction with the simplified procedure, wherein a smooth design spectrum is recommended, but is used here to provide direct comparison with the results obtained from the refined analysis procedure.

### Computation of Earthquake Forces

The dam is analyzed by the simplified analysis procedure for the four cases listed in Table 7. Implementation of the step-by-step analysis procedure described in the preceding section is summarized next with additional details available in Appendix C; all computations are performed for a unit width of the monolith:

1. For  $E_s = 3.25 \times 10^6$  psi and  $H_s = 400$  ft, from Eq. 10,  $T_1 = (1.4)(400)/\sqrt{3.25 \times 10^6} = 0.311$  sec.
2. For  $E_s = 3.0 \times 10^6$  psi (rounded down from  $3.25 \times 10^6$  psi),  $\alpha = 0.50$  and  $H/H_s = 381/400 = 0.95$ , Fig. 5 or Table 2 gives  $R = 1.213$ , so  $\tilde{T}_1 = (1.213)(0.311) = 0.377$  sec.
3. From Eq. 11,  $T_1' = (4)(381)/4720 = 0.323$  sec. and  $R_w = 0.323/0.377 = 0.86$ .
4. For  $E_f/E_s = 1$ , Fig. 6 or Table 3 gives  $R_f = 1.187$ , so  $\tilde{T}_1 = (1.187)(0.311) = 0.369$  sec for Case 3, and  $\tilde{T}_1 = (1.187)(0.377) = 0.448$  sec for Case 4.
5. For Cases 2 and 4,  $\xi_r = 0.030$  from Fig. 5 or Table 2 for  $E_s = 3.0 \times 10^6$  psi (rounded down from  $3.25 \times 10^6$  psi),  $\alpha = 0.50$ , and  $H/H_s = 0.95$ . For Cases 3 and 4,  $\xi_f = 0.068$  from Fig. 7 or Table 3 for  $E_f/E_s = 1$  and  $\eta_f = 0.10$ . With  $\xi_1 = 0.05$ , Eq. 5 gives:  $\tilde{\xi} = (0.05)/(1.213) + 0.030 = 0.071$  for Case 2;  $\tilde{\xi}_1 = (0.05)/(1.187)^3 + 0.068 = 0.098$  for Case 3; and  $\tilde{\xi}_1 = (0.05)/[(1.213)(1.187)^3] + 0.030 + 0.068 = 0.123$  for Case 4.
6. The values of  $gp(y)$  presented in Table 8 at eleven equally spaced levels were obtained from Fig. 8 or Table 4 for  $R_w = 0.90$  (by rounding  $R_w = 0.86$  from Step 3) and  $\alpha = 0.50$ , and multiplied by  $(0.0624)(381)(.95)^2 = 21.5$  k/ft.
7. Evaluating Eq. 7a in discrete form gives  $M_1 = (1/g)(500 \text{ kip})$ . From Eq. 12a,  $\tilde{M}_1 = (1.213)^2(1/g)(500) = (736 \text{ kip})/g$ .
8. Equation 7b in discrete form gives  $L_1 = (1390 \text{ kip})/g$ . From Table 5,  $A_p = 0.274$  for  $R_w = 0.90$  and  $\alpha = 0.50$ . Equation 12b then gives  $\tilde{L}_1 = 1390/g + [(0.0624)(381)^2/2g](0.95)^2(0.274) = (2510 \text{ kip})/g$ . Consequently, for Cases 1 and 3,  $L_1/M_1 = 1390/500 = 2.78$ , and for Cases 2 and 4,  $\tilde{L}_1/\tilde{M}_1 = 2510/736 = 3.41$ .



9. For each of the four cases, Eq. 8 was evaluated at eleven equally spaced intervals along the height of the dam, including the top and bottom, by substituting values for the quantities computed in the preceding steps, computing the weight of the dam per unit height  $w_s(y)$  from the monolith dimensions (Fig. 12) and the unit weight of concrete, by substituting  $\phi(y)$  from Fig. 3a or Table 1, and the  $S_a(\tilde{T}_1, \tilde{\xi}_1)$  from Fig. 13 corresponding to the  $\tilde{T}_1$  and  $\tilde{\xi}_1$  obtained in Steps 4 and 5 (Table 7). the resulting equivalent lateral forces  $f_1(y)$  are presented in Table 8 for each case.
10. The static stress analysis of the dam subjected to the equivalent lateral forces  $f_1(y)$ , from Step 9, applied to the upstream face of the dam is described in the next subsection, leading to response value  $r_1$  at a particular location in the dam.
11. For each of the four cases, Eq. 14 was evaluated at eleven equally spaced intervals along the height of the dam, including the top and bottom, by substituting numerical values for the quantities computed in the preceding steps; obtaining  $gp_o(y)$  from Fig. 11 or Table 6, which is presented in Table 8; using Eq. 15 to compute  $B_1 = 0.052[(0.0624)(381)^2/2g](0.95)^2 = (212.5 \text{ kip})/g$ , leading to  $B_1/M_1 = 212.5/500 = 0.425$ ; and substituting  $a_g = 0.18 g$ . The resulting equivalent lateral forces  $f_{sc}(y)$  are presented in Table 8 for each case.
12. The static stress analysis of the dam subjected to the equivalent lateral forces  $f_{sc}(y)$ , from Step 11, applied to the upstream face of the dam is described in the next subsection, leading to response value  $r_{sc}$  at a particular location in the dam.
13. Compute the maximum total value of any response quantity by combining  $r_1$  from step 10,  $r_{sc}$  from step 12, and  $r_{st}$ , the initial value prior to the earthquake, according to Eq. 18; this is described further in the next subsection.

### Computation of Stresses

The equivalent lateral earthquake forces  $f_1(y)$  and  $f_{sc}(y)$  representing the maximum effects of the fundamental and higher vibration modes, respectively, were computed in Steps 9 and 11. Dividing the dam into ten blocks of equal height, each of these sets of distributed forces is replaced

by statically equivalent concentrated forces at the centroids of the blocks. Considering the dam monolith to be a cantilever beam, the bending stresses at the upstream and downstream faces of the monolith are computed at the bottom of each block using elementary formulas for stresses in beams. The normal bending stresses at the monolith faces are then transformed to principal stresses (Ref. 13, page 42). In this simple stress analysis, the foundation rock is implicitly assumed to be rigid.

Because the upstream face of Pine Flat Dam is nearly vertical and the effects of tail water at the downstream face are negligible, as shown in Appendix C, the principal stresses  $\sigma_1$  and  $\sigma_{sc}$  at any location in the dam due to the forces  $f_1(y)$  and  $f_{sc}(y)$ , respectively, may be combined using the ABSUM or SRSS combination rules, Eqs. 16 and 17. The combined values  $\sigma_d$  based on both these rules, along with the fundamental mode values  $\sigma_1$  for the maximum principal stresses, are presented in Table 9 for the four analysis cases. These stresses occur at the upstream face when the earthquake forces act in the downstream direction, and at the downstream face when the earthquake forces act in the upstream direction. Obtained by using only the SRSS combination rule, the maximum principal stresses at both faces of the monolith are presented in Figs. 14 and 15.

#### **Comparison with Refined Analysis Procedure**

The dam monolith of Fig. 12 was analyzed by the computer program EAGD-84 (9) in which the response history of the dam, idealized as a finite element system, due to the Taft ground motion is computed considering rigorously the effects of dam-water-foundation rock interaction and of reservoir bottom absorption. The results from Ref. 6 at some intermediate steps of the analysis, in particular the resonant period and damping ratio of the fundamental resonant response, are presented in Table 7, and the envelope values of the earthquake-induced maximum principal stresses are presented in Table 9 and in Figs. 14 and 15.

It is apparent from Table 7 that the simplified procedure leads to excellent estimates of the resonant vibration period and the damping ratio for the fundamental mode. Because the response of concrete gravity dams is dominated by the fundamental mode, this comparison provides a confirmation that the simplified analysis procedure is able to represent the important effects of dam-

water interaction, reservoir bottom absorption, and dam-foundation rock interaction.

As shown in Table 9, the stresses obtained by the simplified procedure considering only the fundamental vibration mode response are about the same as those obtained by including higher mode responses in the SRSS combination rule. For the system parameters and excitation considered in this example, the higher mode responses add only 2 to 10 psi to the stresses, indicating that these can be neglected in this case and many other cases. However, in some cases, depending on the vibration periods and mode shapes of the dam and on the shape of the earthquake response spectrum, the higher mode responses may be more significant and should be included. The ABSUM combination rule is overly conservative in representing the higher mode responses and therefore not recommended or included in the subsequent observations.

Considering only the fundamental mode response or obtaining the SRSS combination of fundamental and higher mode responses, the simplified procedure provides estimates of the maximum stress on the upstream face that are sufficiently accurate -- in comparison with the "exact" results -- to be useful in the preliminary design phase. The accuracy of these stresses depends, in part, on how well the resonant vibration period and damping ratio for the fundamental mode are estimated in the simplified procedure; e.g., in case 4, the maximum stress at the upstream face is overestimated by the simplified procedure primarily because it underestimates the damping ratio by about 2% (Table 7). While the simplified procedure provides excellent estimates of the maximum stress on the upstream face, at the same time it overestimates by 25 to 50% the maximum stress on the downstream face. This large discrepancy is primarily due to the limitations of elementary beam theory in predicting stresses near sloped faces. Similarly, the beam theory is incapable of reproducing the stress concentration in the heel area of dams predicted by the refined analysis (Figs. 14 and 15), and the stresses in that area are therefore underestimated.

Figures 16 and 17 show the maximum principal stresses, including the static stresses. The simplified procedure gives conservative, but reasonable, maximum stresses, with the exception of the heel area of dams with full reservoir. The quality of the approximation is satisfactory for the preliminary phase in the design of new dams and in the safety evaluation of existing dams,

considering the complicated effects of dam-water-foundation rock interactions and reservoir bottom absorption, the number of approximations necessary to develop the simplified analysis procedure, and noting that the results generally err on the conservative side.

## CONCLUSIONS

A procedure was presented in 1978 for earthquake resistant design of new concrete gravity dams and for the seismic safety evaluation of existing dams (3). The procedure was based on two performance requirements: firstly, dams should remain essentially within the elastic range of behavior for the most intense ground shaking, expected to occur during the useful life of the structure; and secondly, some cracking, which is limited enough that it does not impair the ability of the dam to contain the impounded water and is economically repairable, may be permitted if the most intense ground shaking that the seismic environment is capable of producing were to occur.

A two-stage procedure was proposed for the analysis phase of elastic design and safety evaluation of dams: a simplified analysis procedure in which the response due only to the fundamental vibration mode is estimated directly from the earthquake design spectrum; and a refined response history analysis procedure for finite element idealizations of the dam monolith. The former was recommended for the preliminary phase of design and safety evaluation of dams and the latter for accurately computing the dynamic response and checking the adequacy of the preliminary evaluation (3).

At the time (1978) the dam design procedure was presented, both of these analysis procedures included the effects of dam-water interaction and compressibility of water, but assumed rigid, non-absorptive reservoir bottom materials and neglected the effects of dam-foundation rock interaction. Recently (1984), the refined response history analysis procedure and computer program have been extended to also include the absorptive effects of reservoir bottom materials and dam-foundation rock interaction effects (8, 9). In this paper, the simplified analysis procedure has been extended to include

these important effects so that they can now also be considered in the preliminary phase of design and safety evaluation of dams. Also included now in the simplified procedure is a "static correction" method to consider the response contributions of the higher vibration modes. Thus the design procedure proposed in 1978 (3), which is conceptually still valid, should utilize the new refined and simplified analysis procedures.

## REFERENCES

1. Anagnostopoulos, S.A., "Wave and Earthquake Response of Offshore Structures: Evaluation of Modal Solutions," *Journal of the Structural Division*, ASCE, Vol. 108, No. ST10, Oct., 1982, pp. 2175-2191.
2. Chopra, A.K., *Dynamics of Structures, A Primer*, Earthquake Engineering Research Institute, Berkeley, California, 1981.
3. Chopra, A.K., "Earthquake Resistant Design of Concrete Gravity Dams," *Journal of the Structural Division*, ASCE, Vol. 104, No. ST6, June, 1978, pp. 953-971.
4. Fenves, G., and Chopra, A.K., "Simplified Earthquake Analysis of Concrete Gravity Dams: Separate Hydrodynamic and Foundation Interaction Effects," *Journal of Engineering Mechanics*, ASCE, Vol. 111, No. 6, June, 1985, pp. 715-735.
5. Fenves, G., and Chopra, A.K., "Simplified Earthquake Analysis of Concrete Gravity Dams: Combined Hydrodynamic and Foundation Interaction Effects," *Journal of Engineering Mechanics*, ASCE, Vol. 111, No. 6, June 1985, pp. 736-756.
6. Fenves, G., and Chopra, A.K., "Effects of Reservoir Bottom Absorption and Dam-Water-Foundation Rock Interaction on Frequency Response Functions for Concrete Gravity Dams," *Earthquake Engineering and Structural Dynamics*, Vol. 13, No. 1, Jan.-Feb., 1985, pp. 13-31.
7. Fenves, G., and Chopra, A.K., "Reservoir Bottom Absorption Effects in Earthquake Response of Concrete Gravity Dams," *Journal of Structural Engineering*, ASCE, Vol. 111, No. 3, March, 1985, pp. 545-562.
8. Fenves, G., and Chopra, A.K., "Earthquake Analysis of Concrete Gravity Dams Including Reservoir Bottom Absorption and Dam-Water-Foundation Rock Interaction," *Earthquake Engineering and Structural Dynamics*, Vol. 12, No. 5, Sept.-Oct., 1984, pp. 663-680.
9. Fenves, G., and Chopra, A.K., "EAGD-84: A Computer Program for Earthquake Analysis of Concrete Gravity Dams," *Report No. UCB/EERC-84/11*, Earthquake Engineering Research Center, University of California, Berkeley, California, Aug., 1984.
10. Fenves, G., and Chopra, A.K., "Effects of Reservoir Bottom Absorption on Earthquake Response of Concrete Gravity Dams," *Earthquake Engineering and Structural Dynamics*, Vol. 11, No. 6, Nov.-Dec., 1983, pp. 809-829.
11. Rosenblueth, E., "Presión Hidrodinámica en Presas Debida a la Aceleración Vertical con Refracción en el Fonda," 2nd Congreso Nacional de Ingeniería Sísmica, Veracruz, Mexico, 1968.
12. Hansteen, O.E., and Bell, K., "On the Accuracy of Mode Superposition Analysis in Structural Dynamics," *Earthquake Engineering and Structural Dynamics*, Vol. 7, No. 5, Sept.-Oct., 1979, pp. 405-411.
13. U.S. Bureau of Reclamation, *Design of Gravity Dams*, U.S. Government Printing Office, Denver, Colorado, 1976.
14. Veletsos, A.S., "Dynamics of Structure-Foundation Systems," in *Structural and Geotechnical Mechanics*, ed. by W.J. Hall, Prentice-Hall, Clifton, New Jersey, 1977.

## NOTATION

The following symbols are used in this report:

$A_p$	=	<i>integral of <math>2gp(\hat{y})/wH</math> over depth of the impounded water for <math>H/H_s = 1</math> as listed in Table 5;</i>
$a_g$	=	maximum ground acceleration;
$B_1$	=	defined in Eq. 15;
$C$	=	velocity of pressure waves in water;
$E_f$	=	Young's modulus of elasticity of foundation rock;
$E_s$	=	Young's modulus of elasticity of dam concrete;
$F_{st}$	=	$\frac{1}{2}wH^2$ ;
$f_1(x,y)$	=	equivalent lateral forces acting on the dam due to fundamental vibration mode as defined in Eq. 1;
$f_1(y)$	=	$\int_0^b f_1(x,y)dx$ , as defined in Eq. 6;
$f_{sc}(y)$	=	equivalent lateral forces acting on dam due to higher vibration modes as defined in Eq. 14;
$g$	=	acceleration due to gravity;
$H$	=	depth of impounded water;
$H_s$	=	height of upstream face of dam;
$L_1$	=	integral defined in Eq. 7b;
$\tilde{L}_1$	=	defined in Eq. 12b;
$M_1$	=	integral defined in Eq. 7a;
$\tilde{M}_1$	=	defined in Eq. 12a;
$m_s(x,y)$	=	unit mass of concrete;
$p_o(y)$	=	hydrodynamic pressure on a rigid dam with water compressibility neglected;
$p(y, \tilde{T}_r)$	=	$Re[\bar{p}_1(y, \tilde{T}_r)]$ ;
$\bar{p}_1(y, \tilde{T}_r)$	=	complex-valued hydrodynamic pressure on the upstream face due to harmonic acceleration of dam, at period $\tilde{T}_r$ , in the fundamental vibration mode;
$R_f$	=	period lengthening ratio due to foundation-rock flexibility effects;

$R_r$	=	period lengthening ratio due to hydrodynamic effects;
$R_w$	=	$T_1^r / \tilde{T}_r$ ;
$r_1$	=	maximum response due to the fundamental vibration mode;
$r_d$	=	maximum dynamic response;
$r_{\max}$	=	maximum total response of dam;
$r_{sc}$	=	maximum response due to the higher vibration modes;
$r_{st}$	=	response due to initial static effects;
$S_a(\tilde{T}_1, \tilde{\xi}_1)$	=	ordinate of pseudo-acceleration response spectrum for the ground motion evaluated at period $\tilde{T}_1$ and damping ratio $\tilde{\xi}_1$ ;
$T_1$	=	fundamental vibration period of dam on rigid foundation rock with empty reservoir given by Eq. 10;
$\tilde{T}_1$	=	fundamental resonant period of dam on flexible foundation rock with impounded water given by Eq. 4c;
$T_1^r$	=	$4H/C$ , fundamental vibration period of impounded water;
$\tilde{T}_f$	=	fundamental resonant period of dam on flexible foundation rock with empty reservoir given by Eq. 4b;
$\tilde{T}_r$	=	fundamental resonant period of dam on rigid foundation rock with impounded water given by Eq. 4a;
$t$	=	time;
$W_s$	=	total weight of dam;
$w$	=	unit weight of water;
$w_s(x, y)$	=	unit weight of dam;
$w_s(y)$	=	weight of dam per unit height;
$x$	=	coordinate along the breadth of the dam;
$y$	=	coordinate along the height of the dam;
$\hat{y}$	=	$y/H$ ;
$\alpha$	=	wave reflection coefficient for reservoir bottom materials;
$\delta(x)$	=	Dirac delta function;
$\eta_f$	=	constant hysteretic damping factor for foundation rock;



- $\xi_1$  = damping ratio of dam on rigid foundation rock with empty reservoir;
- $\tilde{\xi}_1$  = damping ratio for dam on flexible foundation rock with impounded water;
- $\xi_f$  = added damping ratio due to foundation-rock flexibility effects;
- $\xi_r$  = added damping ratio due to hydrodynamic effects;
- $\phi(y)$  = fundamental vibration mode shape of dam at upstream face, i.e.  $\phi_1^x(O, y)$ ; and
- $\phi_1^k(x, y)$  = fundamental vibration mode of dam on rigid foundation rock with empty reservoir, where  $k = x, y$  denotes  $x$  and  $y$  components of modal displacements, respectively.



## TABLES

- Table 1 Standard Fundamental Mode Shape of Vibration for Concrete Gravity Dams
- Table 2(a) Standard Values for  $R_r$  and  $\xi_r$ , the Period Lengthening Ratio and Added Damping Ratio due to Hydrodynamic Effects for Modulus of Elasticity of Concrete,  $E_s = 5$  and 4.5 million psi
- Table 2(b) Standard Values for  $R_r$  and  $\xi_r$ , the Period Lengthening Ratio and Added Damping Ratio due to Hydrodynamic Effects for Modulus of Elasticity of Concrete,  $E_s = 4, 3.5,$  and 3 million psi
- Table 2(c) Standard Values for  $R_r$  and  $\xi_r$ , the Period Lengthening Ratio and Added Damping Ratio due to Hydrodynamic Effects for Modulus of Elasticity of Concrete,  $E_s = 2.5, 2$  and 1 million psi
- Table 3 Standard Values for  $R_f$  and  $\xi_f$ , the Period Lengthening Ratio and Added Damping Ratio due to Dam-Foundation Rock Interaction
- Table 4(a) Standard Values for the Hydrodynamic Pressure Function  $p(\hat{y})$  for Full Reservoir, i.e.,  $H/H_s = 1; \alpha = 1.00$
- Table 4(b) Standard Values for the Hydrodynamic Pressure Function  $p(\hat{y})$  for Full Reservoir, i.e.,  $H/H_s = 1; \alpha = 0.90$
- Table 4(c) Standard Values for the Hydrodynamic Pressure Function  $p(\hat{y})$  for Full Reservoir, i.e.,  $H/H_s = 1; \alpha = 0.75$
- Table 4(d) Standard Values for the Hydrodynamic Pressure Function  $p(\hat{y})$  for Full Reservoir, i.e.,  $H/H_s = 1; \alpha = 0.50$
- Table 4(e) Standard Values for the Hydrodynamic Pressure Function  $p(\hat{y})$  for Full Reservoir, i.e.,  $H/H_s = 1; \alpha = 0.25$
- Table 4(f) Standard Values for the Hydrodynamic Pressure Function  $p(\hat{y})$  for Full Reservoir, i.e.,  $H/H_s = 1; \alpha = 0.00$
- Table 5(a) Standard Values for  $A_p$ , the Hydrodynamic Force Coefficient in  $\tilde{L}_1; \alpha = 1$
- Table 5(b) Standard Values for  $A_p$ , the Hydrodynamic Force Coefficient in  $\tilde{L}_1; \alpha = 0.90, 0.75, 0.50, 0.25$  and 0.
- Table 6 Standard Values for the Hydrodynamic Pressure Function  $p_o(\hat{y})$
- Table 7 Pine Flat Dam Analysis Cases, Simplified Procedure Parameters, and Fundamental Mode Properties from Simplified and Refined Analysis Procedures
- Table 8 Equivalent Lateral Earthquake Forces on Pine Flat Dam due to S69E Component of Taft Ground Motion
- Table 9 Maximum Principal Stresses (in psi) in Pine Flat Dam due to S69E Component of Taft Ground Motion



Table 1 -- Standard Fundamental Mode Shape  
of Vibration for Concrete Gravity Dams

$y/H_s$	$\phi(y)$
1.0	1.000
.95	.866
.90	.735
.85	.619
.80	.530
.75	.455
.70	.389
.65	.334
.60	.284
.55	.240
.50	.200
.45	.165
.40	.135
.35	.108
.30	.084
.25	.065
.20	.047
.15	.034
.10	.021
.05	.010
0	0

Preceding page blank

Table 2(a) -- Standard Values for  $R_r$  and  $\xi_r$ , the Period Lengthening Ratio and Added Damping Ratio due to Hydrodynamic Effects for Modulus of Elasticity of Concrete,  $E_s = 5$  and 4.5 million psi

$H/H_s$	$\alpha$	$E_s = 5$ million psi		$E_s = 4.5$ million psi	
		$R_r$	$\xi_r$	$R_r$	$\xi_r$
1.0	1.0	1.454	0	1.409	0
	.90	1.462	.043	1.416	.030
	.75	1.456	.060	1.412	.051
	.50	1.355	.067	1.344	.060
	.25	1.284	.054	1.285	.050
	0	1.261	.038	1.259	.036
.95	1.0	1.368	0	1.323	0
	.90	1.376	.044	1.330	.031
	.75	1.366	.056	1.323	.049
	.50	1.255	.060	1.256	.053
	.25	1.208	.045	1.208	.042
	0	1.192	.032	1.191	.030
.90	1.0	1.289	0	1.247	0
	.90	1.297	.041	1.253	.029
	.75	1.284	.050	1.247	.042
	.50	1.181	.050	1.185	.044
	.25	1.151	.036	1.152	.033
	0	1.139	.025	1.139	.023
.85	1.0	1.215	0	1.179	0
	.90	1.224	.033	1.185	.023
	.75	1.206	.042	1.177	.034
	.50	1.129	.039	1.131	.033
	.25	1.111	.027	1.109	.025
	0	1.100	.019	1.099	.018
.80	1.0	1.148	0	1.121	0
	.90	1.156	.024	1.126	.015
	.75	1.140	.032	1.121	.024
	.50	1.092	.028	1.092	.024
	.25	1.078	.019	1.078	.018
	0	1.071	.014	1.071	.013
.75	1.0	1.092	0	1.078	0
	.90	1.099	.014	1.080	.008
	.75	1.089	.021	1.078	.014
	.50	1.065	.018	1.064	.015
	.25	1.055	.013	1.055	.012
	0	1.049	.009	1.050	.009

Table 2(a). - Continued

$H/H_s$	$\alpha$	$E_s = 5$ million psi		$E_s = 4.5$ million psi	
		$R_r$	$\xi_r$	$R_r$	$\xi_r$
.70	1.0	1.055	0	1.048	0
	.90	1.057	.006	1.050	.003
	.75	1.055	.011	1.050	.007
	.50	1.045	.011	1.044	.009
	.25	1.038	.009	1.037	.008
	0	1.034	.006	1.035	.006
.65	1.0	1.033	0	1.031	0
	.90	1.034	.002	1.031	.001
	.75	1.034	.005	1.031	.003
	.50	1.030	.006	1.029	.005
	.25	1.026	.005	1.027	.005
	0	1.024	.004	1.025	.004
.60	1.0	1.020	0	1.020	0
	.90	1.020	.001	1.020	.001
	.75	1.020	.002	1.020	.001
	.50	1.019	.003	1.018	.003
	.25	1.017	.003	1.018	.003
	0	1.016	.003	1.016	.002
.55	1.0	1.013	0	1.012	0
	.90	1.013	.000	1.012	.000
	.75	1.013	.001	1.012	.001
	.50	1.013	.002	1.012	.001
	.25	1.012	.002	1.012	.002
	0	1.011	.002	1.012	.001
.50	1.0	1.009	0	1.008	0
	.90	1.009	.000	1.008	.000
	.75	1.009	.000	1.008	.000
	.50	1.008	.001	1.008	.001
	.25	1.008	.001	1.008	.001
	0	1.008	.001	1.008	.001

Table 2(b) -- Standard Values for  $R_r$  and  $\xi_r$ , the Period Lengthening Ratio and Added Damping Ratio due to Hydrodynamic Effects for Modulus of Elasticity of Concrete,  $E_s = 4, 3.5,$  and  $3$  million psi

$H/H_s$	$\alpha$	$E_s = 4$ million psi		$E_s = 3.5$ million psi		$E_s = 3$ million psi.	
		$R_r$	$\xi_r$	$R_r$	$\xi_r$	$R_r$	$\xi_r$
1.0	1.0	1.370	0	1.341	0	1.320	0
	.90	1.374	.021	1.344	.013	1.319	.008
	.75	1.374	.040	1.341	.029	1.312	.021
	.50	1.333	.051	1.316	.042	1.289	.035
	.25	1.285	.045	1.282	.040	1.264	.036
	0	1.259	.034	1.256	.032	1.247	.030
.95	1.0	1.289	0	1.259	0	1.241	0
	.90	1.292	.020	1.263	.012	1.240	.007
	.75	1.289	.038	1.259	.027	1.233	.019
	.50	1.247	.045	1.238	.036	1.213	.030
	.25	1.208	.038	1.208	.033	1.194	.030
	0	1.191	.028	1.188	.026	1.181	.025
.90	1.0	1.214	0	1.191	0	1.176	0
	.90	1.220	.017	1.193	.010	1.176	.006
	.75	1.214	.033	1.193	.022	1.171	.015
	.50	1.179	.037	1.174	.029	1.155	.024
	.25	1.152	.030	1.152	.026	1.141	.024
	0	1.139	.022	1.136	.020	1.131	.019
.85	1.0	1.152	0	1.136	0	1.126	0
	.90	1.157	.013	1.139	.007	1.125	.004
	.75	1.155	.024	1.136	.016	1.122	.011
	.50	1.129	.028	1.124	.023	1.111	.017
	.25	1.109	.022	1.109	.020	1.101	.017
	0	1.099	.017	1.099	.016	1.093	.015
.80	1.0	1.104	0	1.095	0	1.087	0
	.90	1.106	.008	1.094	.004	1.087	.003
	.75	1.106	.016	1.090	.011	1.085	.007
	.50	1.089	.019	1.080	.016	1.079	.012
	.25	1.078	.016	1.071	.014	1.071	.012
	0	1.071	.012	1.066	.011	1.066	.011
.75	1.0	1.070	0	1.063	0	1.059	0
	.90	1.069	.004	1.063	.003	1.059	.002
	.75	1.065	.010	1.061	.006	1.058	.004
	.50	1.056	.013	1.055	.010	1.054	.007
	.25	1.050	.011	1.050	.010	1.050	.008
	0	1.046	.009	1.046	.008	1.046	.007



Table 2(b) -- Continued

$H/H_s$	$\alpha$	$E_s = 4$ million psi		$E_s = 3.5$ million psi		$E_s = 3$ million psi	
		$R_r$	$\xi_r$	$R_r$	$\xi_r$	$R_r$	$\xi_r$
.70	1.0	1.044	0	1.041	0	1.039	0
	.90	1.044	.002	1.041	.001	1.039	.001
	.75	1.042	.005	1.040	.003	1.038	.002
	.50	1.038	.007	1.037	.006	1.036	.004
	.25	1.034	.007	1.034	.006	1.034	.005
	0	1.031	.006	1.031	.005	1.031	.005
.65	1.0	1.028	0	1.026	0	1.025	0
	.90	1.028	.001	1.026	.001	1.025	.000
	.75	1.027	.002	1.026	.002	1.025	.001
	.50	1.025	.004	1.024	.003	1.024	.002
	.25	1.023	.004	1.022	.004	1.022	.003
	0	1.021	.004	1.021	.003	1.021	.003
.60	1.0	1.017	0	1.016	0	1.016	0
	.90	1.017	.000	1.016	.000	1.016	.000
	.75	1.017	.001	1.016	.001	1.016	.001
	.50	1.016	.002	1.015	.002	1.015	.001
	.25	1.015	.002	1.014	.002	1.014	.002
	0	1.013	.002	1.013	.002	1.013	.002
.55	1.0	1.010	0	1.010	0	1.010	0
	.90	1.010	.000	1.010	.000	1.010	.000
	.75	1.010	.001	1.010	.000	1.010	.000
	.50	1.010	.001	1.010	.001	1.009	.001
	.25	1.009	.001	1.009	.001	1.009	.001
	0	1.009	.001	1.009	.001	1.009	.001
.50	1.0	1.006	0	1.006	0	1.006	0
	.90	1.006	.000	1.006	.000	1.006	.000
	.75	1.006	.000	1.006	.000	1.006	.000
	.50	1.006	.001	1.006	.000	1.006	.000
	.25	1.005	.001	1.005	.001	1.005	.001
	0	1.005	.001	1.005	.001	1.005	.001

Table 2(c) -- Standard Values for  $R_r$  and  $\xi_r$ , the Period Lengthening Ratio and Added Damping Ratio due to Hydrodynamic Effects for Modulus of Elasticity of Concrete,  $E_s = 2.5, 2$  and 1 million psi

$H/H_s$	$\alpha$	$E_s = 2.5$ million psi		$E_s = 2$ million psi		$E_s = 1$ million psi	
		$R_r$	$\xi_r$	$R_r$	$\xi_r$	$R_r$	$\xi_r$
1.0	1.0	1.301	0	1.286	0	1.263	0
	.90	1.301	.005	1.285	.003	1.263	.001
	.75	1.287	.014	1.284	.009	1.262	.004
	.50	1.283	.025	1.275	.018	1.260	.008
	.25	1.264	.030	1.262	.024	1.256	.013
	0	1.247	.027	1.247	.024	1.247	.017
.95	1.0	1.224	0	1.212	0	1.193	0
	.90	1.224	.005	1.211	.003	1.193	.001
	.75	1.221	.012	1.210	.008	1.193	.003
	.50	1.209	.022	1.203	.015	1.191	.007
	.25	1.194	.025	1.192	.020	1.187	.011
	0	1.181	.022	1.181	.020	1.181	.014
.90	1.0	1.164	0	1.154	0	1.140	0
	.90	1.163	.004	1.154	.002	1.140	.001
	.75	1.161	.009	1.152	.006	1.140	.002
	.50	1.152	.017	1.148	.012	1.139	.005
	.25	1.141	.020	1.140	.016	1.136	.008
	0	1.131	.018	1.131	.016	1.131	.011
.85	1.0	1.117	0	1.110	0	1.100	0
	.90	1.116	.003	1.110	.002	1.100	.001
	.75	1.115	.007	1.109	.004	1.100	.002
	.50	1.109	.012	1.106	.009	1.100	.004
	.25	1.101	.014	1.100	.012	1.097	.006
	0	1.093	.013	1.093	.012	1.093	.008
.80	1.0	1.081	0	1.077	0	1.071	0
	.90	1.081	.002	1.077	.001	1.071	.000
	.75	1.080	.004	1.076	.003	1.071	.001
	.50	1.076	.008	1.074	.006	1.070	.003
	.25	1.071	.010	1.071	.008	1.069	.005
	0	1.066	.010	1.066	.008	1.066	.006
.75	1.0	1.055	0	1.053	0	1.049	0
	.90	1.055	.001	1.053	.001	1.049	.000
	.75	1.054	.003	1.052	.002	1.049	.001
	.50	1.053	.005	1.051	.004	1.048	.002
	.25	1.050	.007	1.049	.005	1.048	.003
	0	1.046	.007	1.046	.006	1.046	.004

Table 2(c) -- Continued

$H/H_s$	$\alpha$	$E_s = 2.5$ million psi		$E_s = 2$ million psi		$E_s = 1$ million psi	
		$R_r$	$\xi_r$	$R_r$	$\xi_r$	$R_r$	$\xi_r$
.70	1.0	1.037	0	1.035	0	1.033	0
	.90	1.037	.001	1.035	.000	1.033	.000
	.75	1.037	.002	1.035	.001	1.033	.000
	.50	1.035	.003	1.034	.002	1.033	.001
	.25	1.033	.004	1.033	.004	1.032	.002
	0	1.031	.004	1.031	.004	1.031	.003
.65	1.0	1.024	0	1.023	0	1.022	0
	.90	1.024	.000	1.023	.000	1.022	.000
	.75	1.024	.001	1.023	.001	1.022	.000
	.50	1.023	.002	1.023	.001	1.022	.001
	.25	1.022	.003	1.022	.002	1.021	.001
	0	1.021	.003	1.021	.003	1.021	.002
.60	1.0	1.016	0	1.016	0	1.014	0
	.90	1.016	.000	1.016	.000	1.014	.000
	.75	1.016	.001	1.016	.001	1.014	.000
	.50	1.015	.001	1.015	.001	1.014	.000
	.25	1.014	.002	1.014	.002	1.014	.001
	0	1.013	.002	1.013	.002	1.013	.001
.55	1.0	1.009	0	1.009	0	1.009	0
	.90	1.009	.000	1.009	.000	1.009	.000
	.75	1.009	.000	1.009	.000	1.009	.000
	.50	1.009	.001	1.009	.000	1.009	.000
	.25	1.009	.001	1.009	.001	1.009	.000
	0	1.009	.001	1.009	.001	1.009	.001
.50	1.0	1.006	0	1.006	0	1.005	0
	.90	1.006	.000	1.006	.000	1.005	.000
	.75	1.006	.000	1.006	.000	1.005	.000
	.50	1.006	.000	1.005	.000	1.005	.000
	.25	1.005	.000	1.005	.000	1.005	.000
	0	1.005	.001	1.005	.000	1.005	.000

Table 3 -- Standard Values for  $R_f$  and  $\xi_f$ , the Period Lengthening Ratio and Added Damping Ratio, due to Dam-Foundation Rock Interaction

$E_f/E_s$	$R_f$	Added Damping Ratio, $\xi_f$			
		$\eta_f=0.01$	$\eta_f=0.10$	$\eta_f=0.25$	$\eta_f=0.50$
5.0	1.043	.015	.014	.019	.024
4.5	1.048	.015	.016	.021	.026
4.0	1.054	.015	.018	.023	.030
3.5	1.062	.015	.020	.027	.034
3.0	1.071	.016	.024	.031	.039
2.5	1.083	.020	.028	.037	.046
2.0	1.099	.028	.035	.046	.057
1.5	1.129	.039	.047	.060	.073
1.4	1.139	.042	.050	.063	.078
1.3	1.150	.044	.053	.068	.084
1.2	1.162	.047	.058	.073	.090
1.1	1.174	.050	.062	.079	.096
1.0	1.187	.054	.068	.086	.105
0.9	1.204	.060	.075	.094	.115
0.8	1.223	.068	.083	.104	.127
0.7	1.248	.077	.093	.116	.142
0.6	1.286	.088	.105	.131	.161
0.5	1.335	.103	.121	.151	.186
0.4	1.400	.117	.143	.178	.221
0.3	1.496	.145	.173	.217	.273
0.2	1.678	.186	.220	.279	.362

Table 4(a) -- Standard Values for the Hydrodynamic Pressure Function  $p(\hat{y})$ ,  
for Full Reservoir, i.e.,  $H/H_s = 1$ ;  $\alpha = 1.00$

$\hat{y} = \frac{y}{H}$	Value of $\frac{g p(\hat{y})}{w H}$												
	$R_w \leq .5$	$R_w = .7$	$R_w = .8$	$R_w = .85$	$R_w = .90$	$R_w = .92$	$R_w = .93$	$R_w = .94$	$R_w = .95$	$R_w = .96$	$R_w = .97$	$R_w = .98$	$R_w = .99$
1.00	0	0	0	0	0	0	0	0	0	0	0	0	0
.95	.070	.073	.076	.079	.083	.086	.088	.090	.092	.096	.102	.111	.133
.90	.112	.118	.124	.129	.138	.143	.147	.151	.157	.164	.176	.195	.238
.85	.127	.135	.144	.152	.164	.172	.178	.184	.193	.204	.221	.249	.313
.80	.133	.144	.155	.165	.182	.193	.200	.208	.220	.235	.257	.295	.379
.75	.141	.154	.168	.180	.201	.214	.223	.234	.248	.267	.294	.340	.445
.70	.145	.161	.178	.192	.216	.232	.242	.255	.272	.294	.327	.382	.506
.65	.143	.161	.180	.197	.224	.242	.254	.269	.288	.313	.351	.414	.558
.60	.139	.159	.180	.199	.230	.250	.264	.280	.301	.330	.373	.444	.605
.55	.137	.159	.183	.203	.237	.260	.274	.293	.316	.348	.395	.473	.651
.50	.135	.159	.184	.206	.244	.269	.284	.304	.329	.364	.415	.500	.694
.45	.130	.155	.182	.206	.246	.272	.289	.310	.338	.375	.430	.522	.730
.40	.124	.151	.179	.204	.247	.275	.293	.315	.345	.384	.442	.540	.762
.35	.121	.149	.179	.205	.250	.279	.298	.322	.353	.395	.456	.559	.793
.30	.118	.147	.178	.206	.252	.283	.303	.328	.360	.403	.467	.575	.820
.25	.113	.143	.175	.204	.252	.284	.304	.330	.363	.408	.475	.587	.840
.20	.109	.139	.172	.202	.252	.284	.305	.332	.366	.412	.481	.596	.856
.15	.107	.138	.172	.202	.252	.286	.307	.334	.369	.417	.487	.604	.871
.10	.106	.137	.172	.202	.253	.287	.309	.337	.372	.420	.491	.611	.881
.05	.103	.135	.169	.200	.252	.286	.308	.336	.372	.420	.492	.613	.886
0	.010	.133	.168	.198	.251	.285	.307	.335	.371	.420	.492	.613	.886

Table 4(b) -- Standard Values for the Hydrodynamic Pressure Function  $p(\hat{y})$ ,  
for Full Reservoir, i.e.,  $H/H_s = 1$ ;  $\alpha = 0.90$

$\hat{y} = \frac{y}{H}$	Value of $\frac{g p(\hat{y})}{w H}$									
	$R_w \leq 0.5$	$R_w = .7$	$R_w = .8$	$R_w = .9$	$R_w = .95$	$R_w = 1.0$	$R_w = 1.05$	$R_w = 1.1$	$R_w = 1.2$	
1.00	0	0	0	0	0	0	0	0	0	
.95	.070	.073	.076	.082	.088	.089	.069	.064	.062	
.90	.112	.118	.124	.136	.149	.149	.110	.100	.095	
.85	.127	.135	.144	.162	.181	.181	.123	.108	.101	
.80	.133	.144	.155	.179	.204	.205	.127	.107	.098	
.75	.141	.154	.168	.197	.228	.229	.133	.108	.097	
.70	.145	.161	.177	.212	.249	.249	.135	.105	.092	
.65	.143	.161	.179	.219	.261	.262	.130	.096	.081	
.60	.139	.159	.179	.234	.271	.272	.124	.085	.067	
.55	.137	.159	.182	.231	.283	.283	.119	.076	.057	
.50	.135	.159	.183	.236	.293	.292	.114	.067	.046	
.45	.130	.155	.181	.238	.299	.298	.106	.055	.032	
.40	.124	.150	.178	.238	.303	.301	.097	.044	.019	
.35	.121	.148	.177	.241	.309	.307	.091	.035	.009	
.30	.118	.146	.177	.243	.313	.311	.086	.027	.000	
.25	.113	.142	.174	.242	.315	.312	.078	.017	.000	
.20	.109	.139	.171	.241	.316	.312	.071	.008	.000	
.15	.107	.137	.170	.242	.318	.313	.067	.003	.000	
.10	.106	.136	.170	.242	.320	.313	.064	.000	.000	
.05	.103	.134	.167	.241	.318	.311	.059	.000	.000	
0	.101	.133	.166	.239	.317	.309	.056	.000	.000	

Table 4(c) -- Standard Values for the Hydrodynamic Pressure Function  $p(\hat{y})$ ,  
for Full Reservoir, i.e.,  $H/H_s = 1$ ;  $\alpha = 0.75$

$\hat{y} = \frac{y}{H}$	Value of $\frac{g p(\hat{y})}{w H}$									
	$R_w \leq 0.5$	$R_w = .7$	$R_w = .8$	$R_w = .9$	$R_w = .95$	$R_w = 1.0$	$R_w = 1.05$	$R_w = 1.1$	$R_w = 1.2$	
1.00	0	0	0	0	0	0	0	0	0	
.95	.070	.073	.075	.079	.080	.078	.073	.068	.065	
.90	.112	.118	.122	.129	.132	.128	.118	.101	.101	
.85	.127	.133	.140	.151	.154	.150	.134	.121	.110	
.80	.133	.143	.152	.166	.171	.163	.142	.125	.110	
.75	.140	.153	.164	.181	.187	.177	.151	.130	.110	
.70	.145	.159	.173	.193	.200	.188	.157	.131	.108	
.65	.143	.159	.174	.197	.205	.191	.155	.126	.099	
.60	.139	.157	.174	.199	.208	.192	.151	.118	.088	
.55	.137	.157	.175	.203	.213	.195	.150	.113	.079	
.50	.135	.156	.176	.206	.216	.196	.147	.107	.070	
.45	.129	.152	.173	.205	.216	.194	.140	.097	.058	
.40	.123	.147	.170	.203	.214	.191	.134	.088	.045	
.35	.120	.145	.169	.204	.215	.190	.129	.080	.036	
.30	.117	.143	.168	.204	.215	.188	.125	.074	.027	
.25	.112	.139	.164	.201	.212	.184	.118	.065	.016	
.20	.108	.135	.161	.199	.209	.180	.111	.056	.007	
.15	.106	.134	.159	.198	.208	.177	.107	.051	.001	
.10	.104	.133	.158	.197	.207	.175	.103	.046	.000	
.05	.102	.130	.156	.194	.204	.171	.098	.040	.000	
0	.100	.128	.154	.192	.201	.167	.093	.036	.000	

Table 4(d) -- Standard Values for the Hydrodynamic Pressure Function  $p(\hat{y})$ ,  
for Full Reservoir, i.e.,  $H/H_s = 1$ ;  $\alpha = 0.50$

$\hat{y} = \frac{y}{H}$	Value of $\frac{g p(\hat{y})}{w H}$									
	$R_w \leq 0.5$	$R_w = .7$	$R_w = .8$	$R_w = .9$	$R_w = .95$	$R_w = 1.0$	$R_w = 1.05$	$R_w = 1.1$	$R_w = 1.2$	
1.00	0	0	0	0	0	0	0	0	0	
.95	.071	.072	.073	.074	.074	.073	.072	.070	.068	
.90	.112	.116	.118	.119	.119	.118	.116	.113	.108	
.85	.125	.132	.135	.136	.135	.134	.130	.127	.120	
.80	.132	.139	.143	.146	.145	.143	.138	.133	.123	
.75	.139	.148	.153	.156	.155	.152	.146	.139	.127	
.70	.144	.154	.160	.163	.162	.158	.151	.143	.128	
.65	.141	.152	.159	.163	.161	.156	.148	.138	.122	
.60	.137	.149	.157	.162	.160	.153	.143	.132	.113	
.55	.135	.148	.156	.161	.158	.151	.141	.128	.107	
.50	.133	.147	.155	.159	.156	.148	.137	.123	.099	
.45	.127	.142	.150	.154	.151	.142	.129	.115	.088	
.40	.121	.136	.145	.149	.145	.136	.122	.106	.077	
.35	.117	.133	.143	.146	.142	.131	.116	.099	.069	
.30	.114	.131	.140	.143	.137	.126	.110	.092	.060	
.25	.109	.126	.135	.137	.131	.119	.102	.083	.050	
.20	.104	.121	.130	.132	.125	.112	.094	.074	.040	
.15	.102	.119	.127	.128	.121	.108	.089	.068	.033	
.10	.100	.117	.125	.125	.118	.104	.083	.062	.026	
.05	.098	.114	.121	.121	.113	.098	.077	.055	.018	
0	.096	.111	.119	.117	.108	.093	.072	.049	.012	



Table 4(e) -- Standard Values for the Hydrodynamic Pressure Function  $p(\hat{y})$ ,  
for Full Reservoir, i.e.,  $H/H_s = 1$ ;  $\alpha = 0.25$

$\hat{y} = \frac{y}{H}$	of $\frac{g p(\hat{y})}{w H}$									
	$R_w \leq 0.5$	$R_w = .7$	$R_w = .8$	$R_w = .9$	$R_w = .95$	$R_w = 1.0$	$R_w = 1.05$	$R_w = 1.1$	$R_w = 1.2$	
1.00	0	0	0	0	0	0	0	0	0	
.95	.069	.070	.071	.071	.071	.071	.070	.070	.070	
.90	.111	.113	.114	.114	.114	.114	.113	.113	.111	
.85	.124	.127	.128	.129	.129	.128	.127	.127	.125	
.80	.130	.133	.134	.135	.135	.134	.133	.132	.129	
.75	.137	.141	.142	.143	.142	.141	.140	.138	.135	
.70	.141	.145	.147	.147	.146	.145	.143	.141	.137	
.65	.137	.142	.144	.144	.143	.142	.140	.137	.131	
.60	.133	.138	.140	.139	.138	.136	.134	.131	.124	
.55	.131	.136	.137	.136	.135	.133	.130	.126	.118	
.50	.128	.133	.134	.133	.131	.128	.125	.121	.112	
.45	.121	.126	.127	.126	.124	.120	.116	.112	.101	
.40	.115	.120	.120	.118	.115	.112	.107	.102	.091	
.35	.111	.116	.116	.113	.110	.106	.100	.095	.082	
.30	.107	.111	.111	.107	.104	.099	.093	.087	.074	
.25	.101	.105	.104	.100	.096	.091	.084	.077	.063	
.20	.096	.099	.098	.093	.088	.082	.076	.068	.052	
.15	.094	.096	.094	.088	.083	.076	.069	.061	.044	
.10	.092	.096	.090	.083	.078	.071	.063	.054	.037	
.05	.088	.088	.085	.077	.071	.064	.055	.046	.028	
0	.086	.085	.081	.072	.065	.057	.048	.039	.020	

Table 4(f) -- Standard Values for the Hydrodynamic Pressure Function  $p(\hat{y})$ ,  
for Full Reservoir, i.e.,  $H/H_s = 1; \alpha = 0.00$

$\hat{y} = \frac{y}{H}$	Value of $\frac{g p(\hat{y})}{w H}$									
	$R_w \leq 0.5$	$R_w = .7$	$R_w = .8$	$R_w = .9$	$R_w = .95$	$R_w = 1.0$	$R_w = 1.05$	$R_w = 1.1$	$R_w = 1.2$	
1.00	0	0	0	0	0	0	0	0	0	
.95	.069	.069	.069	.069	.069	.069	.070	.070	.070	
.90	.109	.110	.110	.111	.111	.111	.112	.112	.112	
.85	.122	.123	.124	.125	.125	.125	.126	.126	.126	
.80	.127	.128	.128	.129	.129	.129	.130	.130	.130	
.75	.133	.134	.134	.135	.135	.135	.136	.136	.136	
.70	.135	.136	.137	.138	.138	.138	.139	.139	.139	
.65	.132	.133	.133	.133	.133	.133	.134	.134	.134	
.60	.127	.127	.127	.127	.127	.127	.127	.127	.127	
.55	.123	.123	.123	.123	.123	.123	.122	.122	.121	
.50	.120	.119	.118	.118	.118	.117	.116	.116	.115	
.45	.113	.111	.110	.109	.109	.108	.107	.106	.105	
.40	.105	.103	.102	.100	.099	.098	.097	.096	.094	
.35	.101	.098	.096	.094	.092	.091	.090	.088	.085	
.30	.096	.092	.090	.087	.085	.084	.082	.080	.076	
.25	.090	.085	.082	.078	.076	.074	.072	.069	.065	
.20	.084	.078	.074	.070	.067	.065	.062	.059	.053	
.15	.080	.073	.068	.064	.061	.058	.055	.051	.045	
.10	.077	.069	.064	.058	.054	.051	.048	.044	.036	
.05	.073	.063	.057	.050	.046	.043	.039	.035	.026	
0	.070	.058	.052	.044	.040	.036	.031	.027	.017	

Table 5(a) -- Standard Values for  $A_p$ , the Hydrodynamic Force Coefficient  
in  $\tilde{L}_1$ ;  $\alpha = 1$

$R_w$	Value of $A_p$ for $\alpha=1$
0.99	1.242
0.98	.893
0.97	.739
0.96	.647
0.95	.585
0.94	.539
0.93	.503
0.92	.474
0.90	.431
0.85	.364
0.80	.324
0.70	.279
$\leq 0.50$	.237

Table 5(b) -- Standard Values for  $A_p$ , the Hydrodynamic Force Coefficient  
in  $\tilde{L}_1$ ;  $\alpha = 0.90, 0.75, 0.50, 0.25$  and  $0$

$R_w$	Value of $A_p$				
	$\alpha=0.90$	$\alpha=0.75$	$\alpha=0.5$	$\alpha=0.25$	$\alpha=0$
1.20	.071	.111	.159	.178	.181
1.10	.110	.177	.204	.197	.186
1.05	.194	.249	.229	.205	.189
1.00	.515	.340	.252	.213	.191
0.95	.518	.378	.267	.219	.193
0.90	.417	.361	.274	.224	.195
0.80	.322	.309	.269	.229	.198
0.70	.278	.274	.256	.228	.201
$\leq 0.50$	.237	.236	.231	.222	.206

Table 6 -- Standard Values  
for the Hydrodynamic Pressure Function  $p_0(\hat{y})$

$\hat{y}=y/H$	$\frac{g p_0}{wH}$
1.0	0
.95	.137
.90	.224
.85	.301
.80	.362
.75	.418
.70	.465
.65	.509
.60	.546
.55	.580
.50	.610
.45	.637
.40	.659
.35	.680
.30	.696
.25	.711
.20	.722
.15	.731
.10	.737
.05	.741
0	.742

Table 7 - Pine Flat Dam Analysis Cases,  
Simplified Procedure Parameters, and Fundamental Mode Properties  
from Simplified and Refined Analysis Procedures

Case	Foundation Rock	Water	Parameters from Simplified Procedure				Fundamental Mode Properties				
			$R_r$	$R_f$	$\xi_r$	$\xi_f$	Vibration Period, in seconds, $\bar{T}_1$		Damping Ratio $\xi_1$		$S_a(\bar{T}_1, \xi_1)$ in $g's^\dagger$
							Simplified Procedure	Refined Procedure*	Simplified Procedure	Refined Procedure*	
1	rigid	empty	1.0	1.0	0	0	0.311	0.317	.050	.050	0.429
2	rigid	full	1.213	1.0	0.030	0	0.377	0.386	.071	.076	0.312
3	flexible	empty	1.0	1.187	0	0.068	0.369	0.386	.098	.126	0.281
4	flexible	full	1.213	1.187	0.030	0.068	0.448	0.482	.123	.144	0.327

\* From Ref. 7.

†  $S_a$  value corresponding to  $\bar{T}_1$  and  $\xi_1$  from simplified procedure.

Table 8 - Equivalent Lateral Earthquake Forces on Pine Flat Dam  
due to S69E Component of Taft Ground Motion

$y$ (ft)	$w_s$ (k/ft)	$\phi$	$w_s \phi$ (k/ft)	$gd$ (k/ft)	$gp_o$ (k/ft)	Lateral Forces, in kips per foot							
						Case 1		Case 2		Case 3		Case 4	
						$f_1$	$f_{sc}$	$f_1$	$f_{sc}$	$f_1$	$f_{sc}$	$f_1$	$f_{sc}$
400	4.96	1.00	4.96	0	0	5.92	-1.60	5.27	-1.98	3.87	-1.60	5.52	-1.98
360	5.18	0.73	3.80	1.68	3.67	4.53	-0.97	5.83	-0.59	2.97	-0.97	6.11	-0.59
320	8.19	0.53	4.35	2.96	7.45	5.19	-0.70	7.78	0.31	3.40	-0.70	8.15	0.31
280	12.7	0.39	4.95	3.39	10.3	5.91	-0.19	8.87	1.29	3.87	-0.19	9.30	1.29
240	17.8	0.28	4.98	3.50	12.5	5.94	0.71	9.02	2.58	3.89	0.71	9.46	2.58
200	23.0	0.20	4.60	3.43	14.1	5.49	1.84	8.54	4.03	3.60	1.84	8.95	4.03
160	28.1	0.13	3.65	3.24	15.5	4.35	3.23	7.34	5.74	2.85	3.23	7.69	5.74
120	33.3	0.084	2.80	3.09	16.4	3.34	4.59	6.27	7.33	2.19	4.59	6.57	7.33
80	38.4	0.047	1.80	2.85	17.1	2.15	6.01	4.95	8.96	1.41	6.01	5.19	8.96
40	43.6	0.021	0.92	2.68	17.5	1.10	7.39	3.83	10.5	0.72	7.39	4.01	10.5
0	48.7	0	0	2.51	17.6	0	8.77	2.67	11.9	0	8.77	2.80	11.9

Table 9 - Maximum Principal Stresses\* (in psi) in Pine Flat Dam  
due to S69E Component of Taft Ground Motion

Case	Foundation Rock	Water	Upstream Face				Downstream Face			
			Fundamental Mode only	ABSUM	SRSS	Exact†	Fundamental Mode only	ABSUM	SRSS	Exact†
1	rigid	empty	241	296	247	223	333	398	338	272
2	rigid	full	263	309	266	261	411	440	413	277
3	flexible	empty	157	213	167	172	218	284	226	181
4	flexible	full	276	322	278	218	431	460	433	229

\*Initial static stresses are excluded.

† From Refined Procedure, Ref. 7.





## FIGURES

- Fig. 1. Dam-Water-Foundation Rock System
- Fig. 2. Distribution of Real (Re) and Imaginary (Im) Valued Components of Equivalent Lateral Earthquake Forces on Upstream Face of a Typical Dam
- Fig. 3. Fundamental Period and Mode Shape of Vibration for Concrete Gravity Dams.  
(a) Standard Period and Mode Shape. (b) Comparison of Standard Values with Properties of Six Dams.
- Fig. 4(a). Standard Values for  $R_r$ , the Period Lengthening Ratio due to Hydrodynamic Effects;  
 $E_s = 5$  million psi.
- Fig. 4(b). Standard Values for  $R_r$ , the Period Lengthening Ratio due to Hydrodynamic Effects;  
 $E_s = 4.5$  million psi.
- Fig. 4(c). Standard Values for  $R_r$ , the Period Lengthening Ratio due to Hydrodynamic Effects;  
 $E_s = 4.0$  million psi.
- Fig. 4(d). Standard Values for  $R_r$ , the Period Lengthening Ratio due to Hydrodynamic Effects;  
 $E_s = 3.5$  million psi.
- Fig. 4(e). Standard Values for  $R_r$ , the Period Lengthening Ratio due to Hydrodynamic Effects;  
 $E_s = 3.0$  million psi.
- Fig. 4(f). Standard Values for  $R_r$ , the Period Lengthening Ratio due to Hydrodynamic Effects;  
 $E_s = 2.5$  million psi.
- Fig. 4(g). Standard Values for  $R_r$ , the Period Lengthening Ratio due to Hydrodynamic Effects;  
 $E_s = 2.0$  million psi.
- Fig. 4(h). Standard Values for  $R_r$ , the Period Lengthening Ratio due to Hydrodynamic Effects;  
 $E_s = 1.0$  million psi.
- Fig. 5(a). Standard Values for  $\xi_r$ , the Added Damping Ratio due to Hydrodynamic Effects;  
 $E_s = 5$  million psi
- Fig. 5(b). Standard Values for  $\xi_r$ , the Added Damping Ratio due to Hydrodynamic Effects;  
 $E_s = 4.5$  million psi
- Fig. 5(c). Standard Values for  $\xi_r$ , the Added Damping Ratio due to Hydrodynamic Effects;  
 $E_s = 4.0$  million psi.
- Fig. 5(d). Standard Values for  $\xi_r$ , the Added Damping Ratio due to Hydrodynamic Effects;  
 $E_s = 3.5$  million psi.
- Fig. 5(e). Standard Values for  $\xi_r$ , the Added Damping Ratio due to Hydrodynamic Effects;  
 $E_s = 3.0$  million psi.
- Fig. 5(f). Standard Values for  $\xi_r$ , the Added Damping Ratio due to Hydrodynamic Effects;  
 $E_s = 2.5$  million psi.
- Fig. 5(g). Standard Values for  $\xi_r$ , the Added Damping Ratio due to Hydrodynamic Effects;  
 $E_s = 2.0$  million psi

- Fig. 5(h). Standard Values for  $\xi_r$ , the Added Damping Ratio due to Hydrodynamic Effects;  
 $E_s = 1.0$  million psi.
- Fig. 6. Standard Values for  $R_f$ , the Period Lengthening Ratio due to Dam-Foundation Rock Interaction
- Fig. 7. Standard Values for  $\xi_f$ , the Added Damping Ratio due to Dam-Foundation Rock Interaction
- Fig. 8(a). Standard Values for the Hydrodynamic Pressure Function  $p(\hat{y})$  for Full Reservoir, i.e.  
 $H/H_s = 1, \alpha = 1.00$ .
- Fig. 8(b). Standard Values for the Hydrodynamic Pressure Function  $p(\hat{y})$  for Full Reservoir, i.e.  
 $H/H_s = 1; \alpha = 0.90$
- Fig. 8(c). Standard Values for the Hydrodynamic Pressure Function  $p(\hat{y})$  for Full Reservoir, i.e.  
 $H/H_s = 1; \alpha = 0.75$  and  $0.50$ .
- Fig. 8(d). Standard Values for the Hydrodynamic Pressure Function  $p(\hat{y})$  for Full Reservoir, i.e.  
 $H/H_s = 1; \alpha = 0.25$  and  $0.00$ .
- Fig. 9. Heightwise Distribution of Maximum Shear Force in Dams with Empty Reservoir due to S69E Component of Taft Ground Motion
- Fig. 10. Heightwise Distribution of Maximum Bending Moment in Dams with Empty Reservoir due to S69E Component of Taft Ground Motion
- Fig. 11. Standard Values for the Hydrodynamic Pressure Function  $p_o(\hat{y})$
- Fig. 12. Tallest, Nonoverflow Monolith of Pine Flat Dam
- Fig. 13. Response Spectrum for the S69E Component of Taft Ground Motion; damping ratios = 0, 2, 5, 10 and 20 percent.
- Fig. 14. Maximum Principal Stresses (in psi) in Pine Flat Dam on Rigid Foundation Rock due to S69E Component of Taft Ground Motion; Cases 1 and 2. Initial Static Stresses are Excluded.
- Fig. 15. Maximum Principal Stresses (in psi) in Pine Flat Dam on Flexible Foundation Rock due to S69E Component of Taft Ground Motion; Cases 3 and 4. Initial Static Stresses are Excluded.
- Fig. 16. Maximum Principal Stresses (in psi) in Pine Flat Dam on Rigid Foundation Rock due to S69E Component of Taft Ground Motion; Cases 1 and 2. Initial Static Stresses are Included.
- Fig. 17. Maximum Principal Stresses (in psi) in Pine Flat Dam on Flexible Foundation Rock due to S69E Component of Taft Ground Motion; Cases 3 and 4. Initial Static Stresses are Included.

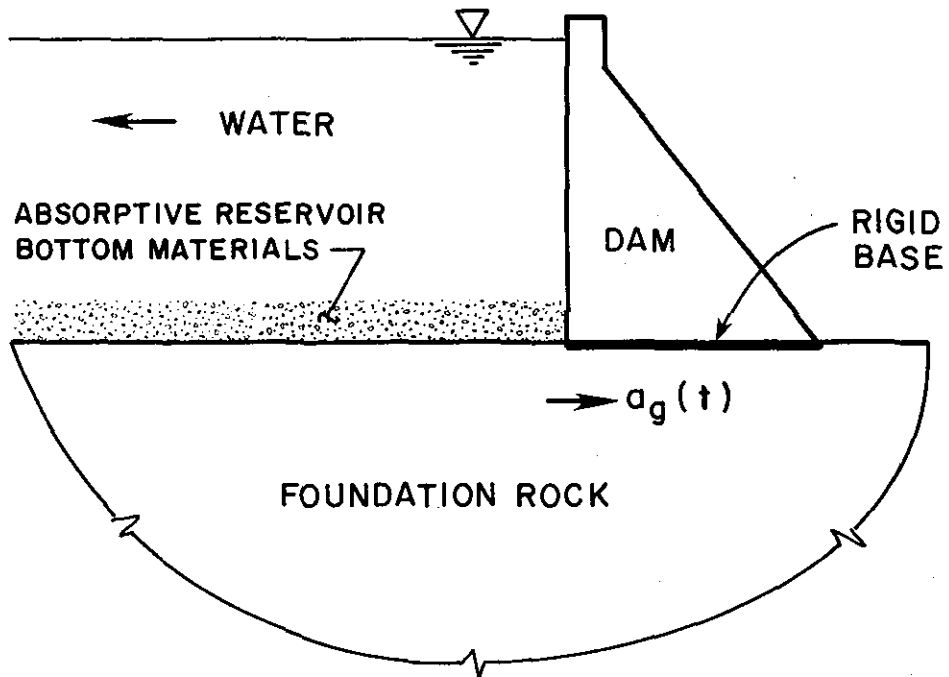


Figure 1. Dam-Water-Foundation Rock System

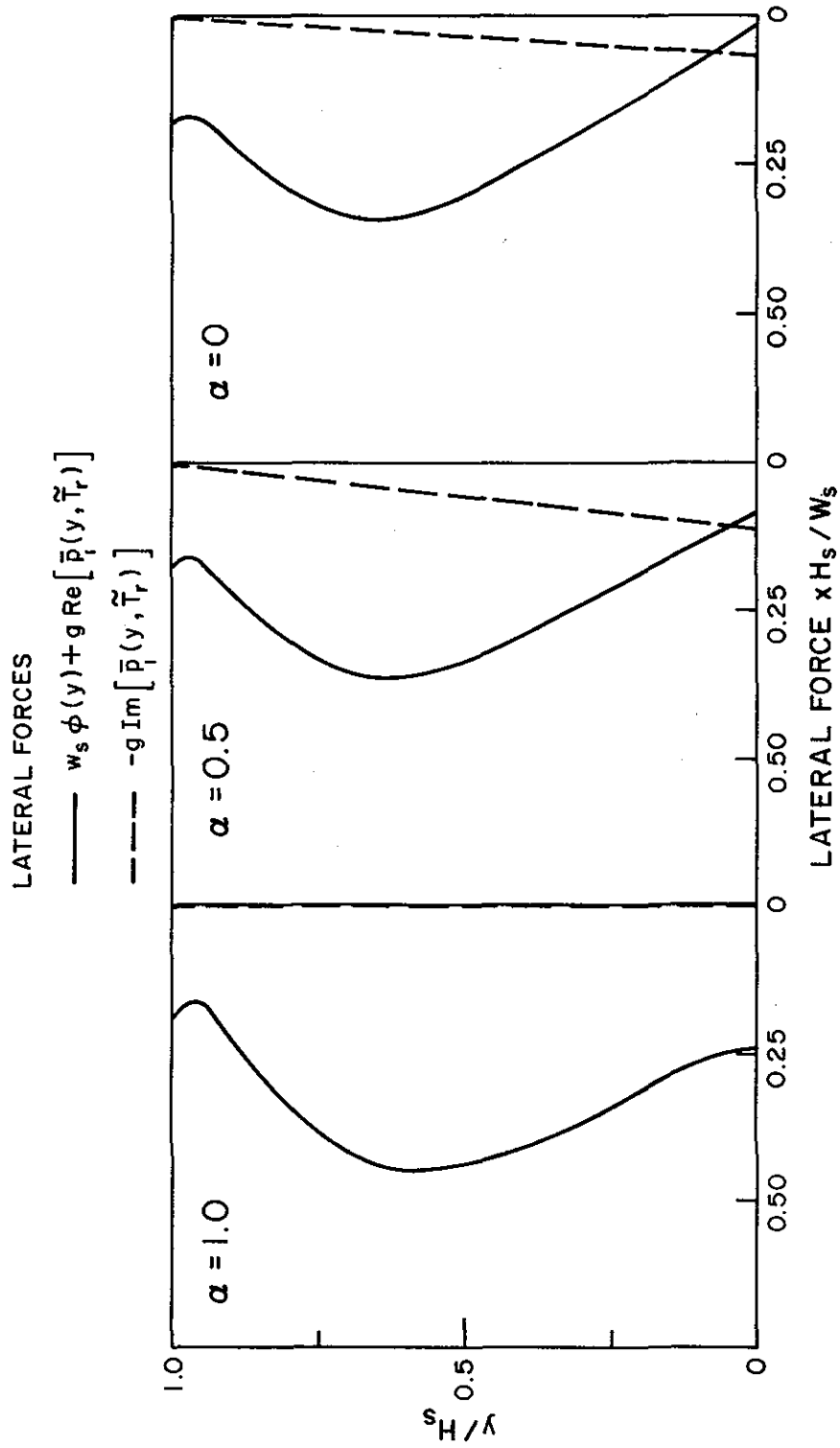


Figure 2. Distribution of Real (Re) and Imaginary (Im) Valued Components of Equivalent Lateral Earthquake Forces on Upstream Face of a Typical Dam

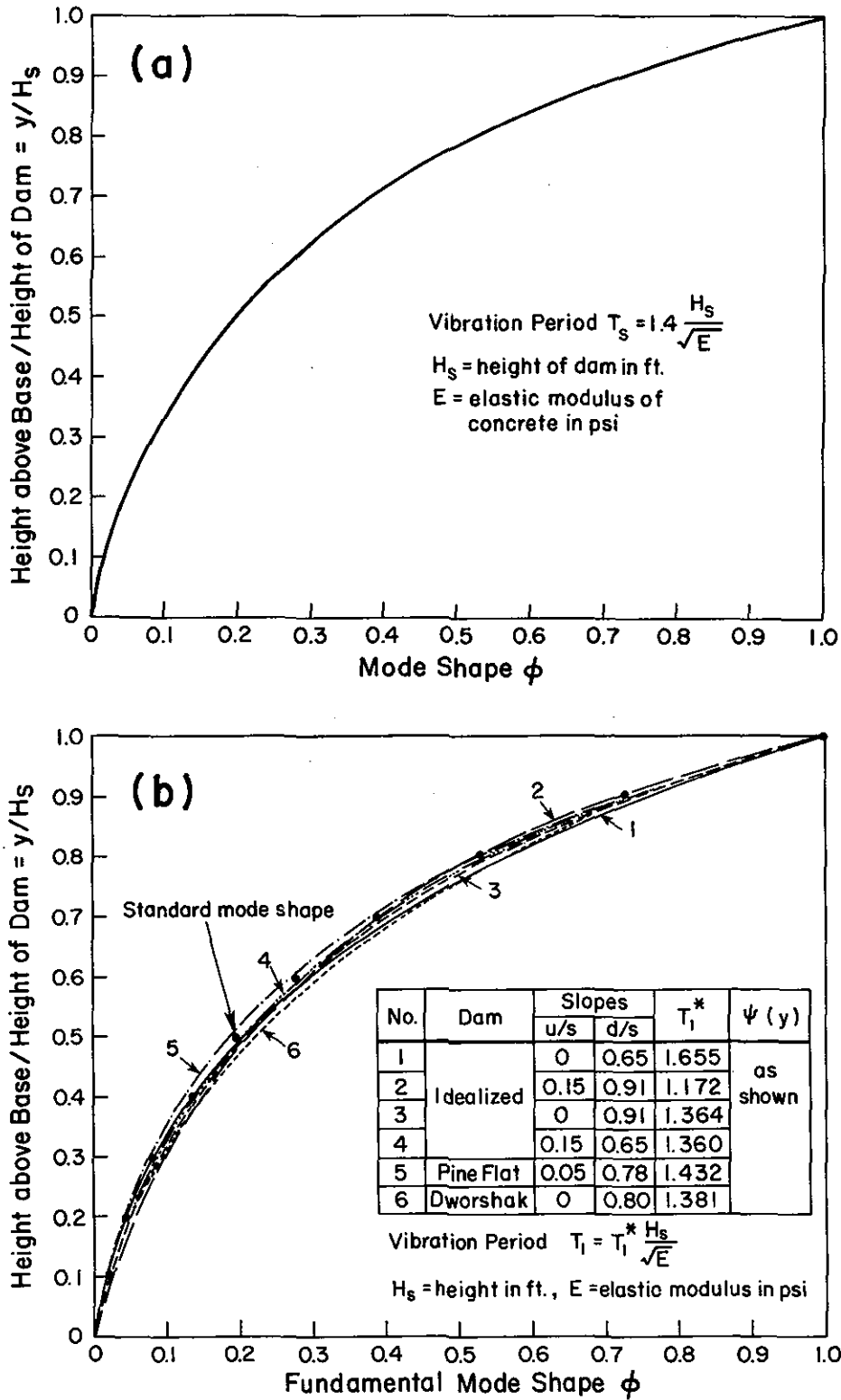


Figure 3. Fundamental Period and Mode Shape of Vibration for Concrete Gravity Dams. (a) Standard Period and Mode Shape. (b) Comparison of Standard Values with Properties of Six Dams.

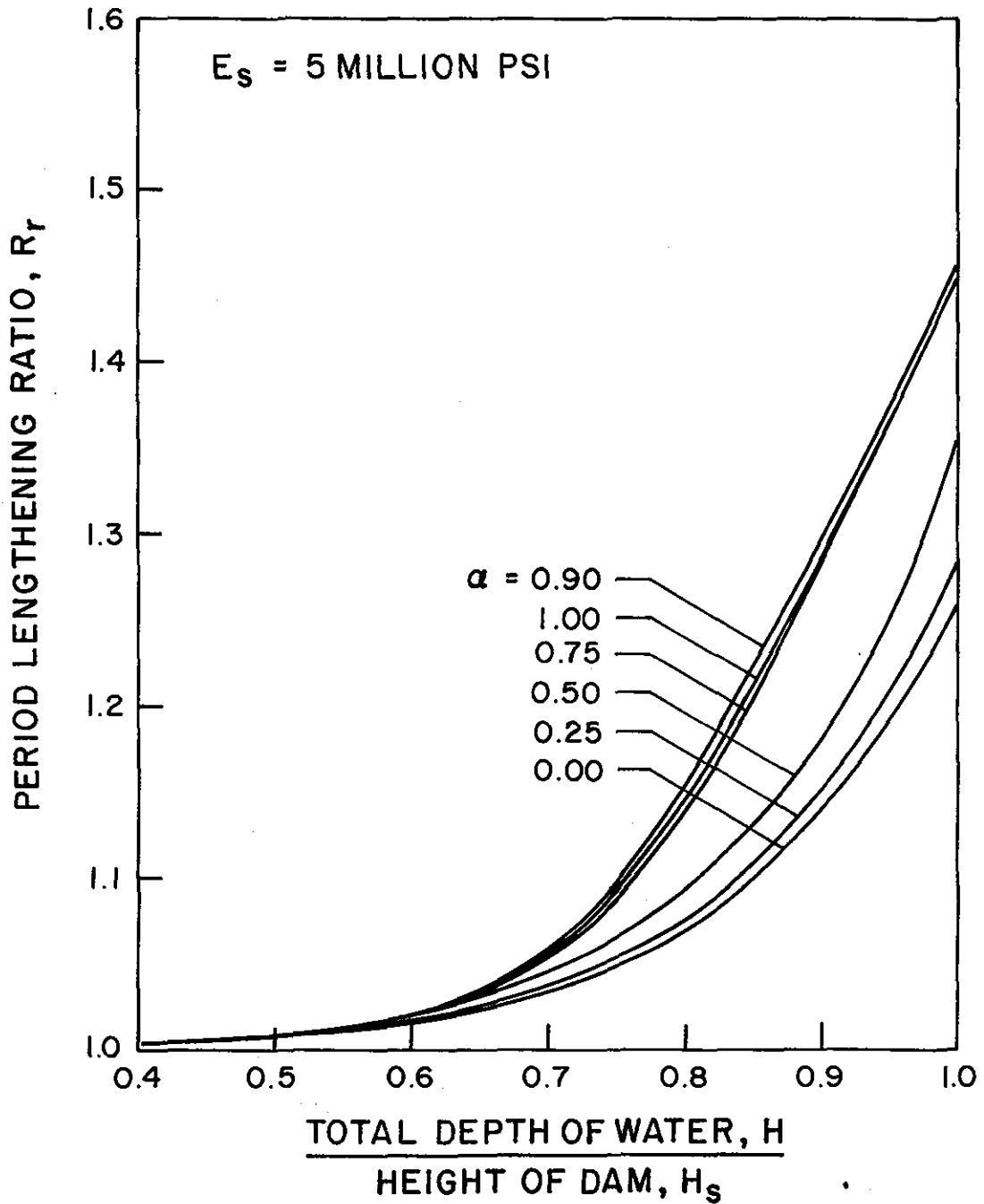


Figure 4(a). Standard Values for  $R_r$ , the Period Lengthening Ratio due to Hydrodynamic Effects;  $E_s = 5$  million psi.

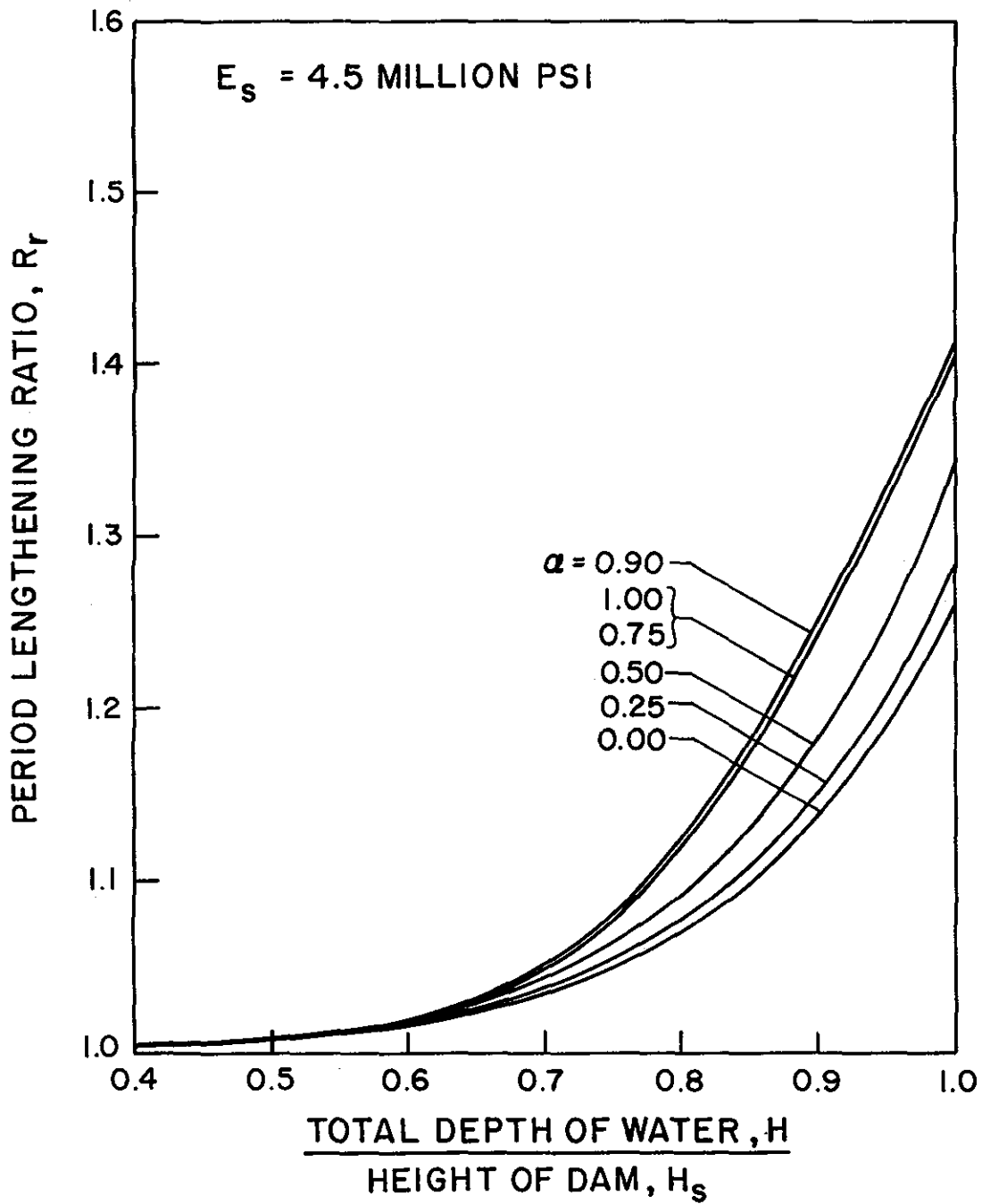


Figure 4(b). Standard Values for  $R_r$ , the Period Lengthening Ratio due to Hydrodynamic Effects;  $E_s = 4.5$  million psi.

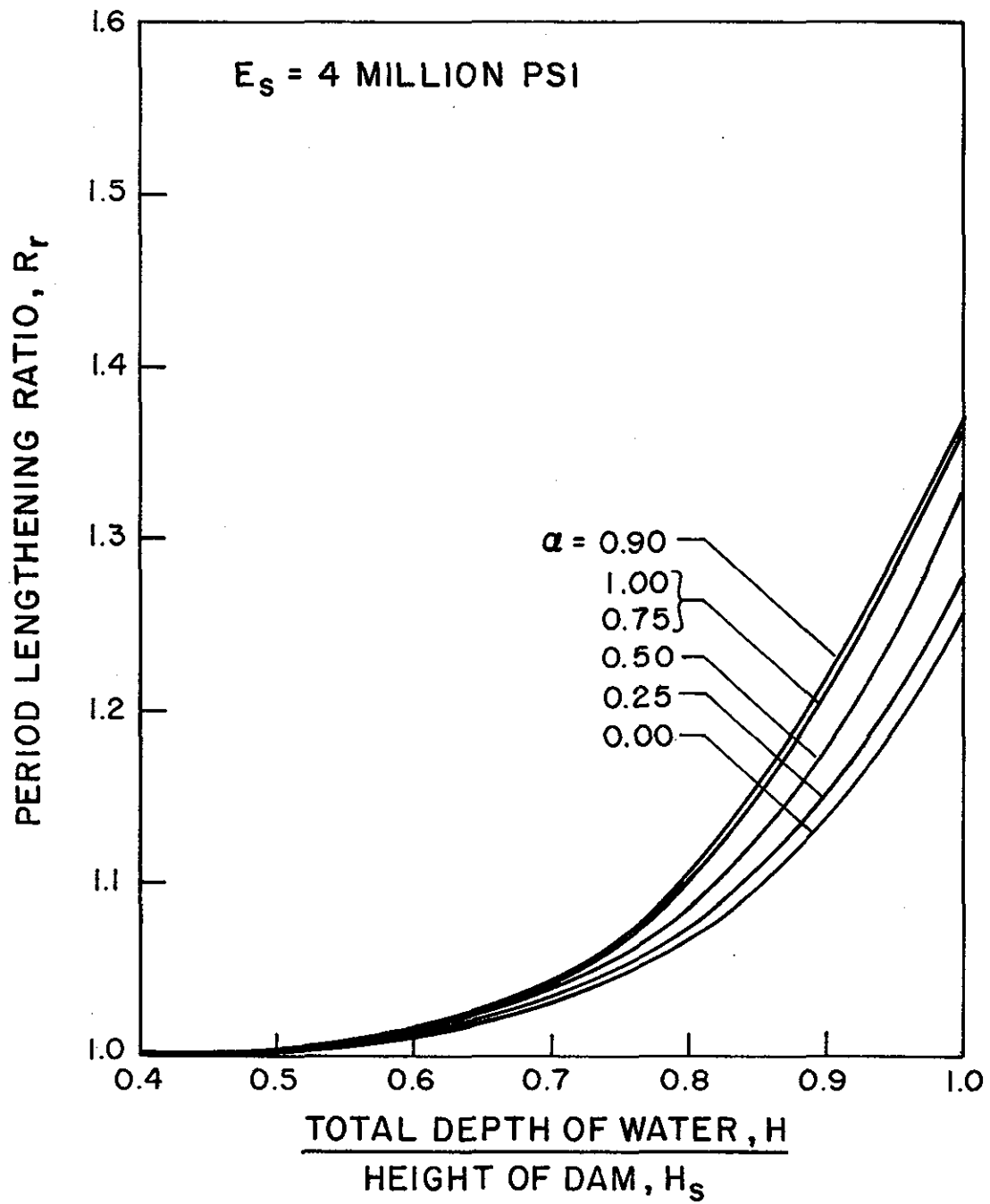


Figure 4(c). Standard Values for  $R_r$ , the Period Lengthening Ratio due to Hydrodynamic Effects;  $E_s = 4.0$  million psi.



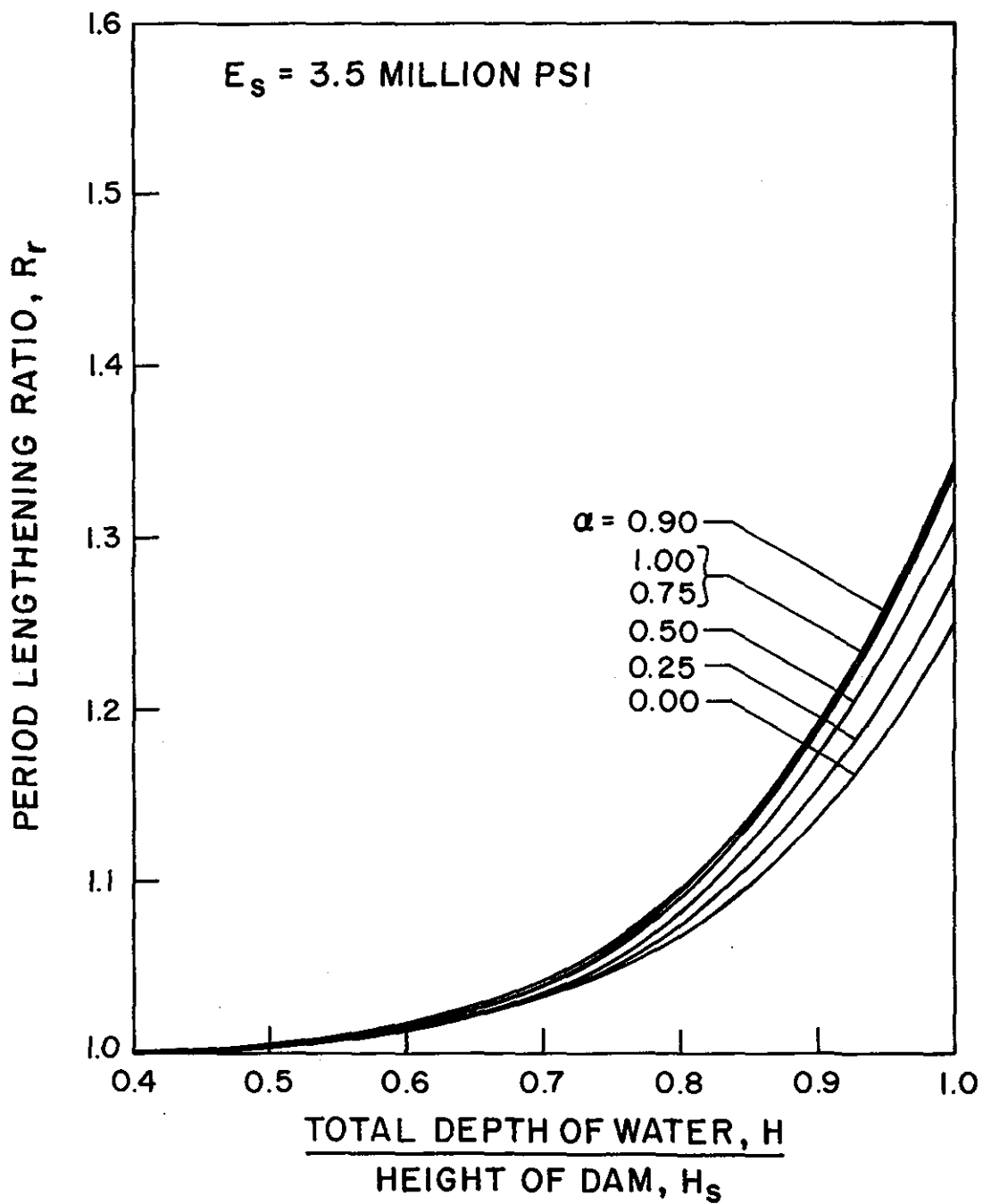


Figure 4(d). Standard Values for  $R_r$ , the Period Lengthening Ratio due to Hydrodynamic Effects;  $E_s = 3.5$  million psi.

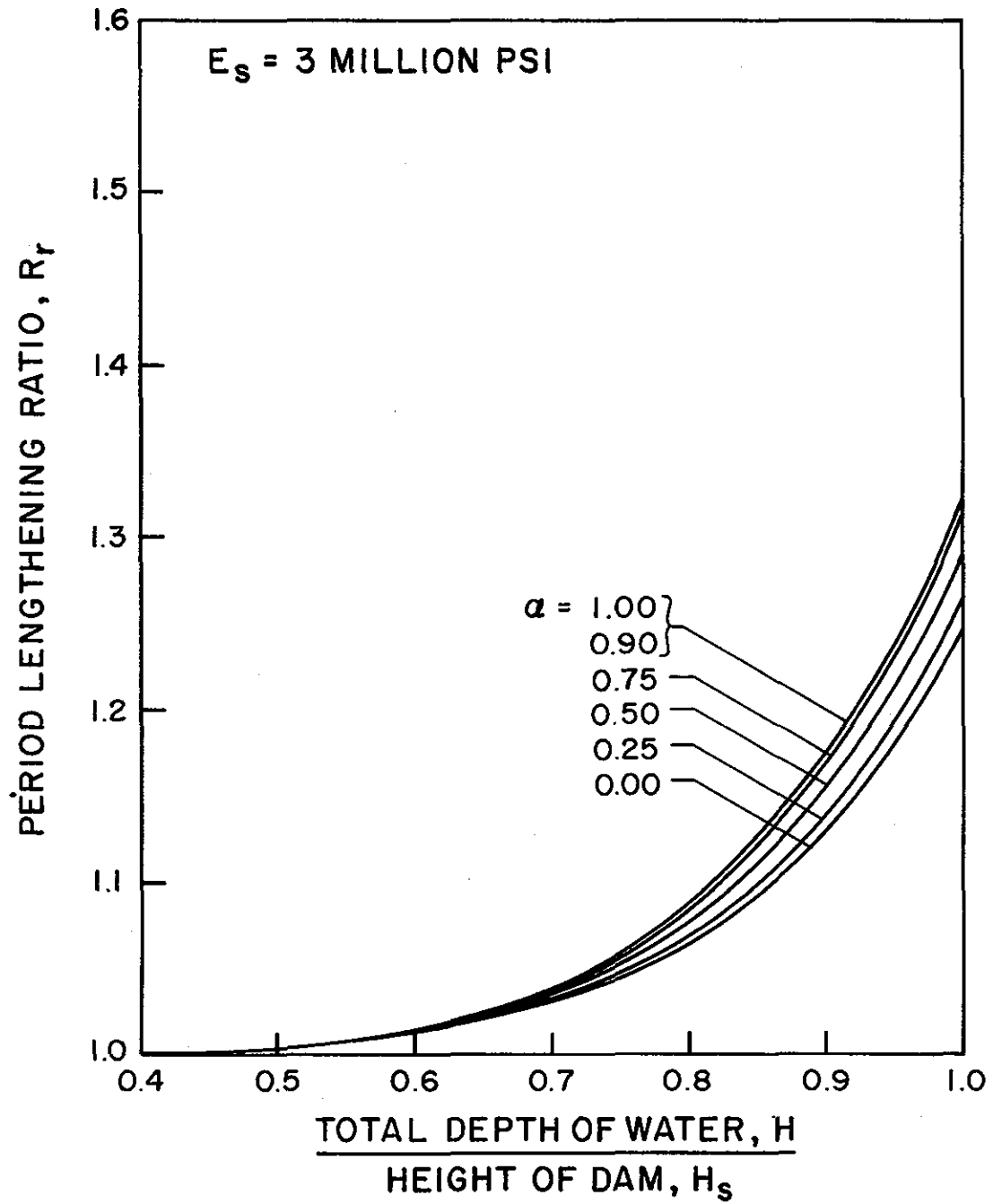


Figure 4(e). Standard Values for  $R_r$ , the Period Lengthening Ratio due to Hydrodynamic Effects;  $E_s = 3.0$  million psi.

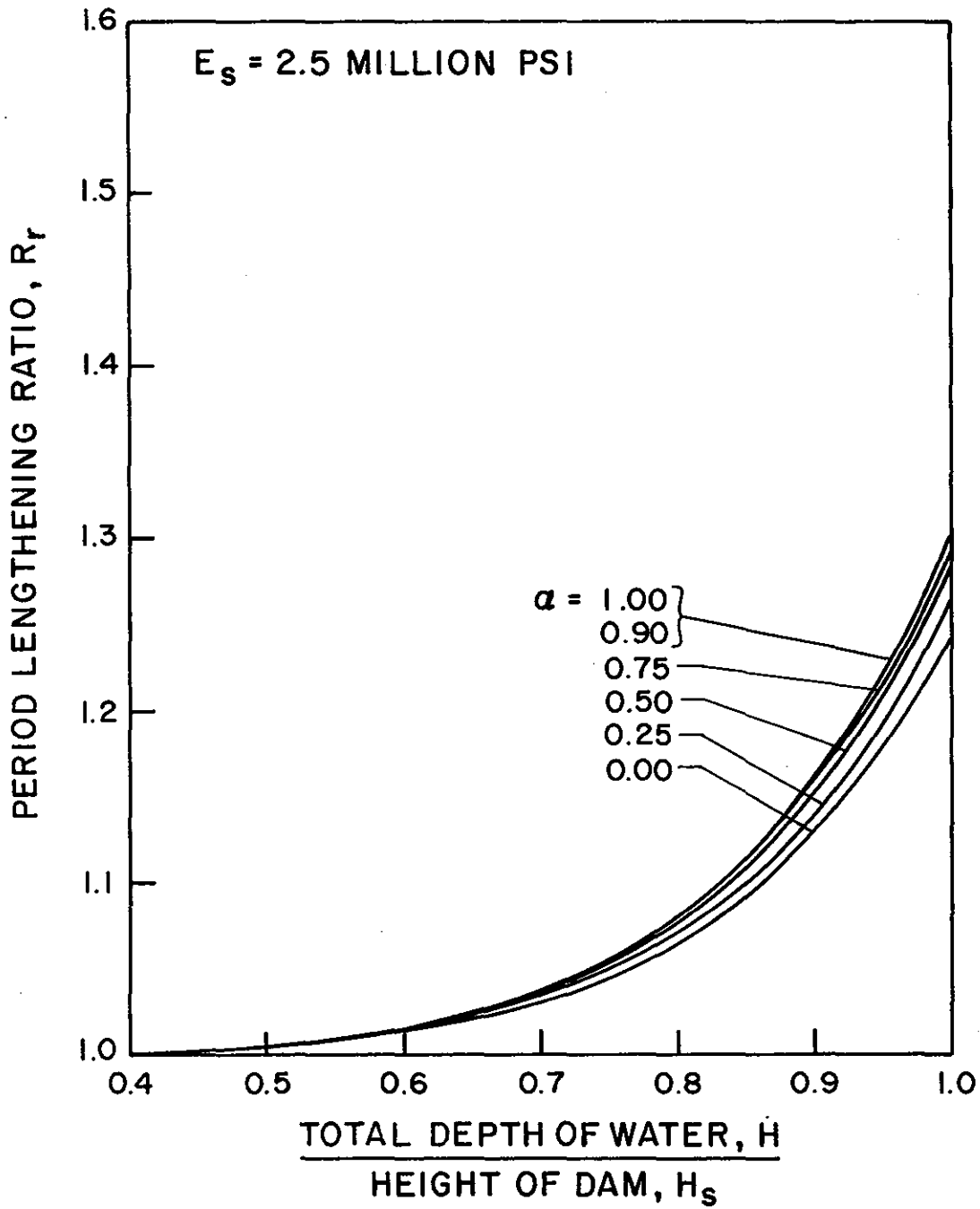


Figure 4(f). Standard Values for  $R_r$ , the Period Lengthening Ratio due to Hydrodynamic Effects;  $E_s = 2.5$  million psi.

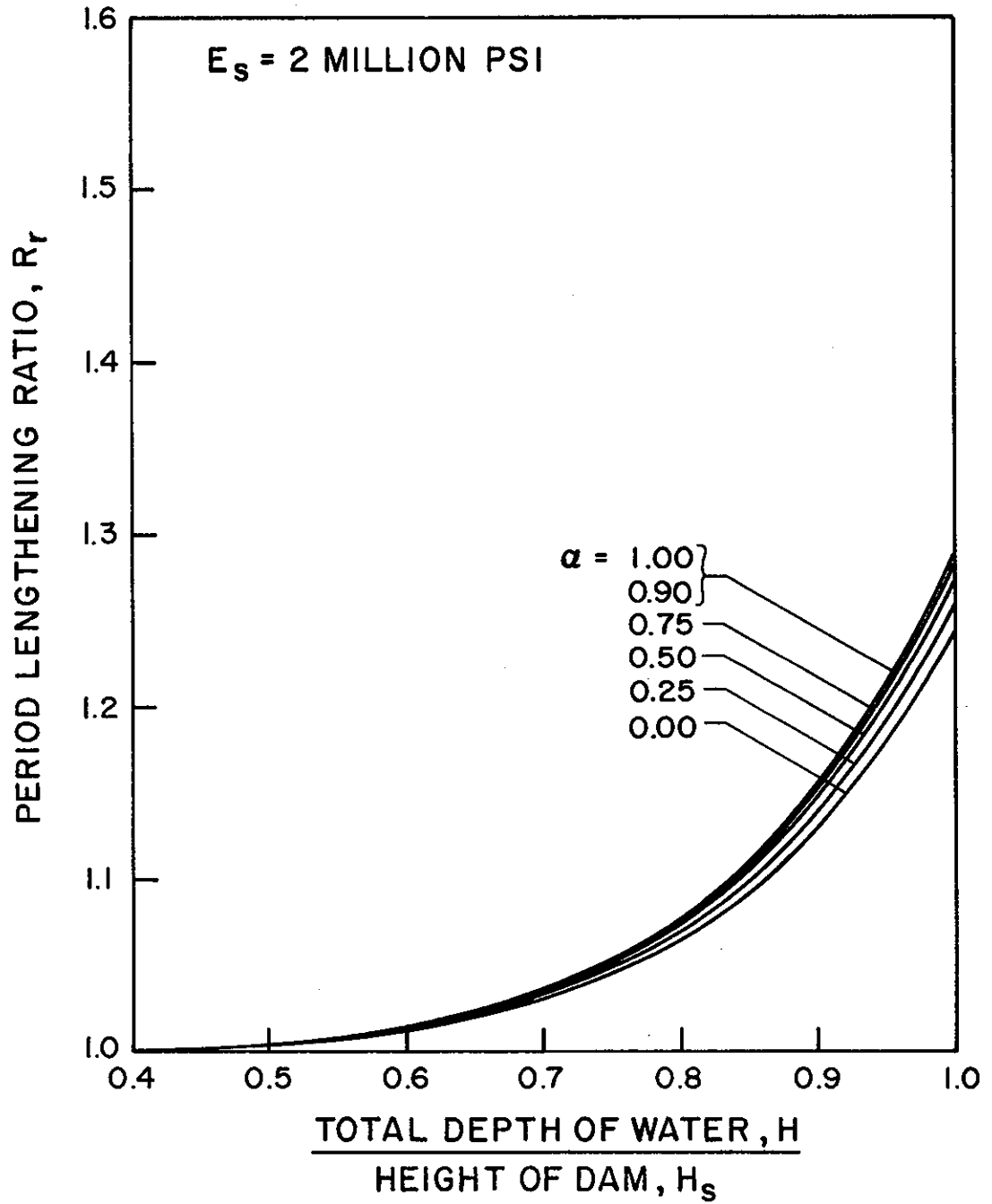


Figure 4(g). Standard Values for  $R_r$ , the Period Lengthening Ratio due to Hydrodynamic Effects;  $E_s = 2.0$  million psi.

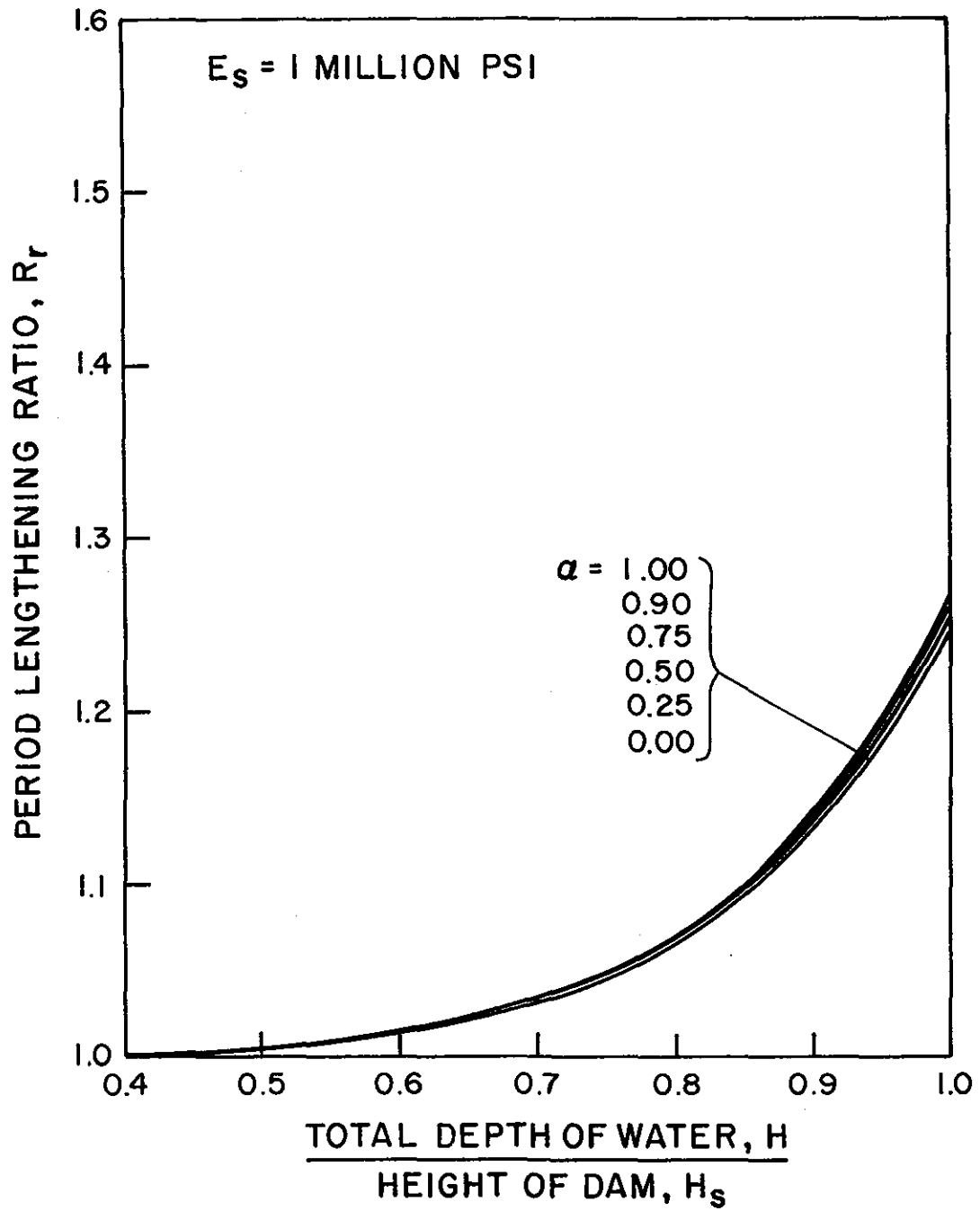


Figure 4(h). Standard Values for  $R_T$ , the Period Lengthening Ratio due to Hydrodynamic Effects;  $E_S = 1.0$  million psi.

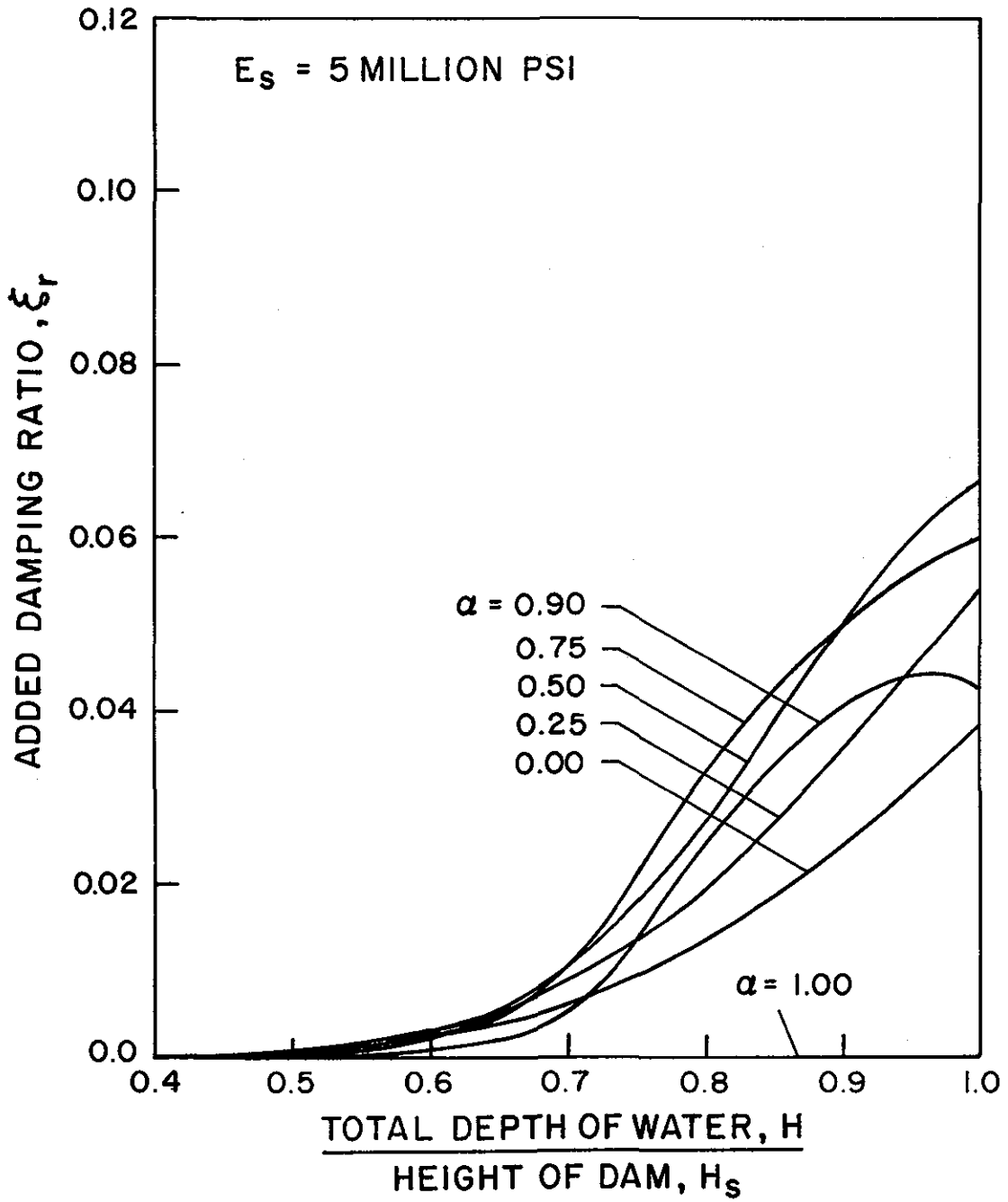


Figure 5(a). Standard Values for  $\xi_r$ , the Added Damping Ratio due to Hydrodynamic Effects;  $E_s = 5$  million psi

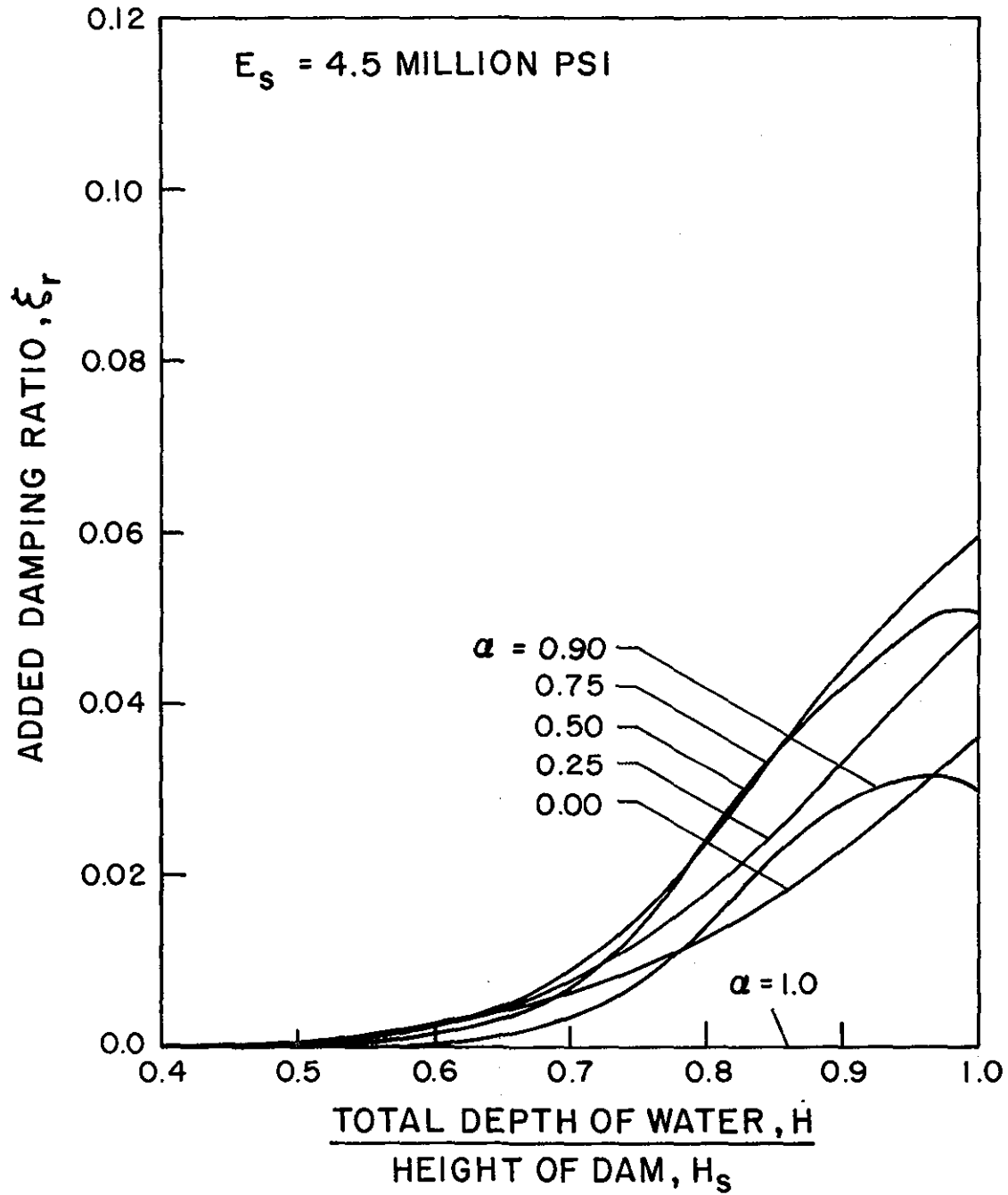


Figure 5(b). Standard Values for  $\xi_r$ , the Added Damping Ratio due to Hydrodynamic Effects;  $E_s = 4.5$  million psi

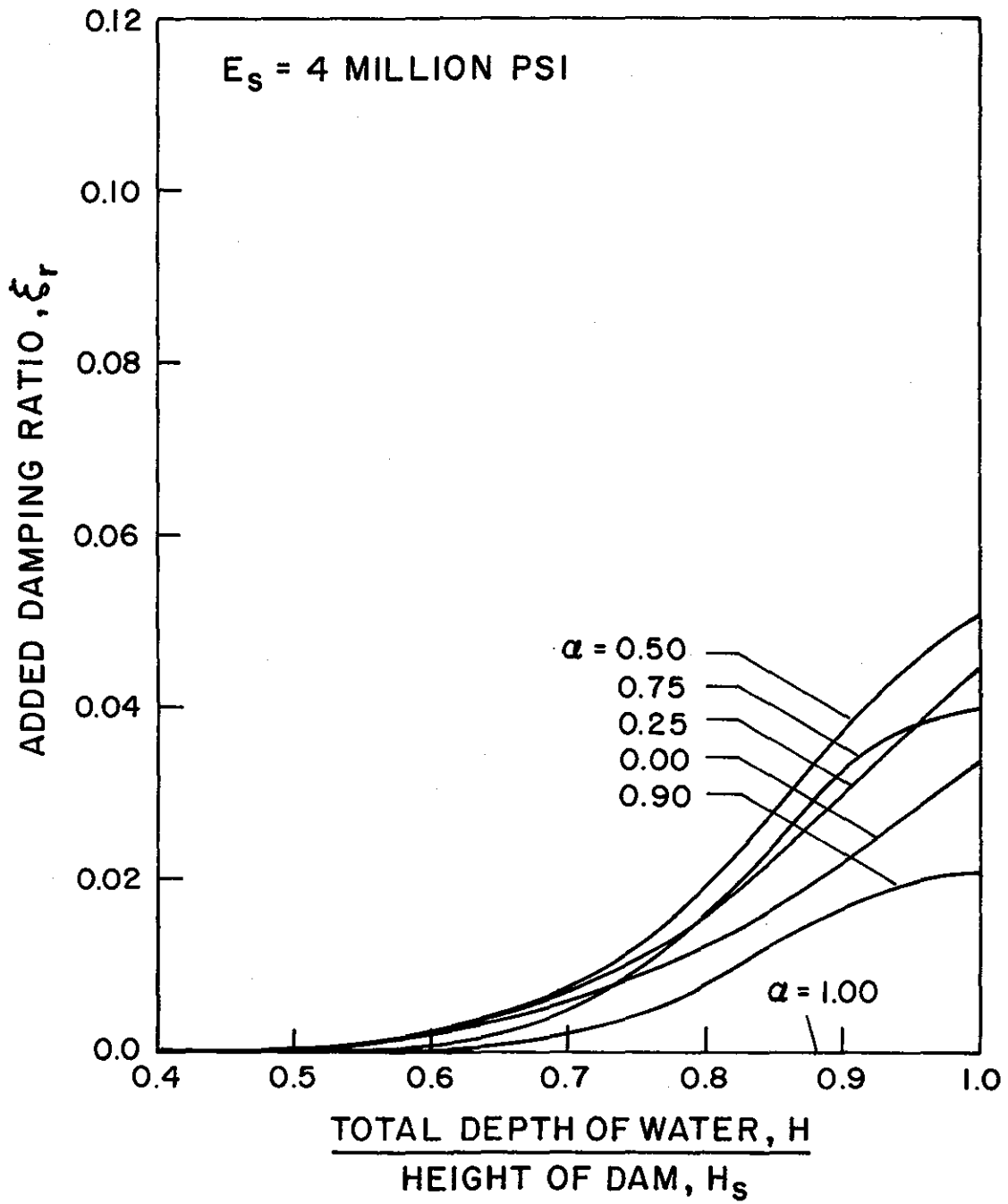


Figure 5(c). Standard Values for  $\xi_r$ , the Added Damping Ratio due to Hydrodynamic Effects;  $E_s = 4.0$  million psi.



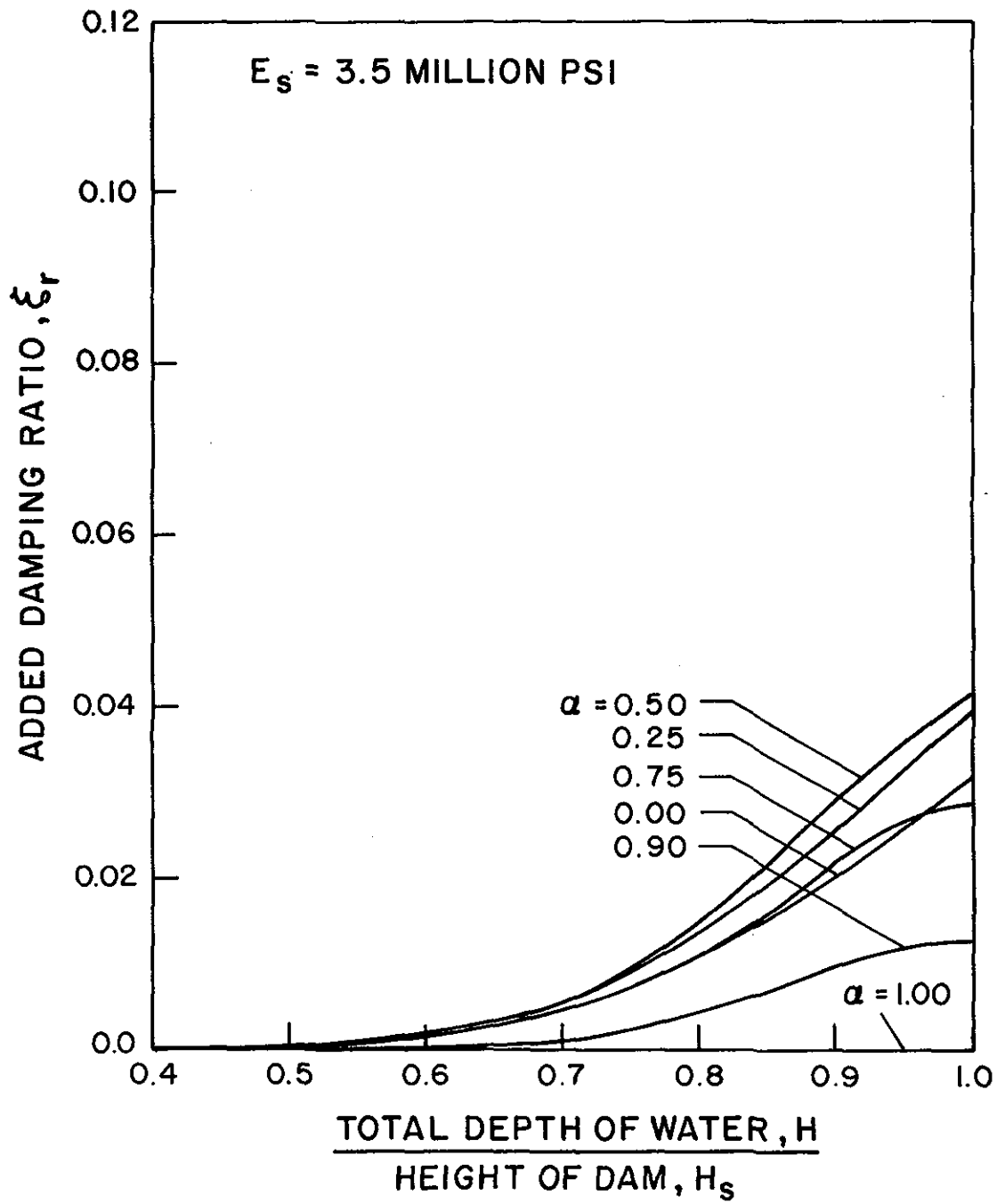


Figure 5(d). Standard Values for  $\xi_r$ , the Added Damping Ratio due to Hydrodynamic Effects;  $E_s = 3.5$  million psi.

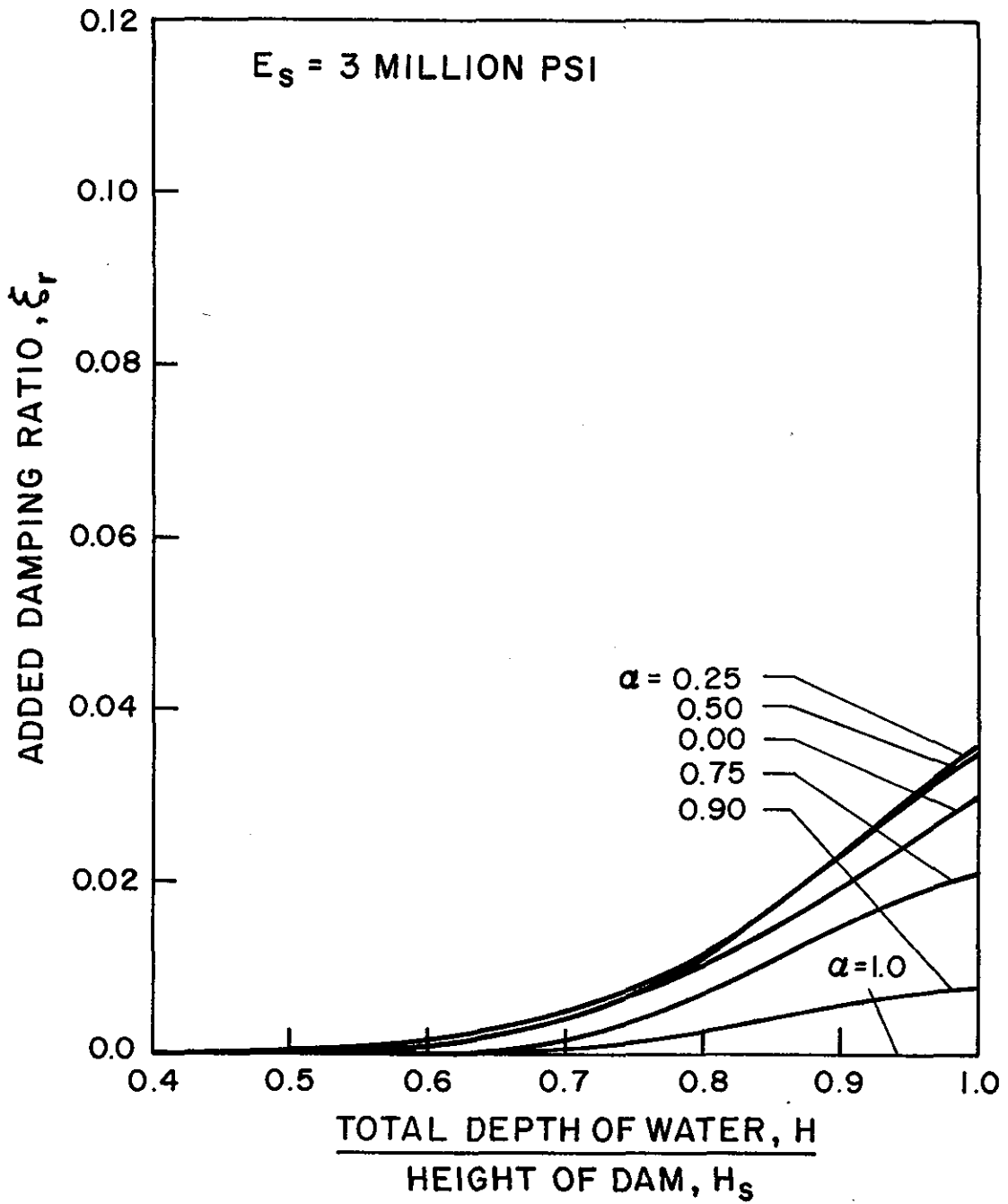


Figure 5(e). Standard Values for  $\xi_r$ , the Added Damping Ratio due to Hydrodynamic Effects;  $E_s = 3.0$  million psi.

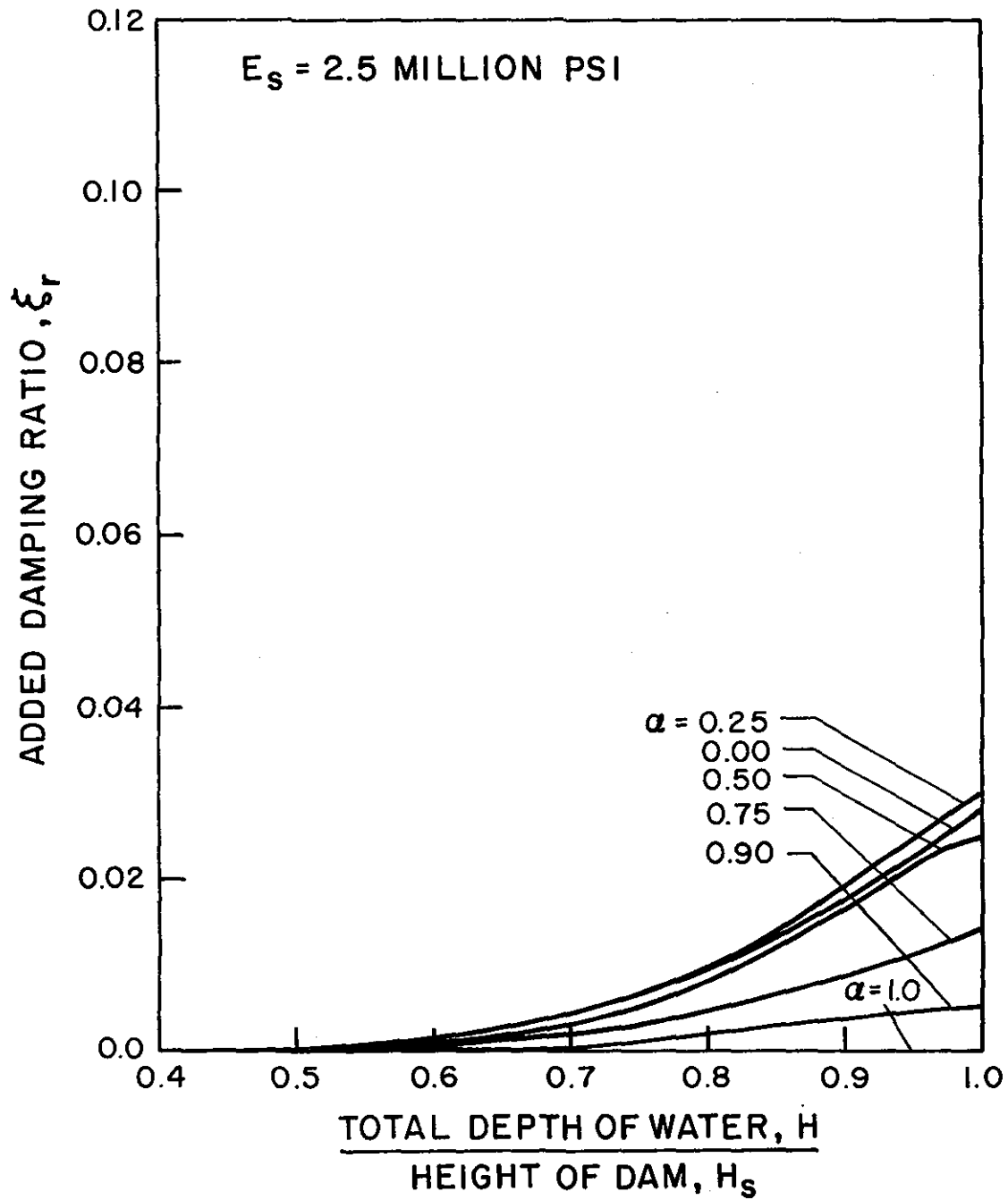


Figure 5(f). Standard Values for  $\xi_r$ , the Added Damping Ratio due to Hydrodynamic Effects;  $E_s = 2.5$  million psi.

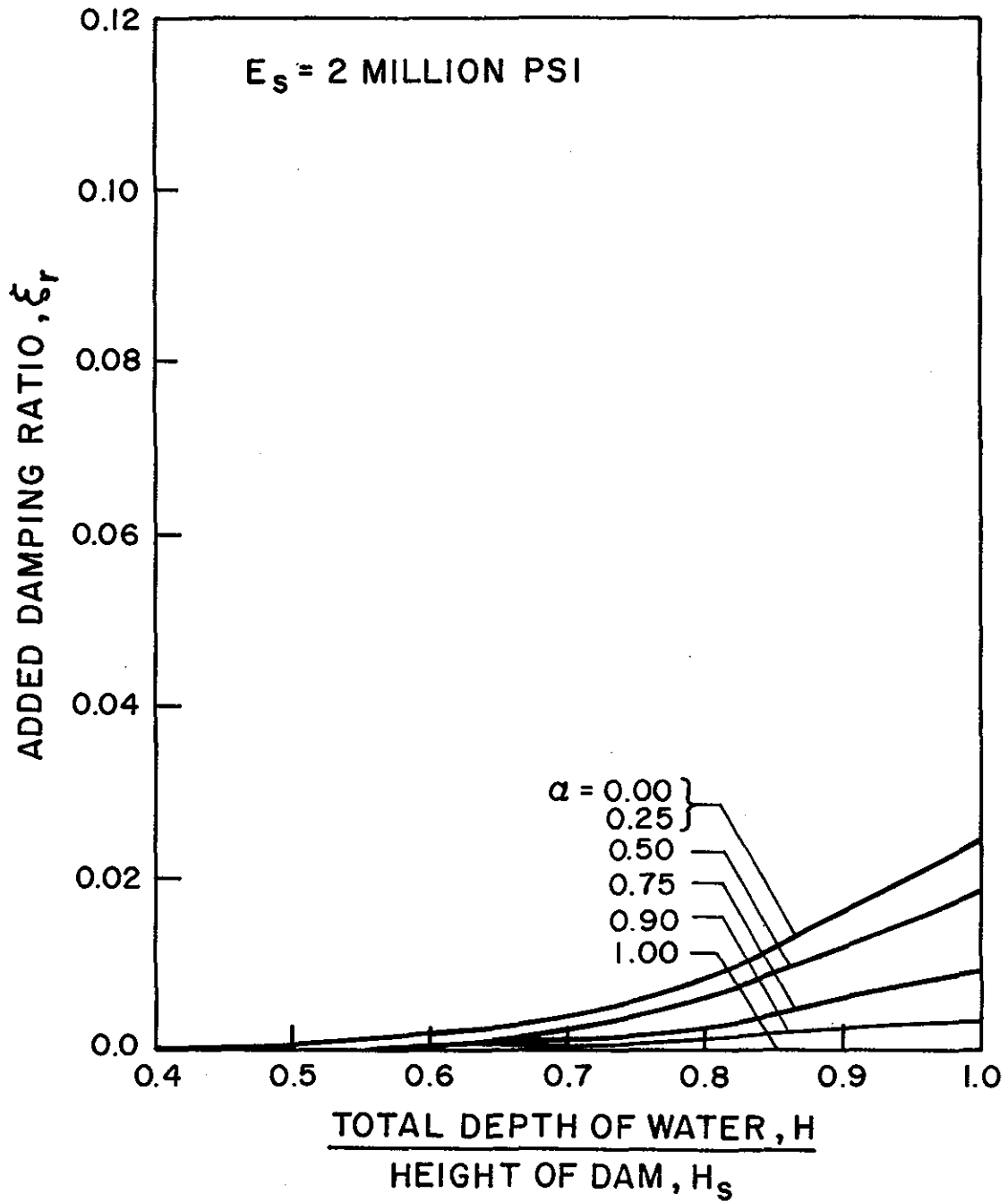


Figure 5(g). Standard Values for  $\xi_r$ , the Added Damping Ratio due to Hydrodynamic Effects;  $E_s = 2.0$  million psi

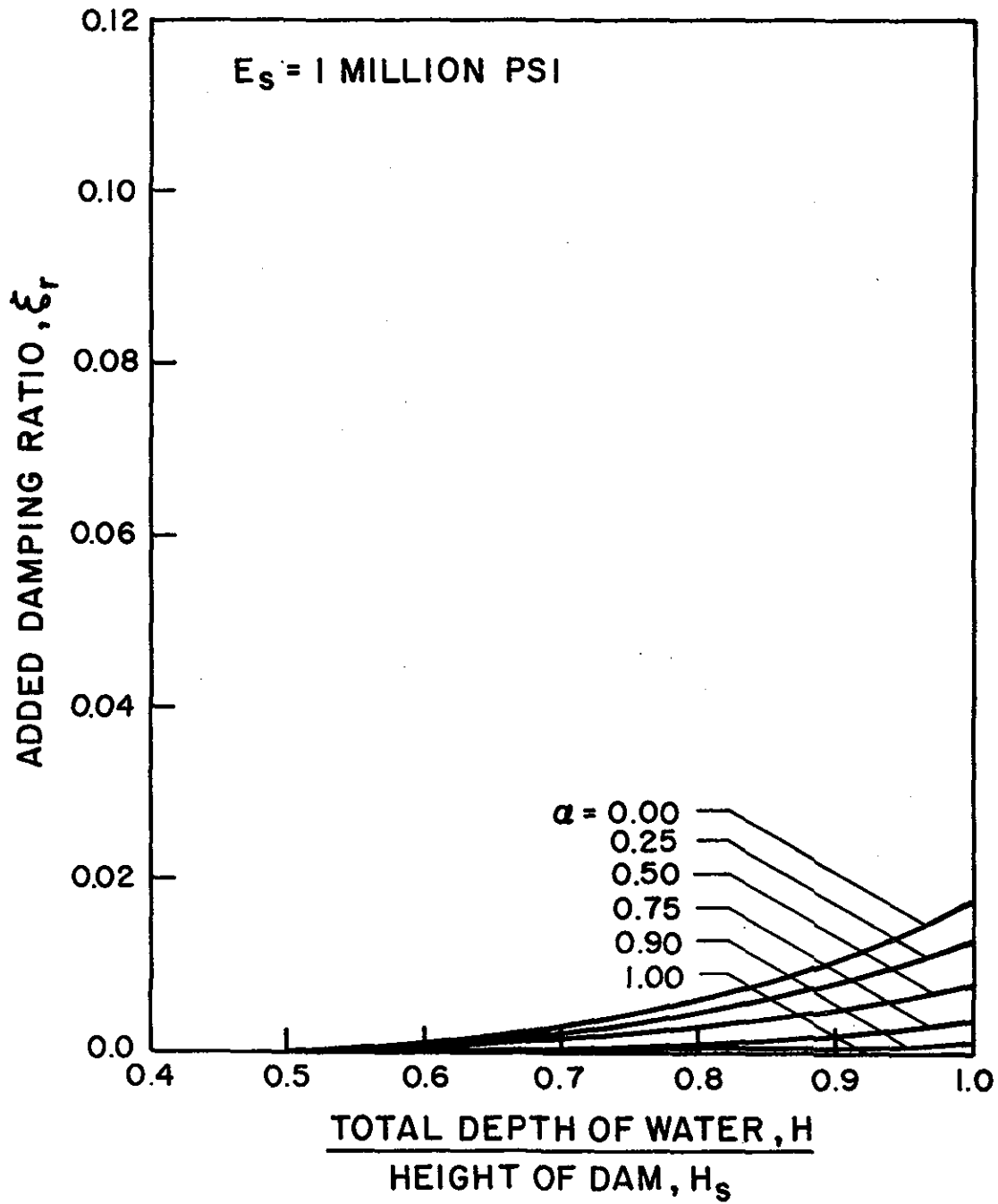


Figure 5(h). Standard Values for  $\xi_r$ , the Added Damping Ratio due to Hydrodynamic Effects;  $E_s = 1.0$  million psi.

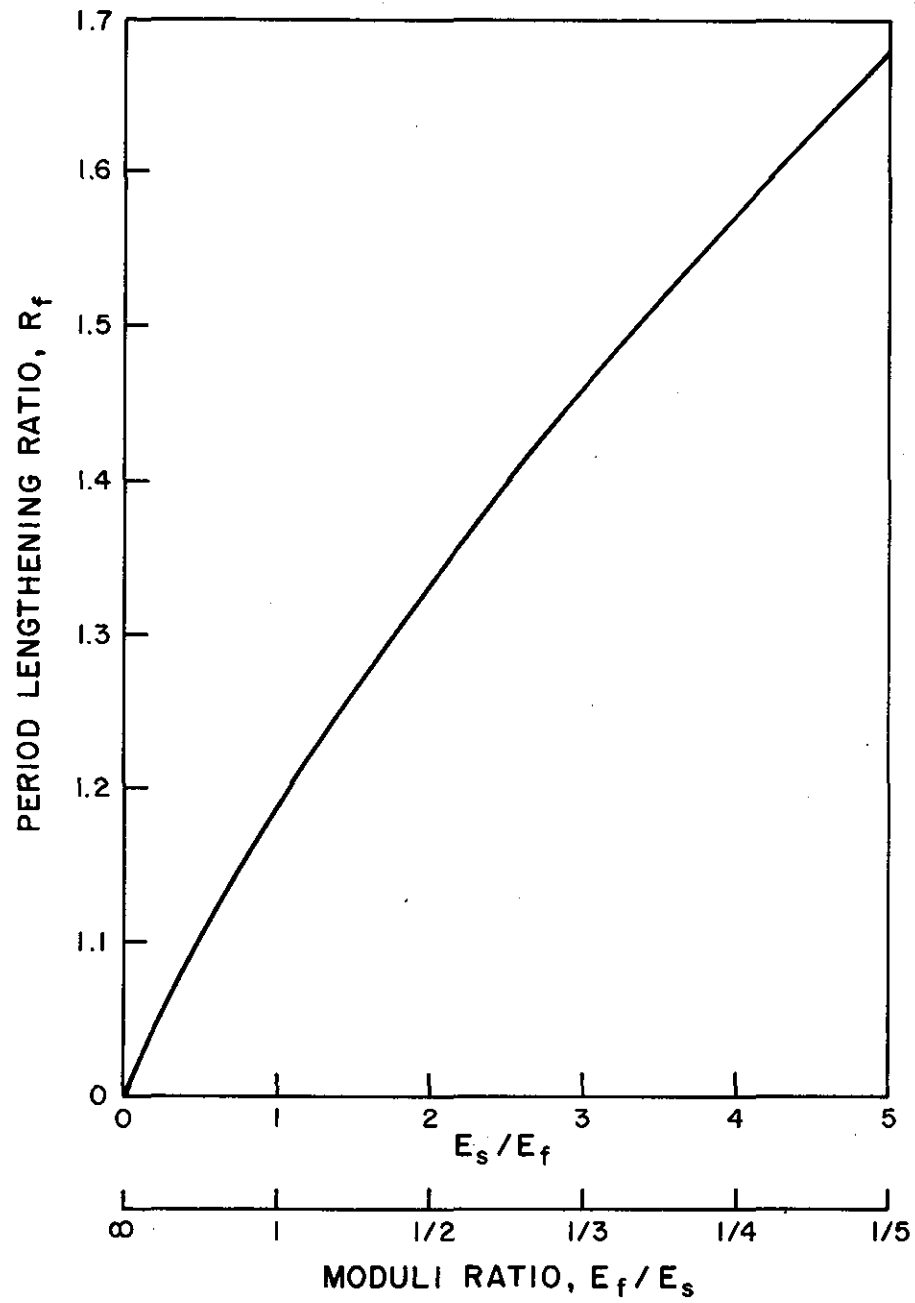


Figure 6. Standard Values for  $R_f$ , the Period Lengthening Ratio due to Dam-Foundation Rock Interaction

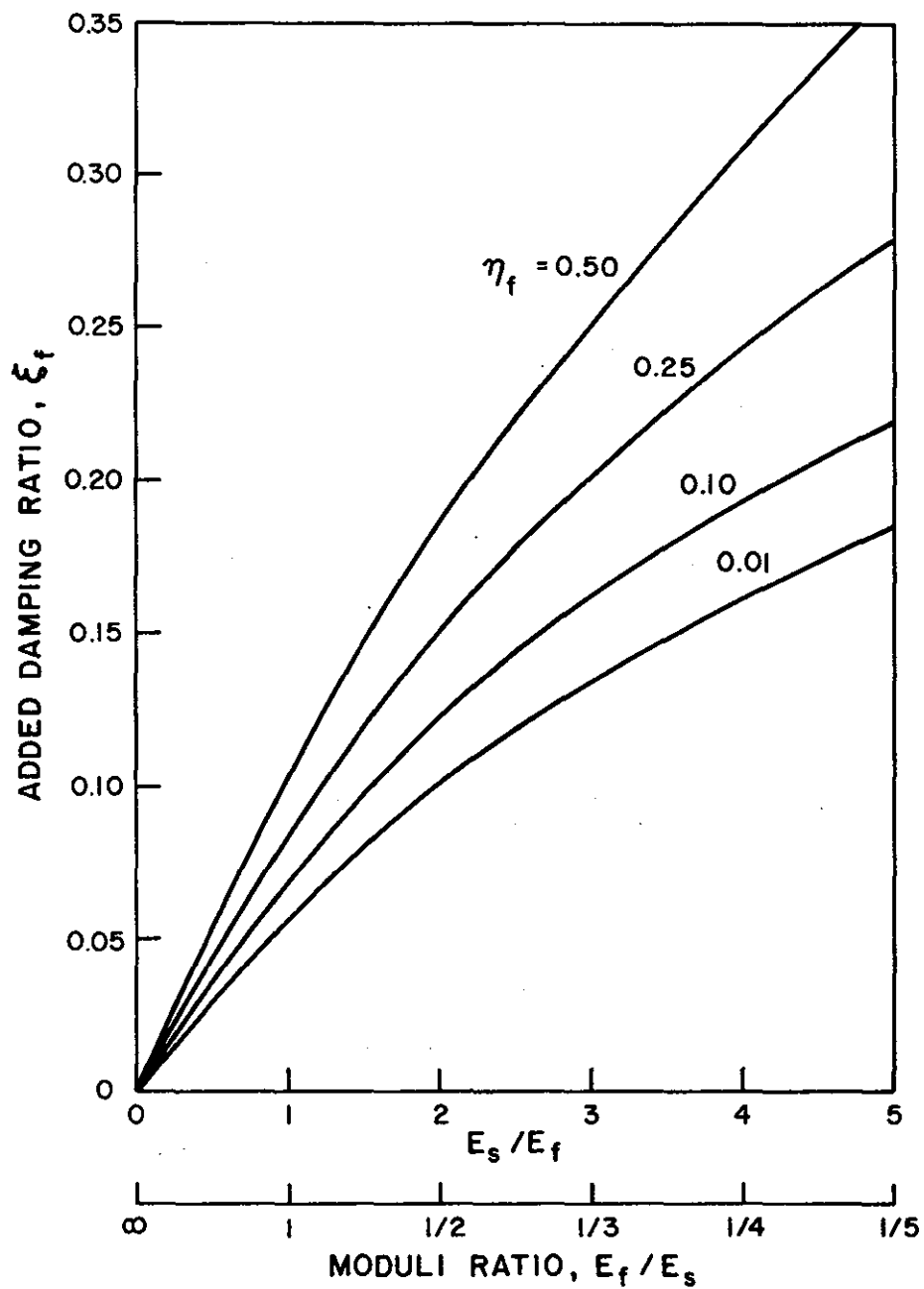


Figure 7. Standard Values for  $\xi_f$ , the Added Damping Ratio due to Dam-Foundation Rock Interaction

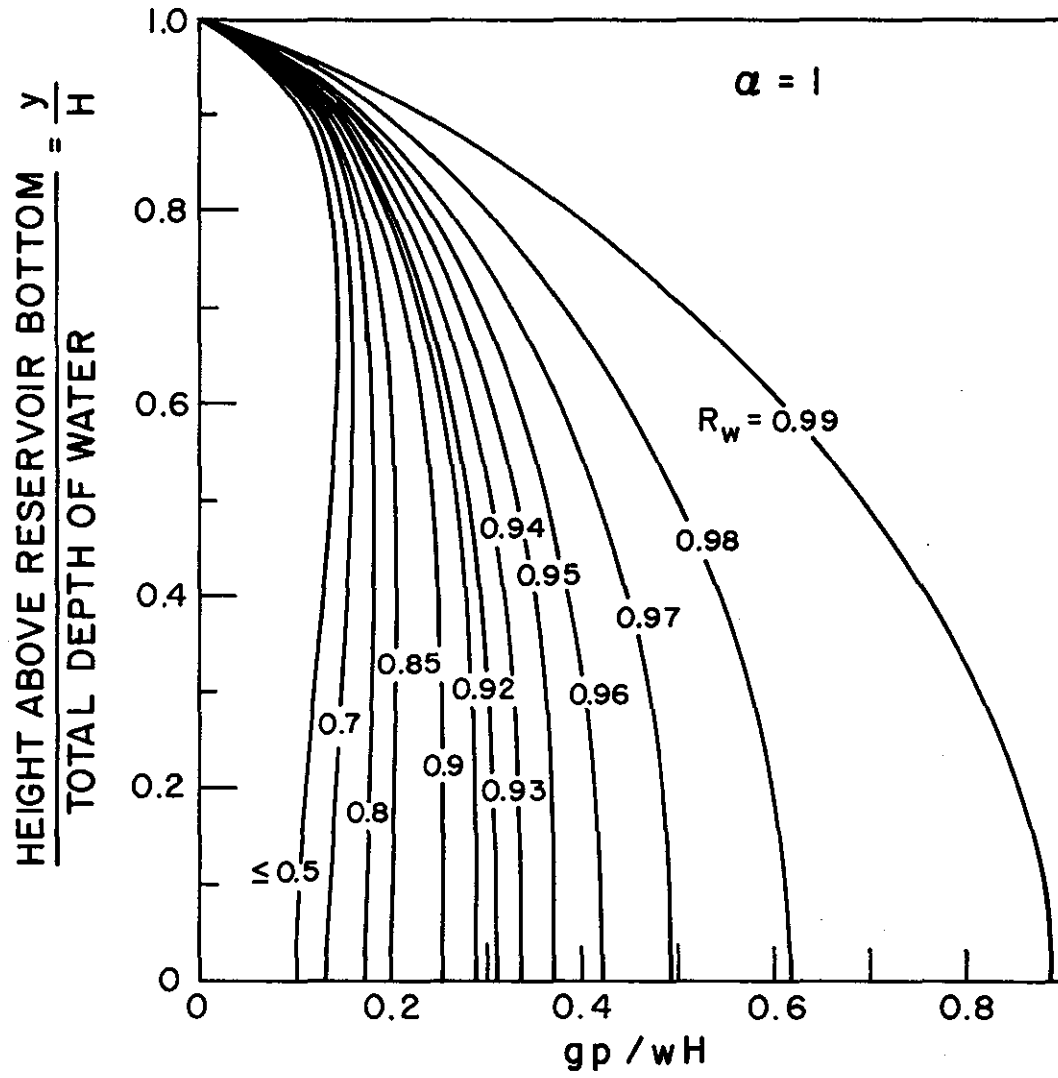


Figure 8(a). Standard Values for the Hydrodynamic Pressure Function  $p(\hat{y})$  for Full Reservoir, i.e.  $H/H_s = 1$ ;  $\alpha = 1.00$ .



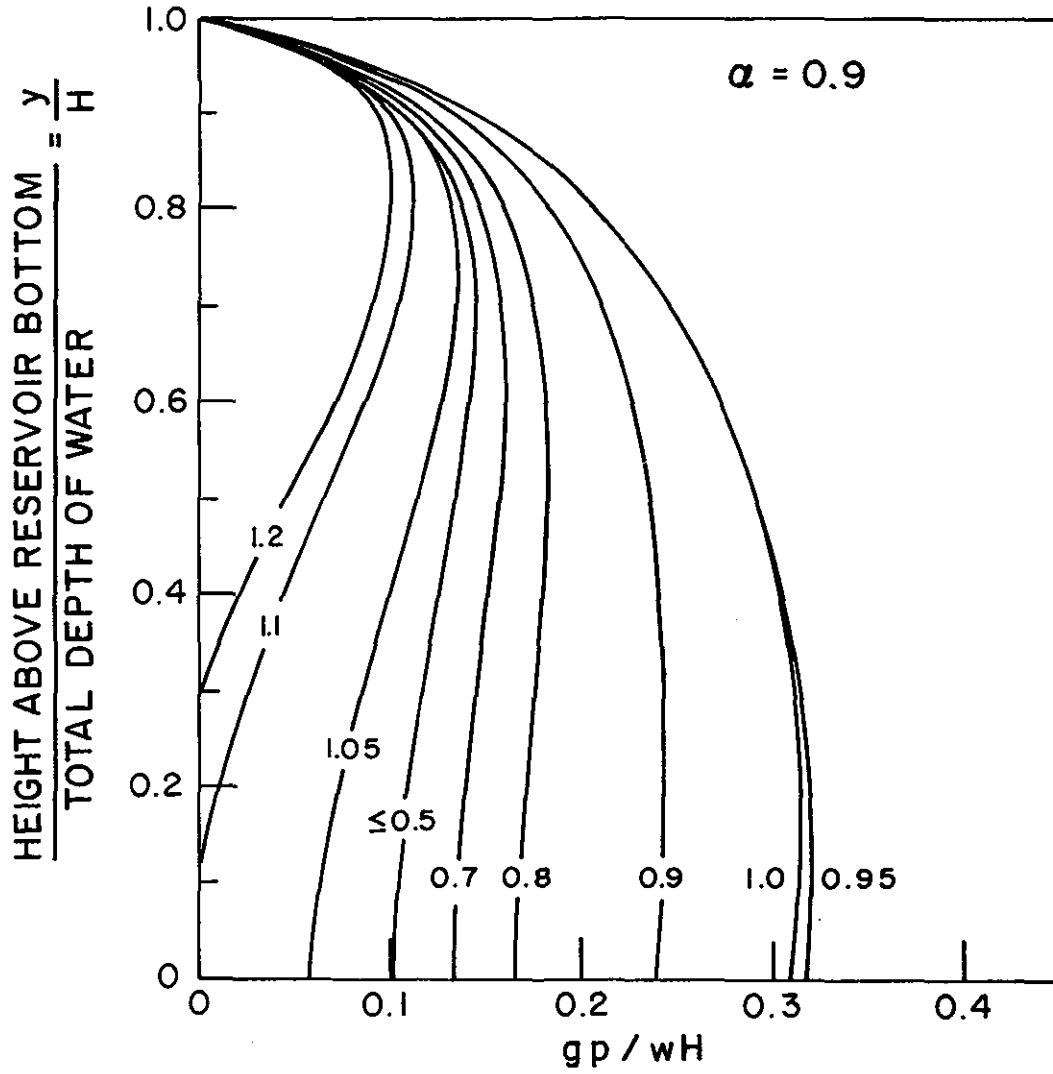


Figure 8(b). Standard Values for the Hydrodynamic Pressure Function  $p(\hat{y})$  for Full Reservoir, i.e.  $H/H_s = 1$ ;  $\alpha = 0.90$

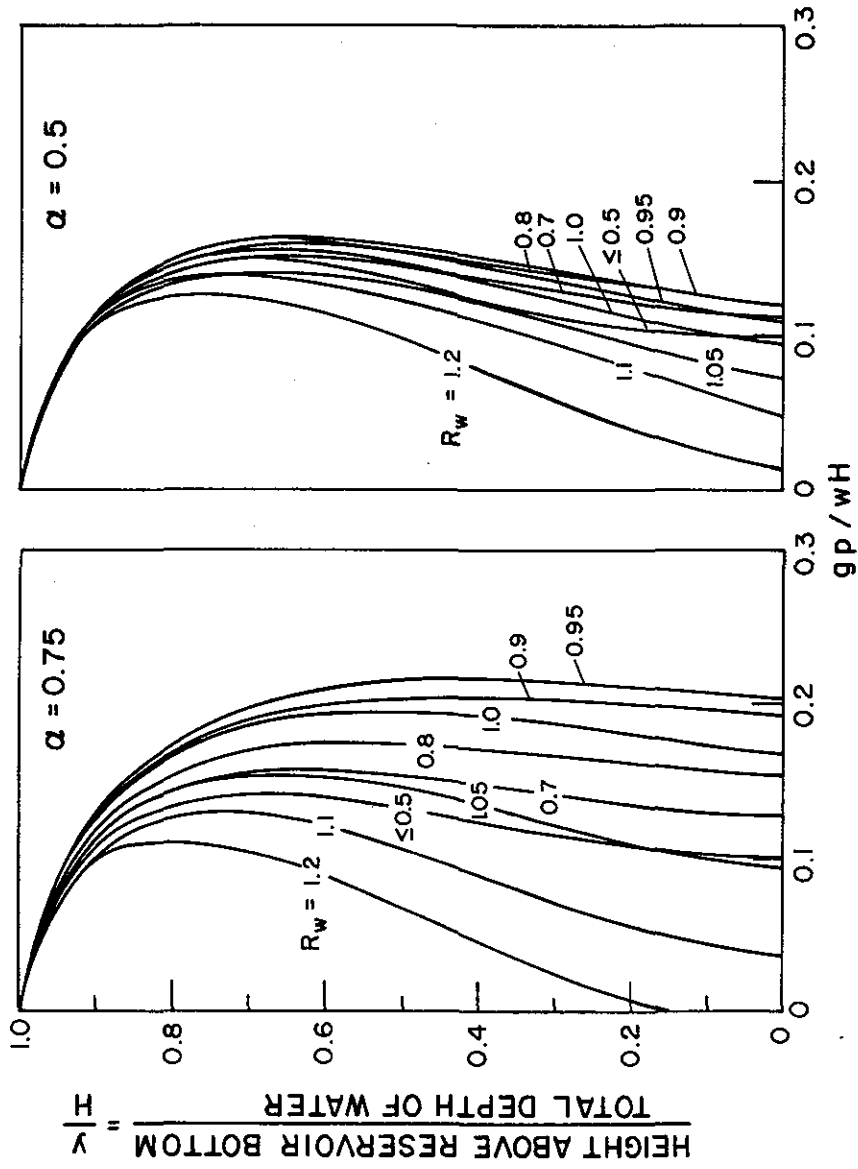


Figure 8(c). Standard Values for the Hydrodynamic Pressure Function  $p(\hat{y})$  for Full Reservoir, i.e.  $H/H_s = 1$ ;  $\alpha = 0.75$  and  $0.50$ .

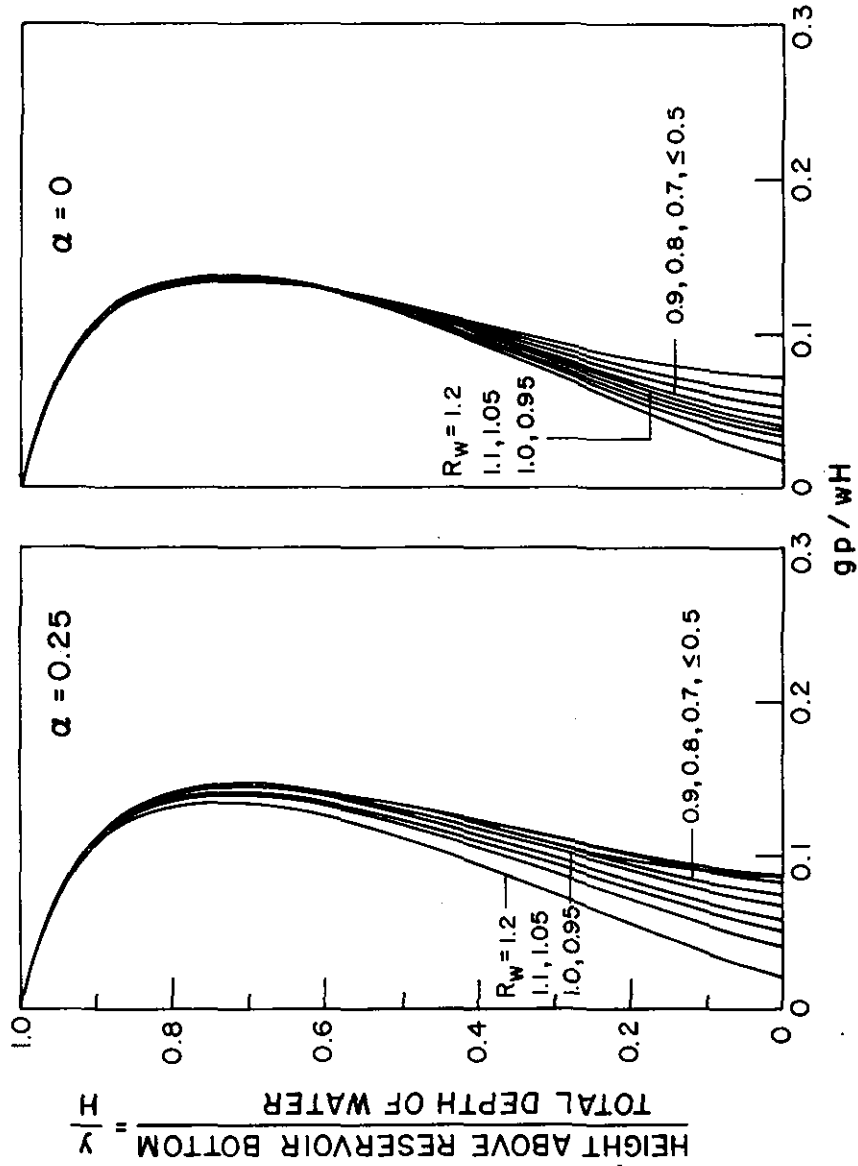


Figure 8(d). Standard Values for the Hydrodynamic Pressure Function  $p(\hat{y})$  for Full Reservoir, i.e.  $H/H_s = 1$ ;  $\alpha = 0.25$  and  $0.00$ .

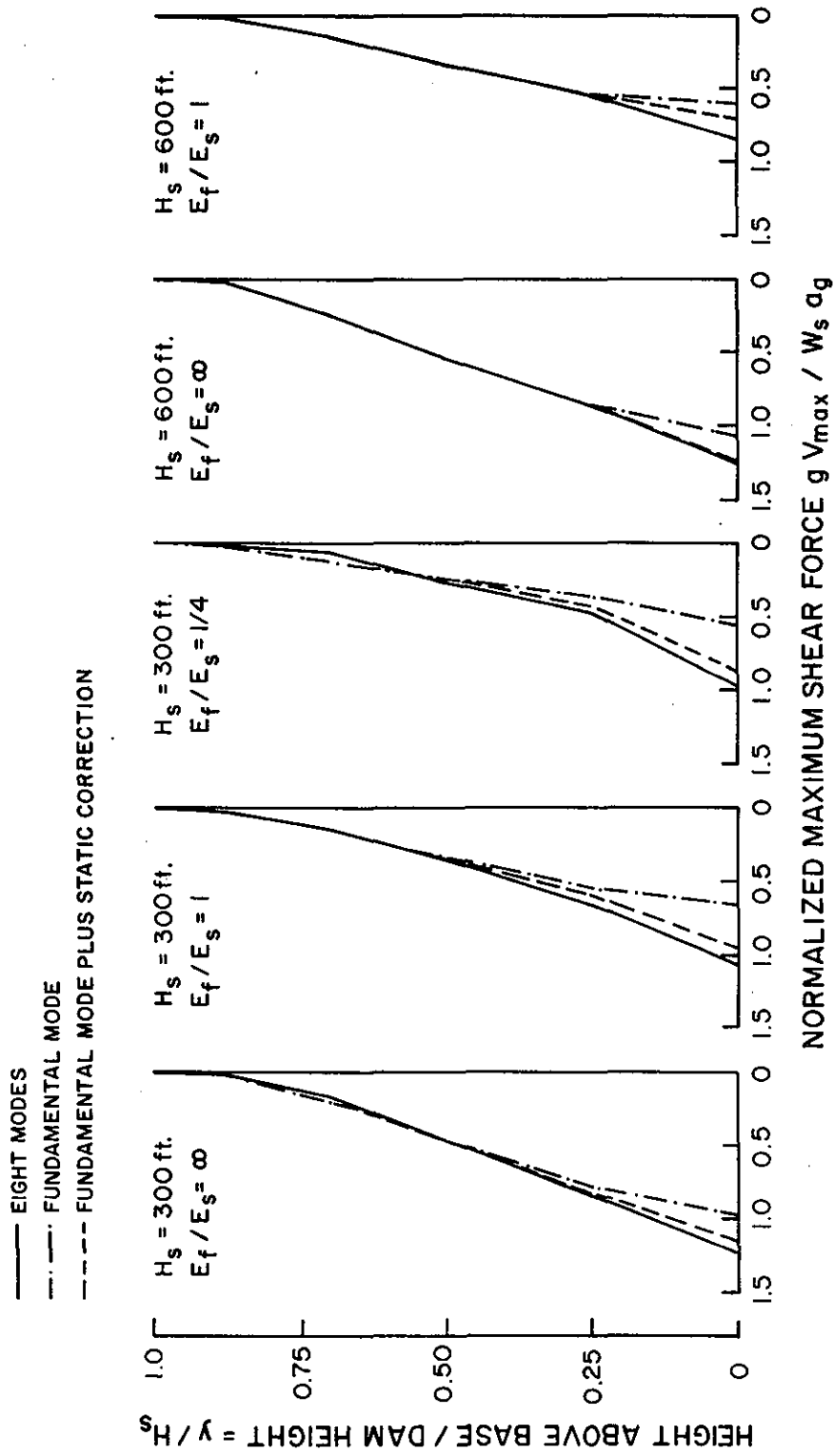


Figure 9. Heightwise Distribution of Maximum Shear Force in Dams with Empty Reservoir due to S69E Component of Taft Ground Motion

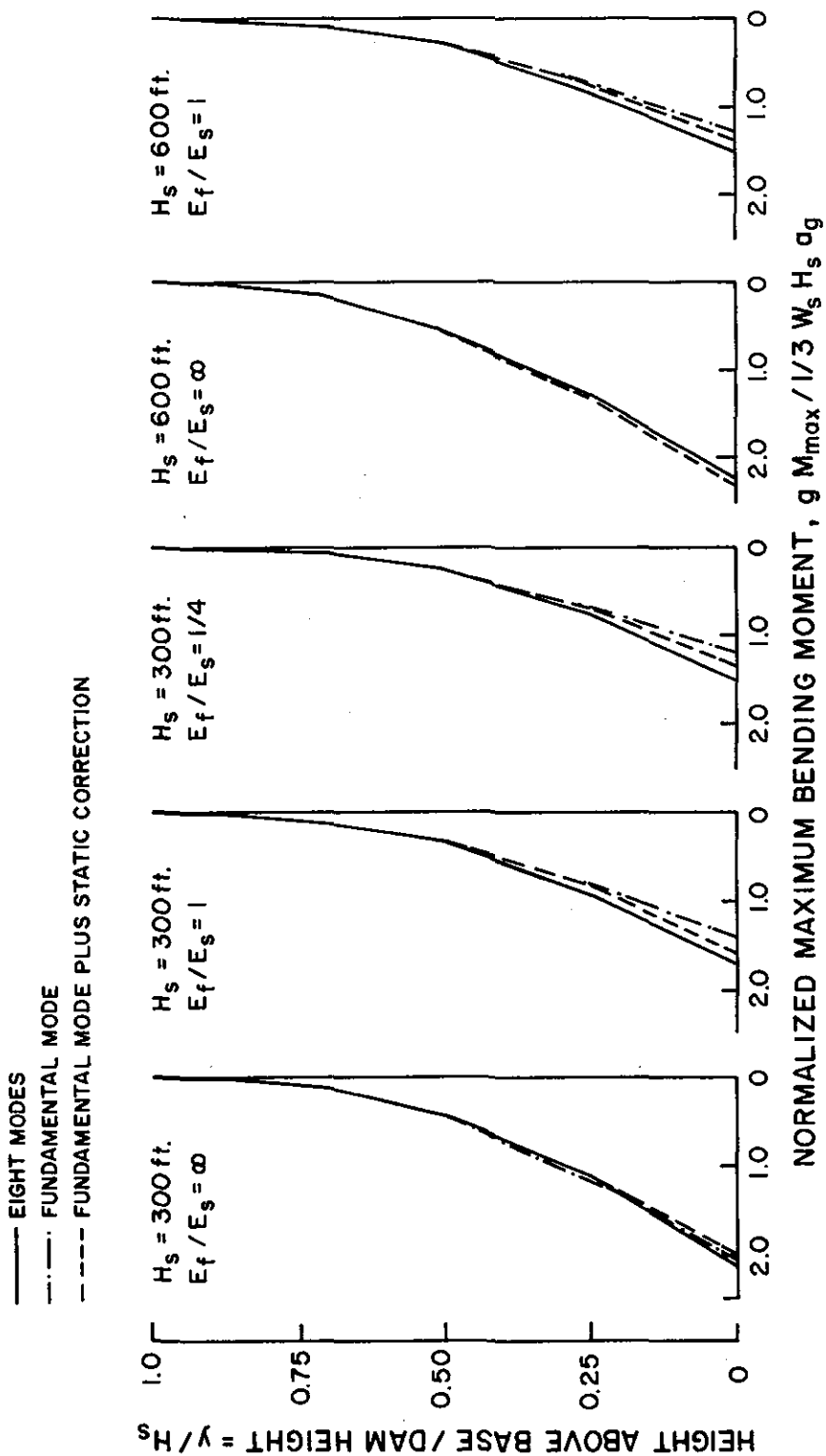


Figure 10. Heightwise Distribution of Maximum Bending Moment in Dams with Empty Reservoir due to S69E Component of Taft Ground Motion

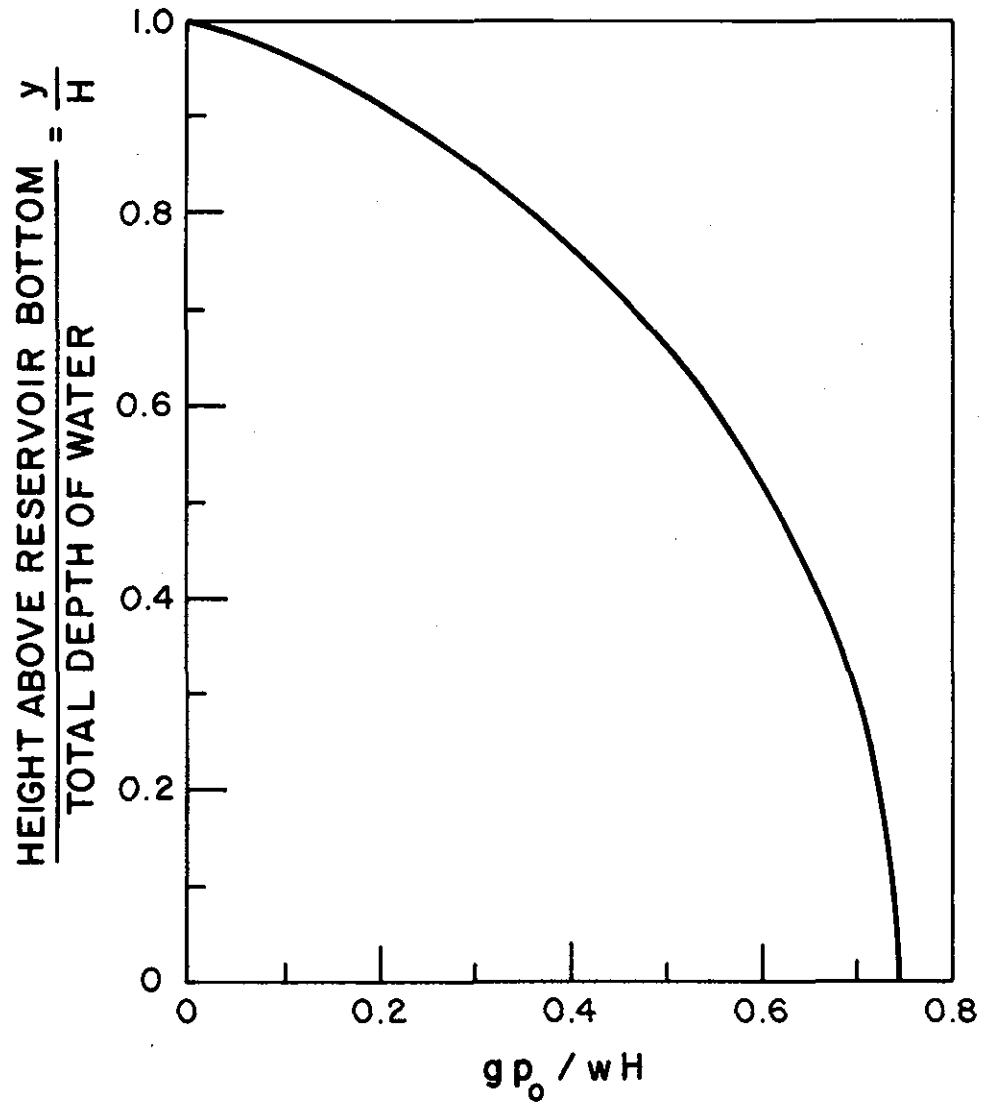


Figure 11. Standard Values for the Hydrodynamic Pressure Function  $p_0(\hat{y})$

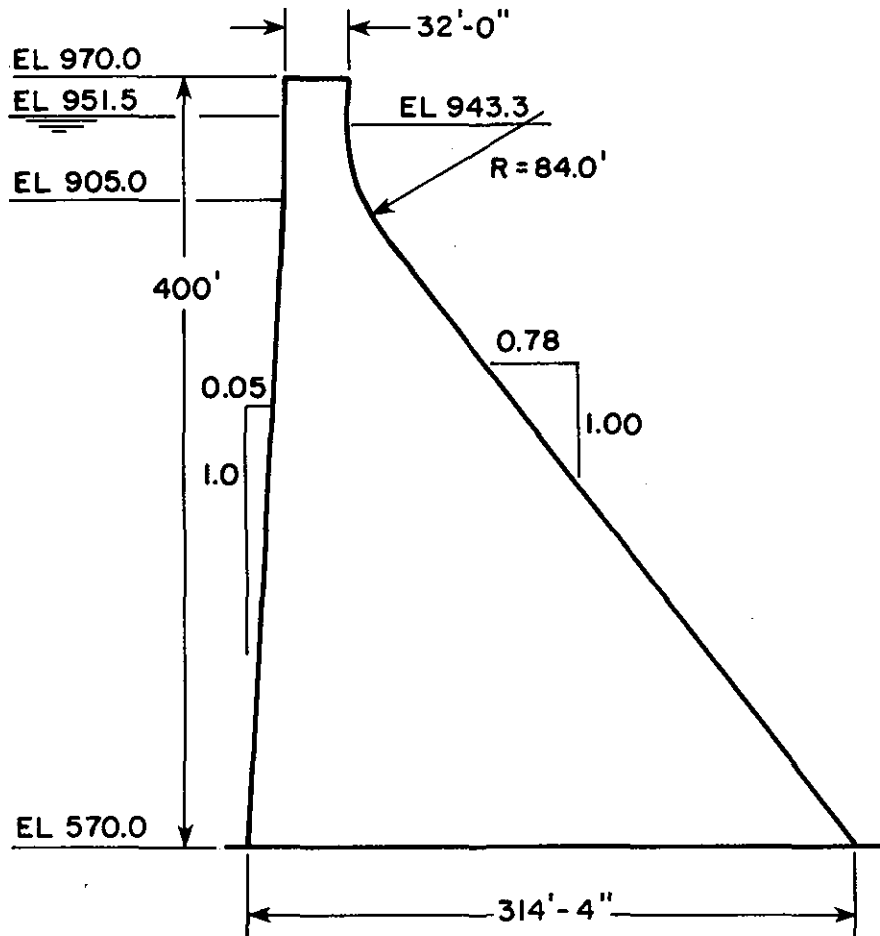


Figure 12. Tallest, Nonoverflow Monolith of Pine Flat Dam

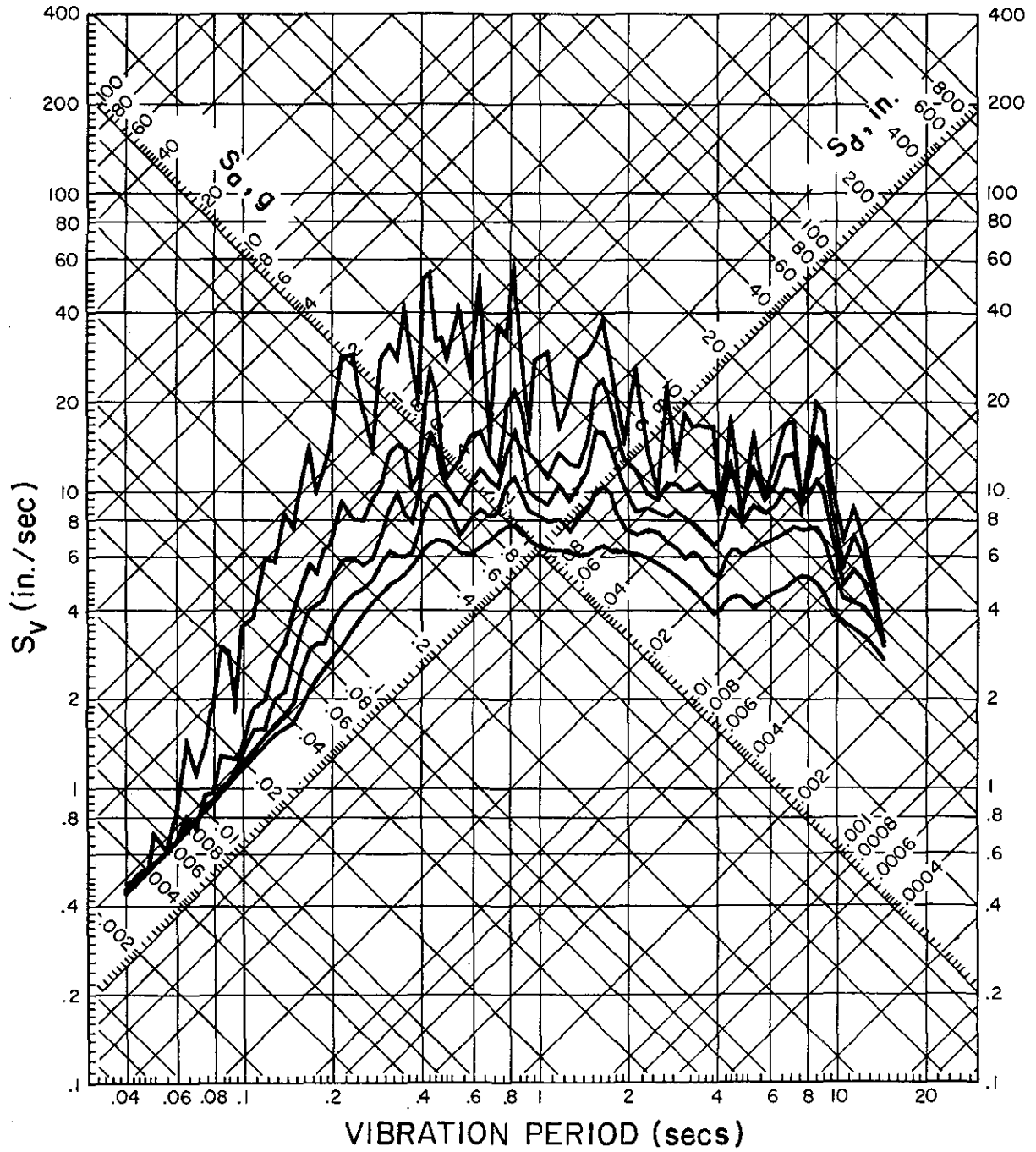
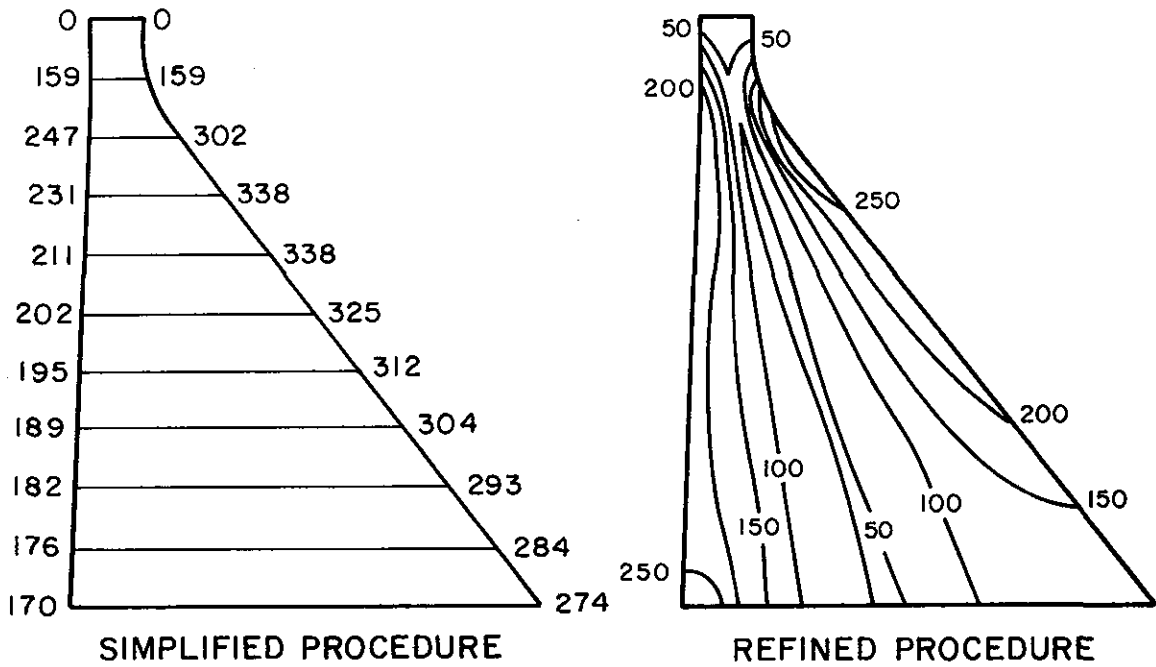
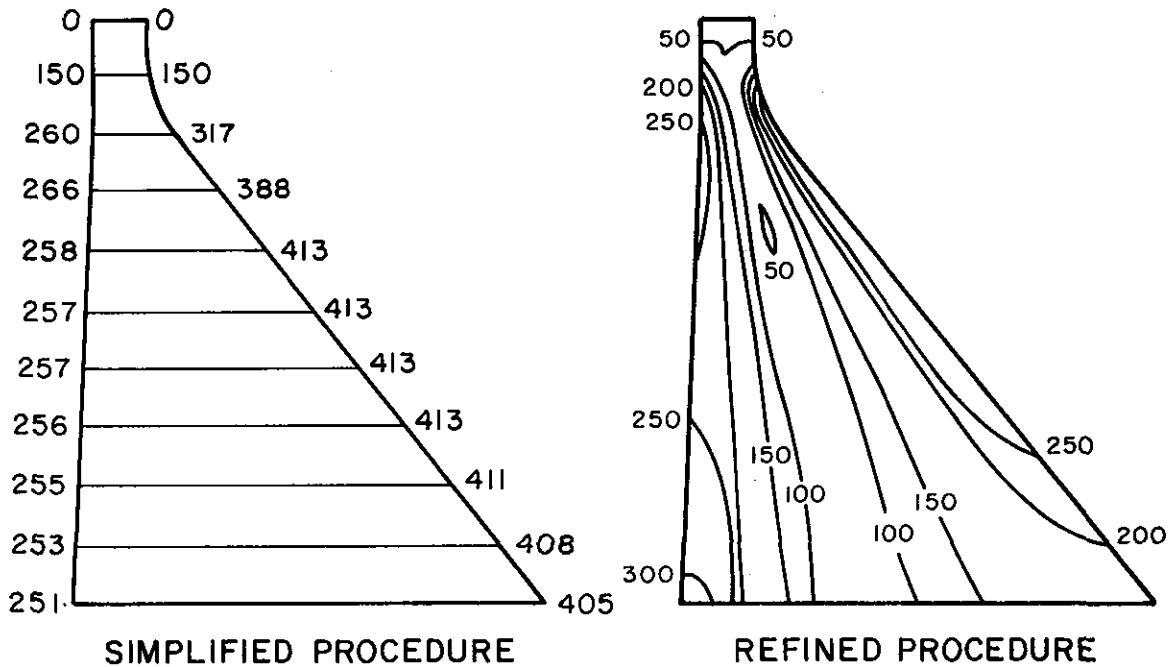


Figure 13. Response Spectrum for the S69E Component of Taft Ground Motion; damping ratios = 0, 2, 5, 10 and 20 percent.



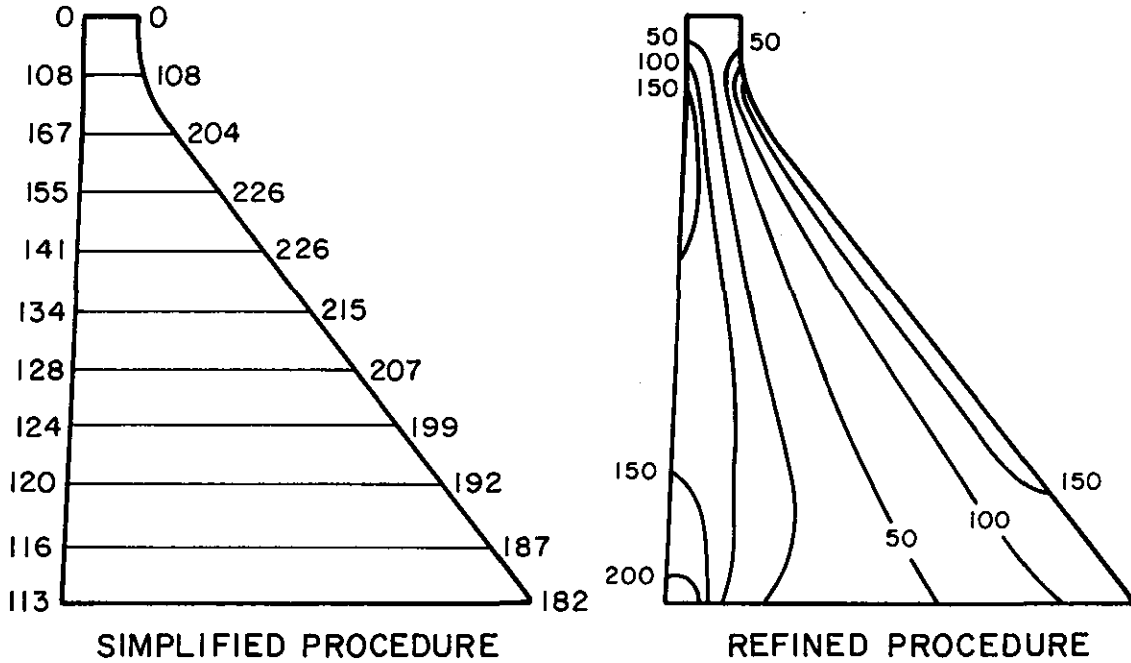


CASE 1. EMPTY RESERVOIR

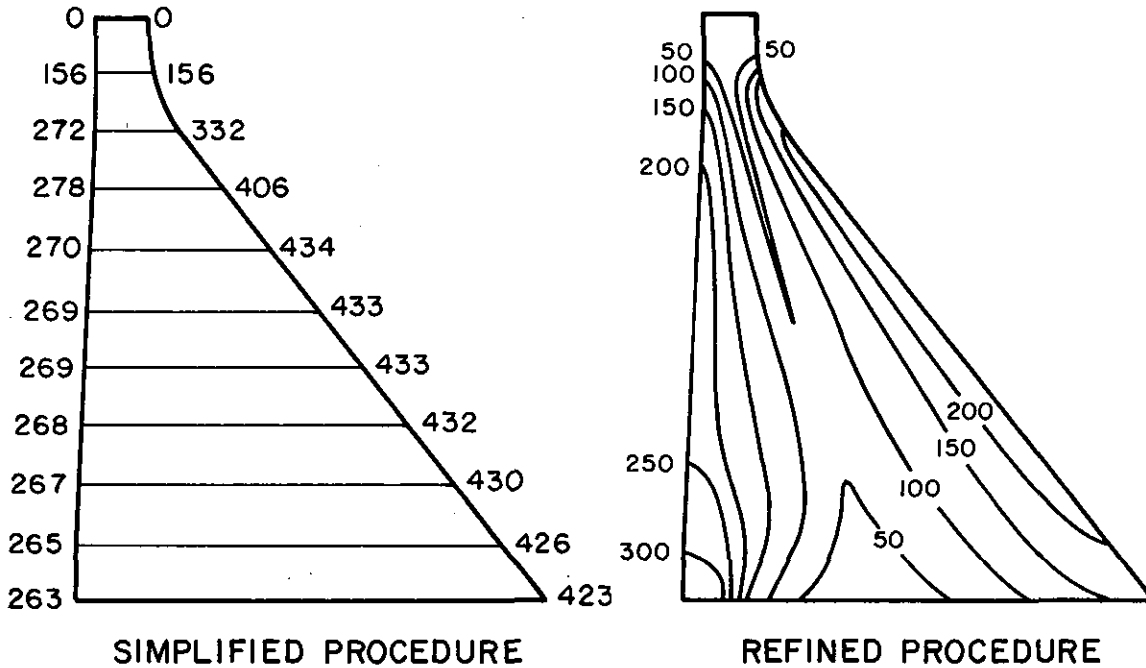


CASE 2. FULL RESERVOIR

Figure 14. Maximum Principal Stresses (in psi) in Pine Flat Dam on Rigid Foundation Rock due to S69E Component of Taft Ground Motion; Cases 1 and 2. Initial Static Stresses are Excluded.

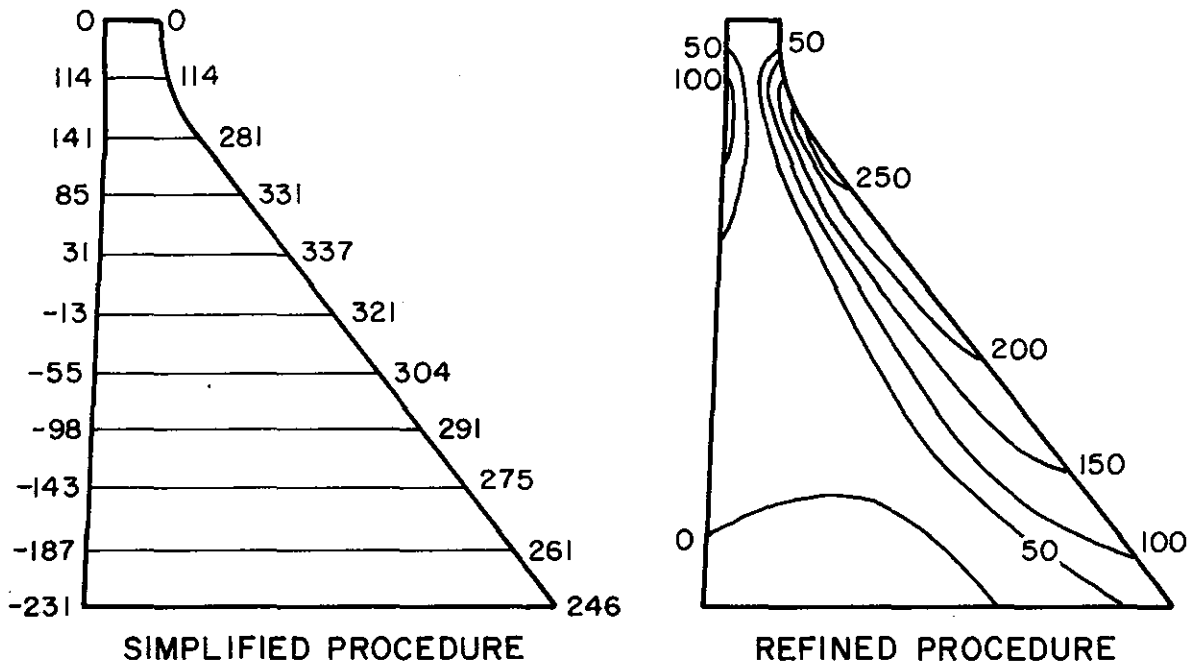


**CASE 3. EMPTY RESERVOIR**

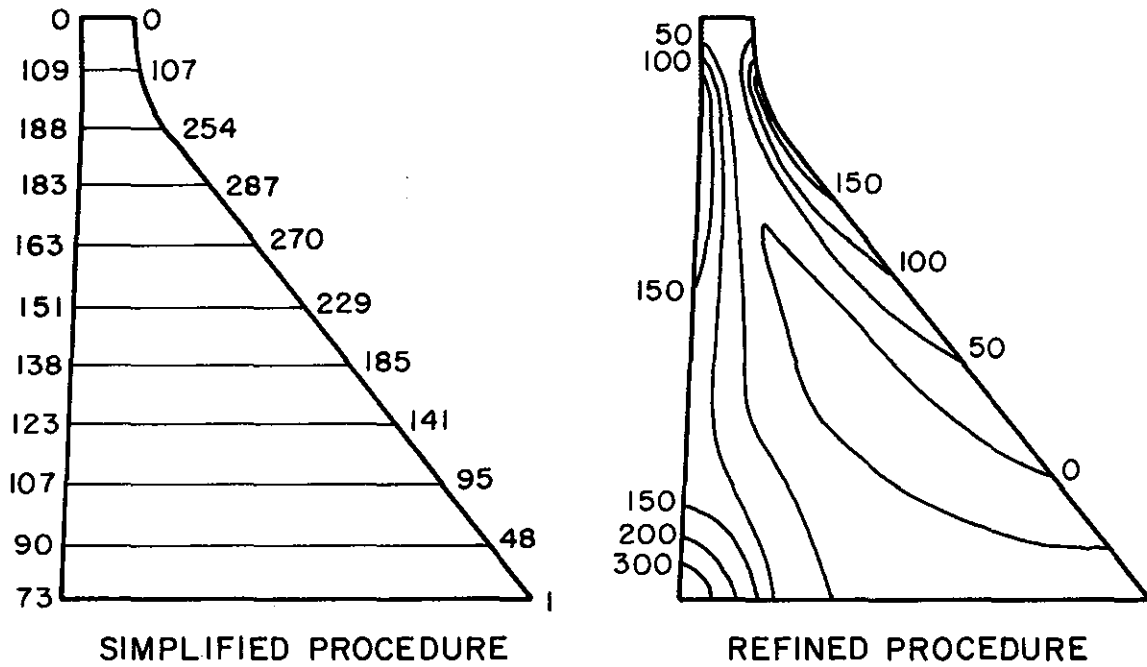


**CASE 4. FULL RESERVOIR**

Figure 15. Maximum Principal Stresses (in psi) in Pine Flat Dam on Flexible Foundation Rock due to S69E Component of Taft Ground Motion; Cases 3 and 4. Initial Static Stresses are Excluded.

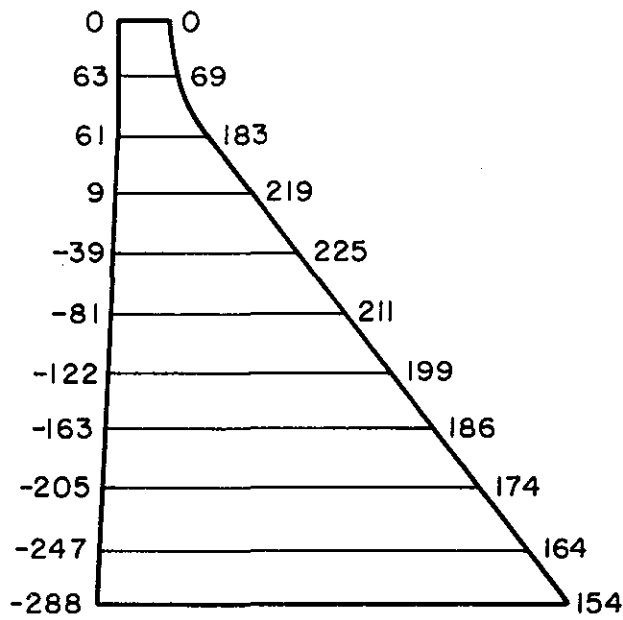


**CASE 1. EMPTY RESERVOIR**

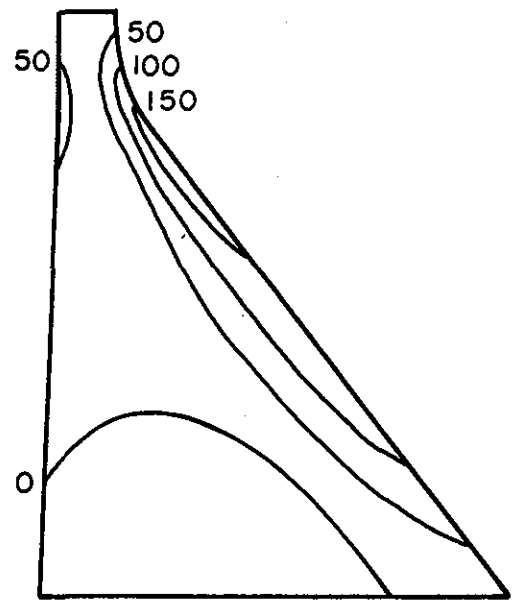


**CASE 2. FULL RESERVOIR**

Figure 16. Maximum Principal Stresses (in psi) in Pine Flat Dam on Rigid Foundation Rock due to S69E Component of Taft Ground Motion; Cases 1 and 2. Initial Static Stresses are Included.

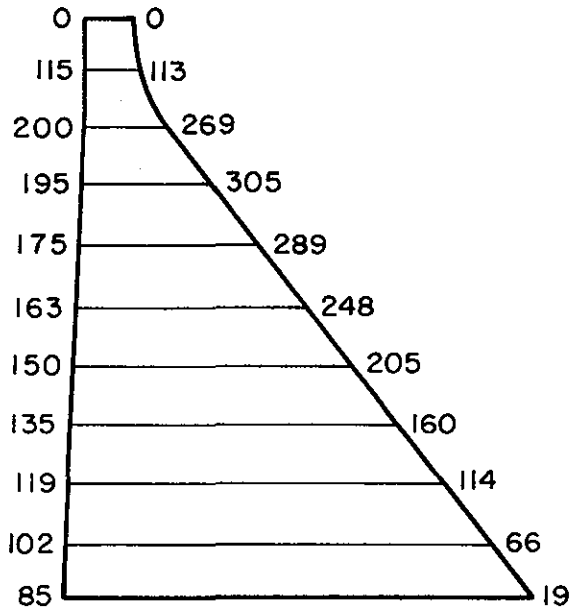


SIMPLIFIED PROCEDURE

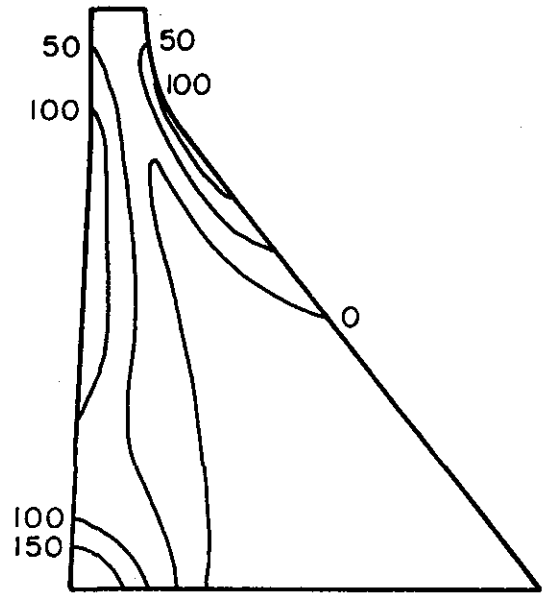


REFINED PROCEDURE

CASE 3. EMPTY RESERVOIR



SIMPLIFIED PROCEDURE



REFINED PROCEDURE

CASE 4. FULL RESERVOIR

Figure 17. Maximum Principal Stresses (in psi) in Pine Flat Dam on Flexible Foundation Rock due to S69E Component of Taft Ground Motion; Cases 3 and 4. Initial Static Stresses are Included.

## APPENDIX A: LIMITATIONS OF THE SIMPLIFIED ANALYSIS PROCEDURE FOR DAM-WATER SYSTEMS

The equivalent SDF system that approximately represents the fundamental mode response of dams was developed in earlier work (see Refs. 4 and 5). In particular, Ref. 4 presented a procedure for computing the vibration properties of the equivalent SDF system for dams on rigid foundation rock including the effects of dam-water interaction and reservoir bottom absorption. The equivalent SDF system representation was shown to be valid for Young's modulus of elasticity of dam concrete,  $E_s$ , of 5 million psi and less (Fig. A.1).

Subsequent investigation has demonstrated that  $E_s = 5$  million psi is an upper limit for which an equivalent SDF system can represent the fundamental mode response of dams including the effects of dam-water interaction and reservoir bottom absorption. Furthermore, while an equivalent SDF system adequately represents the fundamental mode response of dam-water systems with  $E_s = 4$  to 5 million psi the simplified expression derived in Ref. 4 for the natural vibration frequency  $\tilde{\omega}_r$  of the equivalent SDF system is not reliable when reservoir bottom absorption effects are included. This appendix describes further the limitations of the simplified analysis procedure for dam-water systems.

### Limitations of the Equivalent SDF System

The exact fundamental mode response of the standard dam monolith due to unit harmonic horizontal ground acceleration is presented in Figs. A.2 and A.10 for  $E_s = 6$  million psi and various values of the wave reflection coefficient,  $\alpha$ , for the reservoir bottom materials and depth ratio,  $H/H_s$ , of the impounded water. The absolute value of the displacement at the dam crest was evaluated by Eqs. 1 and 6 in Ref. 4. For  $H/H_s \geq 0.75$  and  $\alpha \geq 0.90$ , the response functions exhibit two resonant peaks (Figs. A.2 to A.4). The peak at the lower excitation frequency has a larger magnitude than the second peak at the higher frequency. This phenomenon, described in Ref. 10, is due to interaction between the compressible water and stiff dam. Also described in Ref. 10 was the observation that for  $\alpha \leq 0.50$  the added damping associated with reservoir bottom absorption results in the two resonant peaks

coalescing into a single resonant peak at an intermediate frequency value (see Figs. A.8 to A.10). Thus the response function exhibits one dominant resonant peak if the reservoir bottom materials are highly absorptive ( $\alpha \leq 0.50$ ) or close to nonabsorptive ( $\alpha \geq 0.90$ ). Because the equivalent SDF system can satisfactorily approximate only a single resonant peak (Fig. A.1), it is effective in representing the dam response for  $\alpha \geq 0.90$  and  $\alpha \leq 0.50$  when  $E_s = 6.0$  million psi.

However, the response functions in Figs. A.5 to A.7 show that dam-water systems with an intermediate absorptiveness of the reservoir bottom materials,  $0.50 < \alpha < 0.90$ , do not have a well-defined resonant peak. This is particularly true in the case of  $\alpha = 0.75$  for  $H/H_s$  between 0.85 and 1.0, where the frequency response function shows nearly flat response over a wide range of excitation frequencies. Clearly the representation of this broad-bandwidth response function by a SDF system is prone to substantial error.

#### Limitations of the Approximate Expression for $R_r$

The period lengthening ratio  $R_r$  is defined as  $\tilde{T}_r/T_1$  where  $\tilde{T}_r = 2\pi/\tilde{\omega}_r$ , the natural vibration period of the equivalent SDF system representing the fundamental mode response of the dam with impounded water, and  $T_1$  is the fundamental vibration period of the dam with empty reservoir. In the simplified procedure, an approximate value for  $\tilde{\omega}_r$  is determined from Eq. 18 of Ref. 4.

In preparation of this report, it was discovered that this approximate expression for  $\tilde{\omega}_r$  is not reliable for dams with  $E_s$  greater than 4 million psi. The assumption behind the expression is that the resonant frequency of the dam-water system is approximately the excitation frequency that makes the real-valued component of the denominator in the exact fundamental mode response function zero. This is a good approximation except for relatively stiff dams, where reservoir bottom absorption may reduce the added hydrodynamic mass to such an extent that the real-valued component of the denominator does not equal zero in the excitation frequency range of interest. For such cases, the resonant frequency should be

determined directly from the exact fundamental mode response function, as opposed to the approximate procedure that seeks to find a zero of the real-valued component in the denominator of the response function. Once the resonant frequency is determined, the added hydrodynamic damping ratio  $\xi_r$  can be evaluated, as before, by Eq. 20 in Ref. 4. This improved procedure was followed for computing the standard values presented in this report for the period lengthening ratio,  $R_r$ , and added hydrodynamic ratio,  $\xi_r$ , for dams with  $E_s = 5.0$  and  $4.5$  million psi, and all  $H/H_s$  values;  $E_s = 4.0$  million psi with  $H/H_s \geq 0.80$ ; and  $E_s = 3.5$  million psi with  $H/H_s \geq 0.85$ . The data for other values of  $E_s$  and  $H/H_s$  were generated by the approximate expression presented in Ref. 4.

#### **Comments on Added Hydrodynamic Damping**

Figures A.2 to A.10 show how the frequency response functions of dams vary with the depth of impounded water; these results have not been presented earlier. It is apparent that the resonant frequency of a dam-water system decreases with increasing water depth because of the increasing added hydrodynamic mass (4). The variation of the resonant response magnitude with water depth depends on the effective damping of the dam-water system which is affected by the absorptiveness of the reservoir bottom materials. As shown in Figs. A.2 to A.4, for essentially non-absorptive reservoir bottom materials ( $\alpha \geq 0.90$ ), the resonant response magnitude does not increase monotonically with increasing water depth (except for  $\alpha = 1.0$ ). On the other hand, Figs. A.8 to A.10 show that, for highly absorptive reservoir bottom materials ( $\alpha \leq 0.5$ ), the resonant response magnitude decreases with increasing water depth. In the intermediate range of reservoir bottom absorptiveness ( $0.5 < \alpha < 0.9$ ), the magnitude of the resonant peak is not very sensitive to the water depth for reservoirs at least three-quarters full (Figs. A.5 to A.7).

The trend in resonant response magnitude can be explained in terms of the overall damping of the dam-water system. There are two sources of damping in the system: damping of the dam alone, and hydrodynamic damping due to propagation of hydrodynamic pressure

waves upstream and refraction into the absorptive reservoir bottom materials (4). The combination of opposing trends in the two contributions to effective damping ratio determine the variation of the resonant response magnitude with depth of the impounded water. As the water depth increases, the effectiveness of the structural damping decreases (3,4), tending to increase the resonant response, but the added hydrodynamic damping ratio generally increases, tending to decrease the resonant response. The increase in the added hydrodynamic damping depends on the absorptiveness of the reservoir bottom materials. For relatively absorptive reservoir bottom materials, the added hydrodynamic damping ratio is greater than the reduction in the effective structural damping, so the overall damping ratio increases as the water depth increases (Figs. A.8 to A.10). The variation with water depth is not as straightforward for relatively non-absorptive reservoir bottom materials, in that the added hydrodynamic damping ratio may increase with water depth and then decrease slightly for  $0.90 < H/H_s \leq 1.0$ . This latter trend develops because with a nearly full reservoir the resonant frequency of a stiff dam is reduced far enough below  $\omega_1^*$ , the fundamental resonant frequency of the impounded water alone, that the added hydrodynamic damping is due mainly to refraction of pressure waves into the relatively non-absorptive reservoir bottom materials, thus limiting the energy radiation. As the water depth decreases below  $H/H_s = 0.90$ , the fundamental resonant frequency shifts closer to  $\omega_1^*$ , thus allowing more radiation of energy by propagation of pressure waves upstream. This phenomenon, which is pronounced for  $E_s = 6$  million psi, further explains the rather complicated looking variation of the added hydrodynamic damping ratio presented in Refs. 4 and 5 and in Fig. 5 of this report for other values of  $E_s$ .



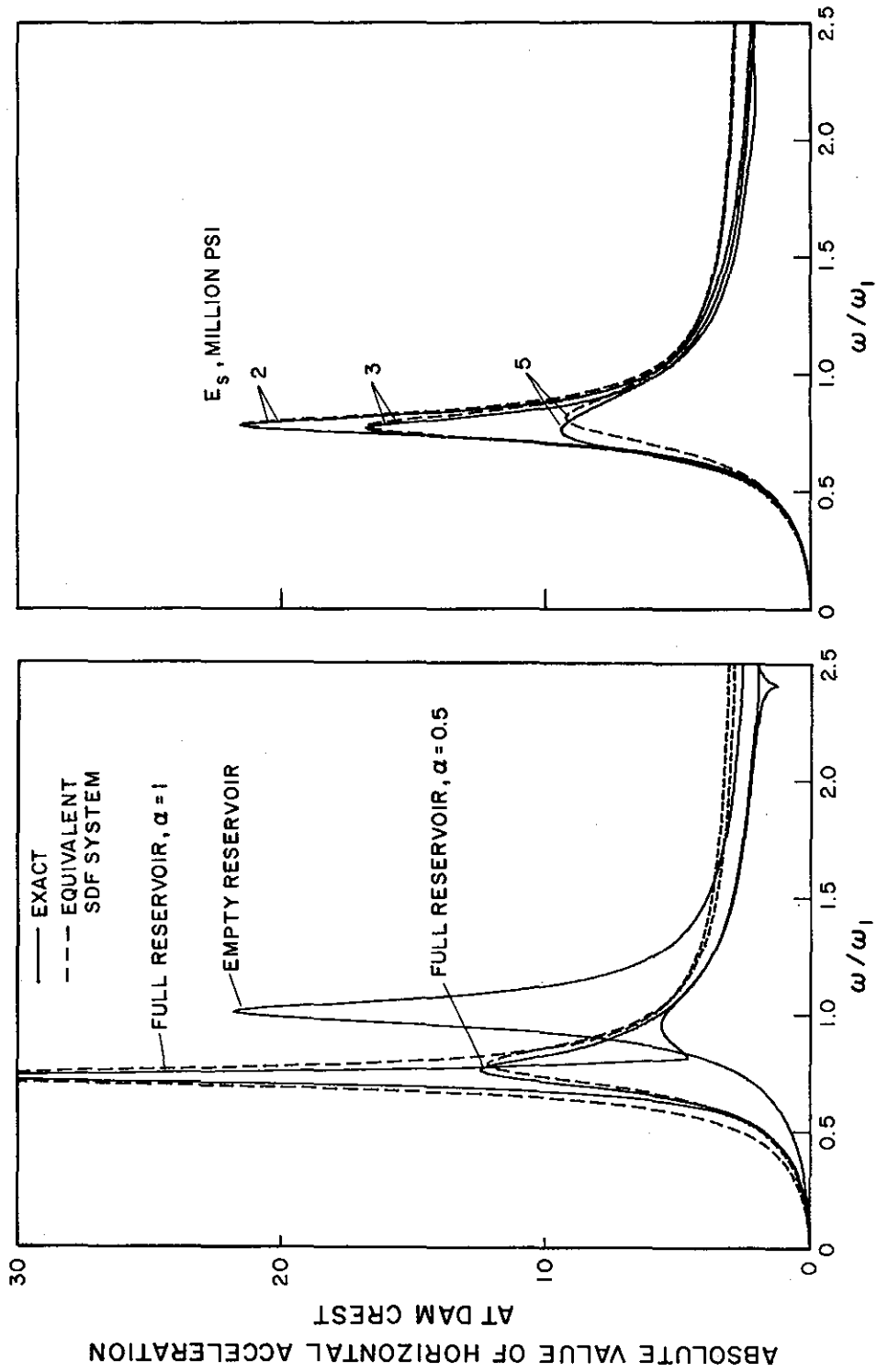


Figure A.1. Comparison of Exact and Equivalent SDF System Response of Dam on Rigid Foundation Rock with Impounded Water due to Harmonic Horizontal Ground Motion.

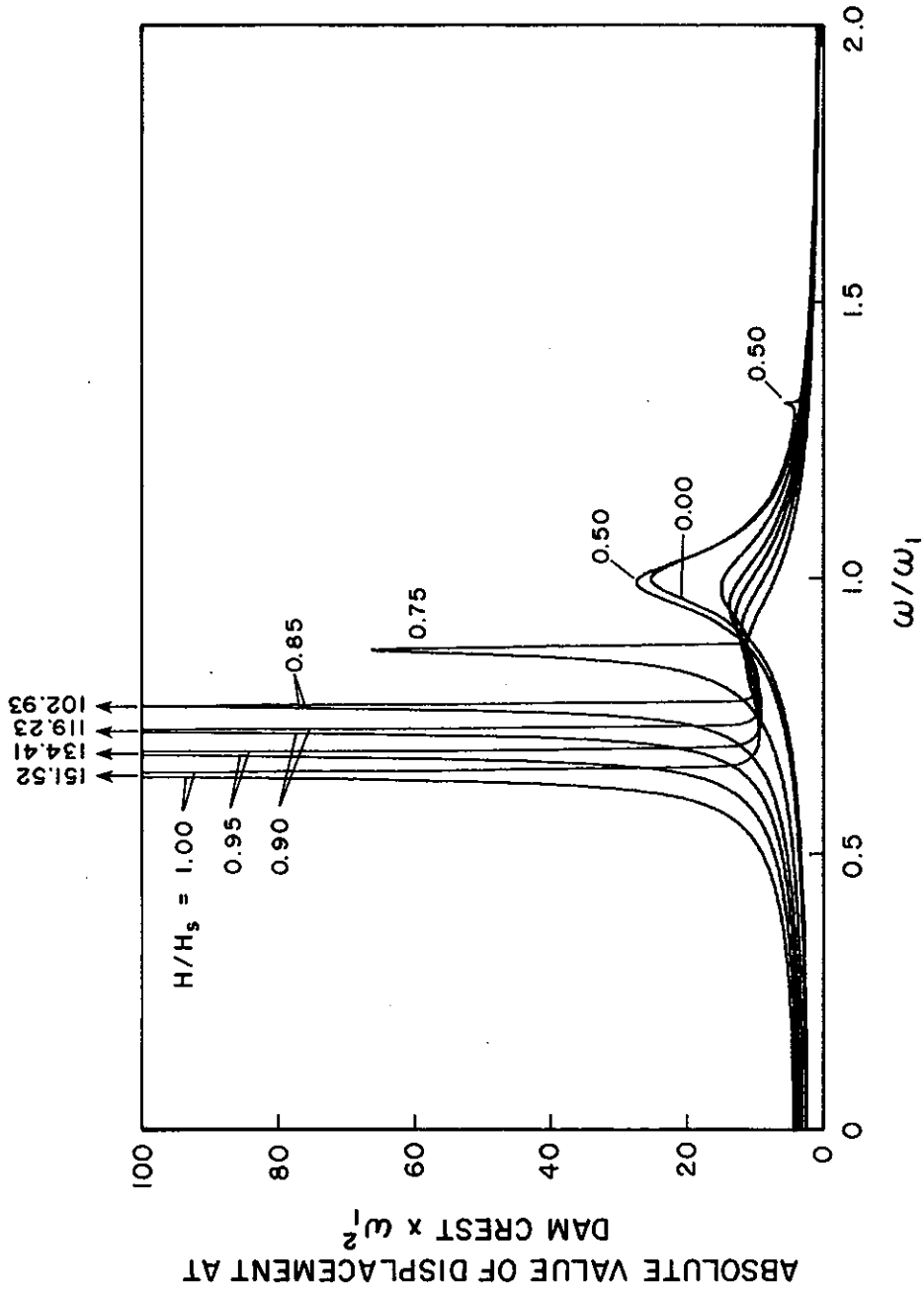


Figure A.2. Fundamental Mode Response of Dams on Rigid Foundation Rock due to Harmonic Horizontal Ground Motion;  $E_s = 6$  million psi,  $\alpha = 1.0$

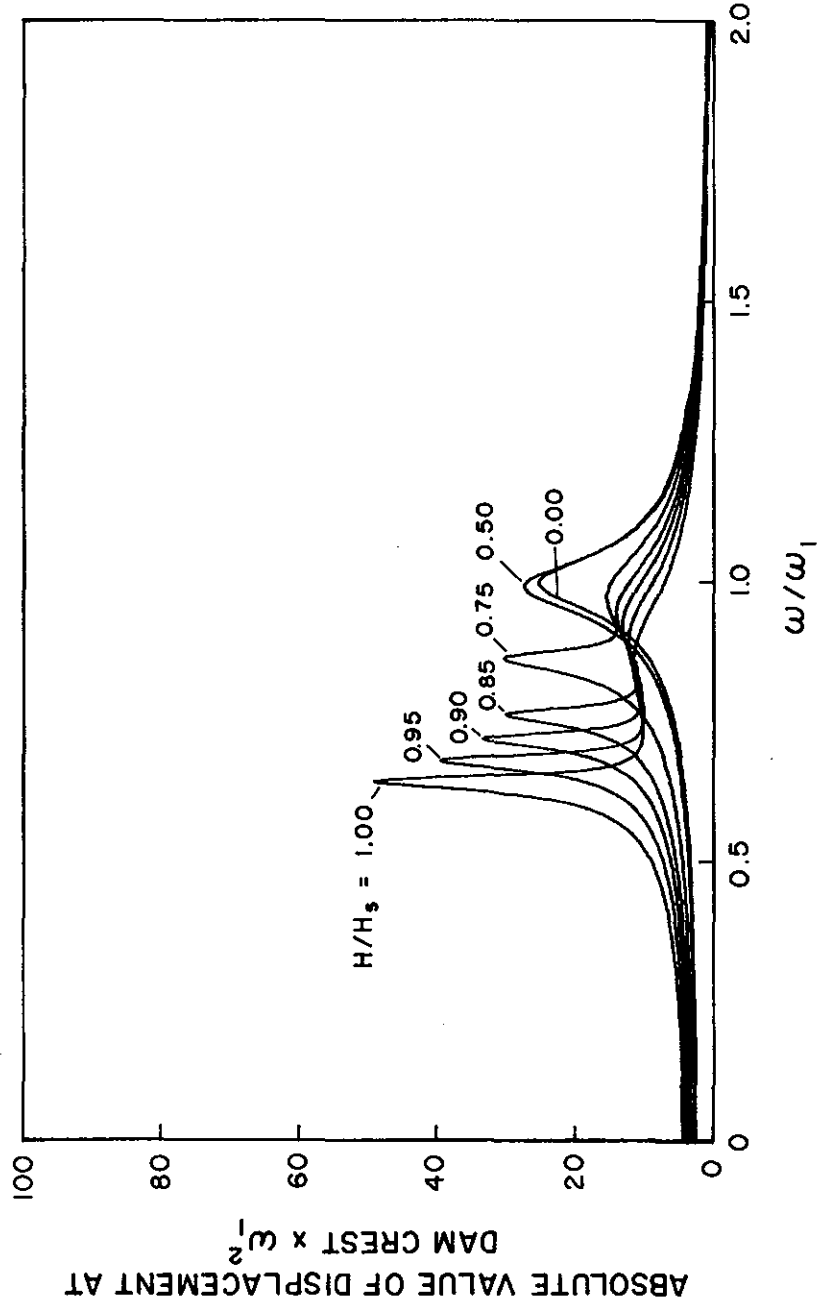


Figure A.3. Fundamental Mode Response of Dams on Rigid Foundation Rock due to Harmonic Horizontal Ground Motion;  $E_s = 6$  million psi,  $\alpha = 0.95$

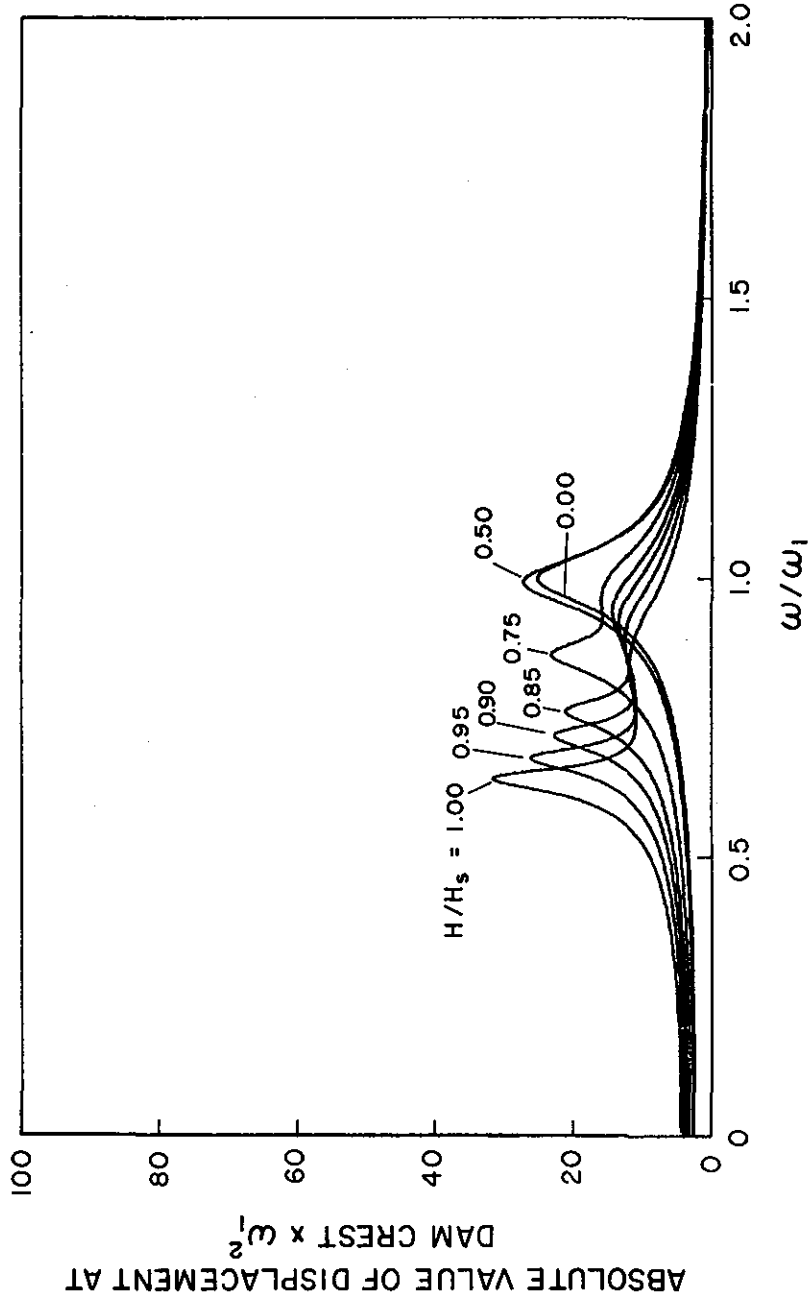


Figure A.4. Fundamental Mode Response of Dams on Rigid Foundation Rock due to Harmonic Horizontal Ground Motion;  $E_s = 6$  million psi,  $\alpha = 0.90$

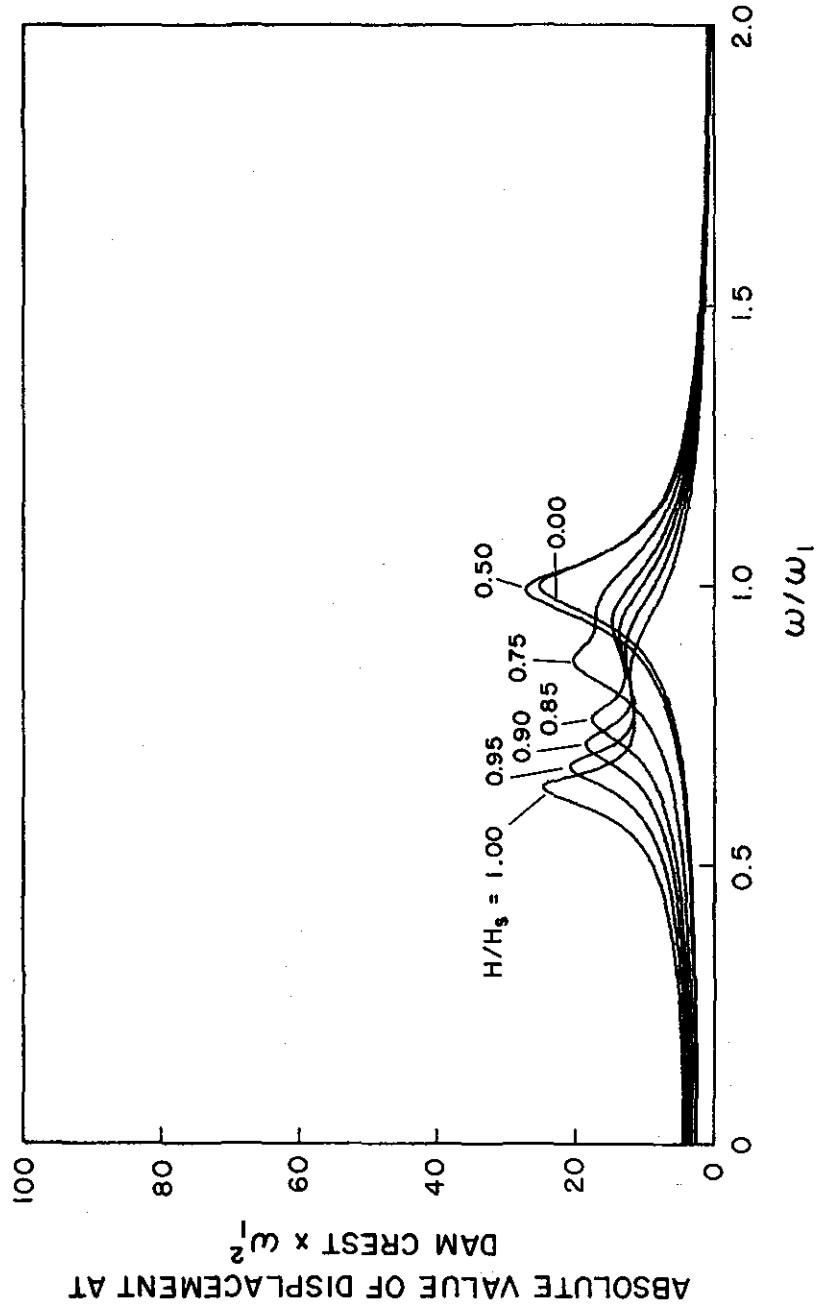


Figure A.5. Fundamental Mode Response of Dams on Rigid Foundation Rock due to Harmonic Horizontal Ground Motion;  $E_s = 6$  million psi,  $\alpha = 0.85$

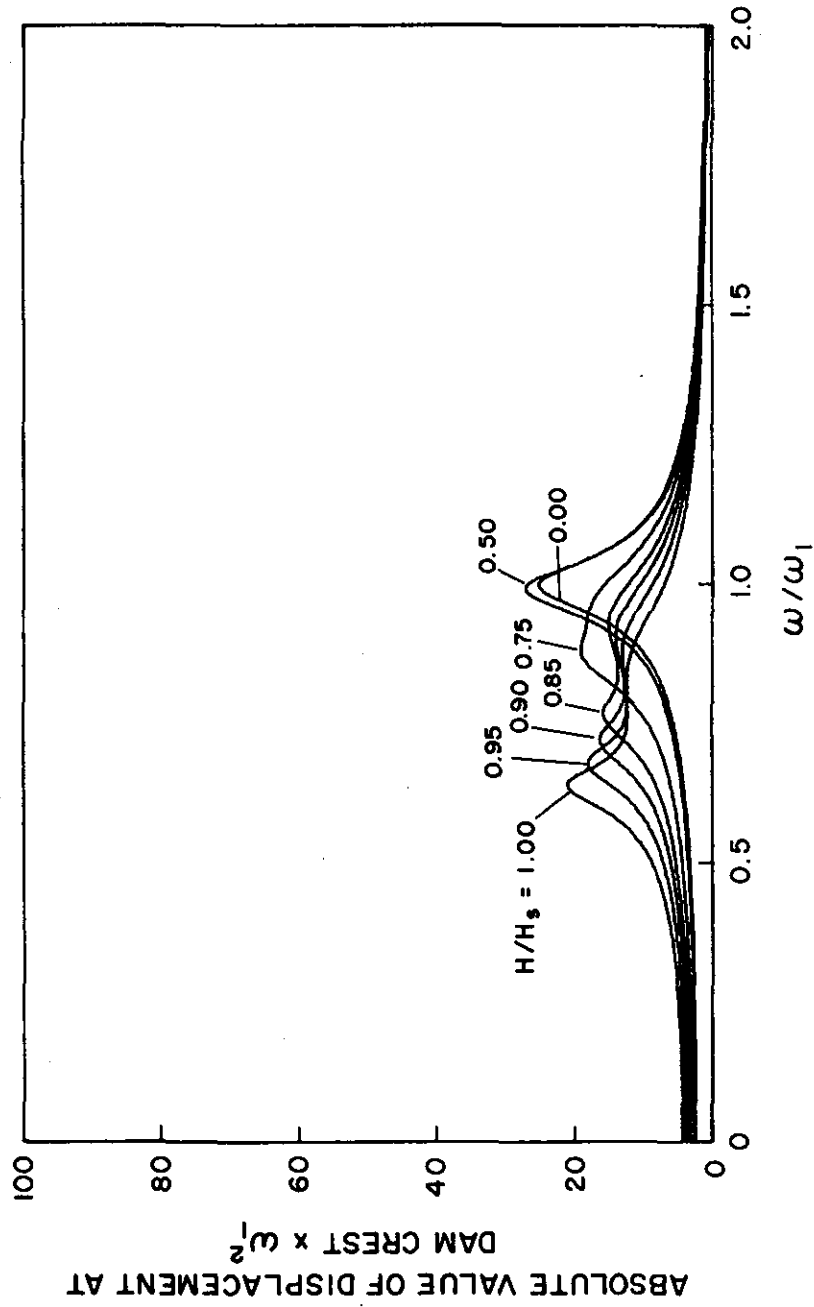


Figure A.6. Fundamental Mode Response of Dams on Rigid Foundation Rock due to Harmonic Horizontal Ground Motion;  $E_s = 6$  million psi,  $\alpha = 0.80$

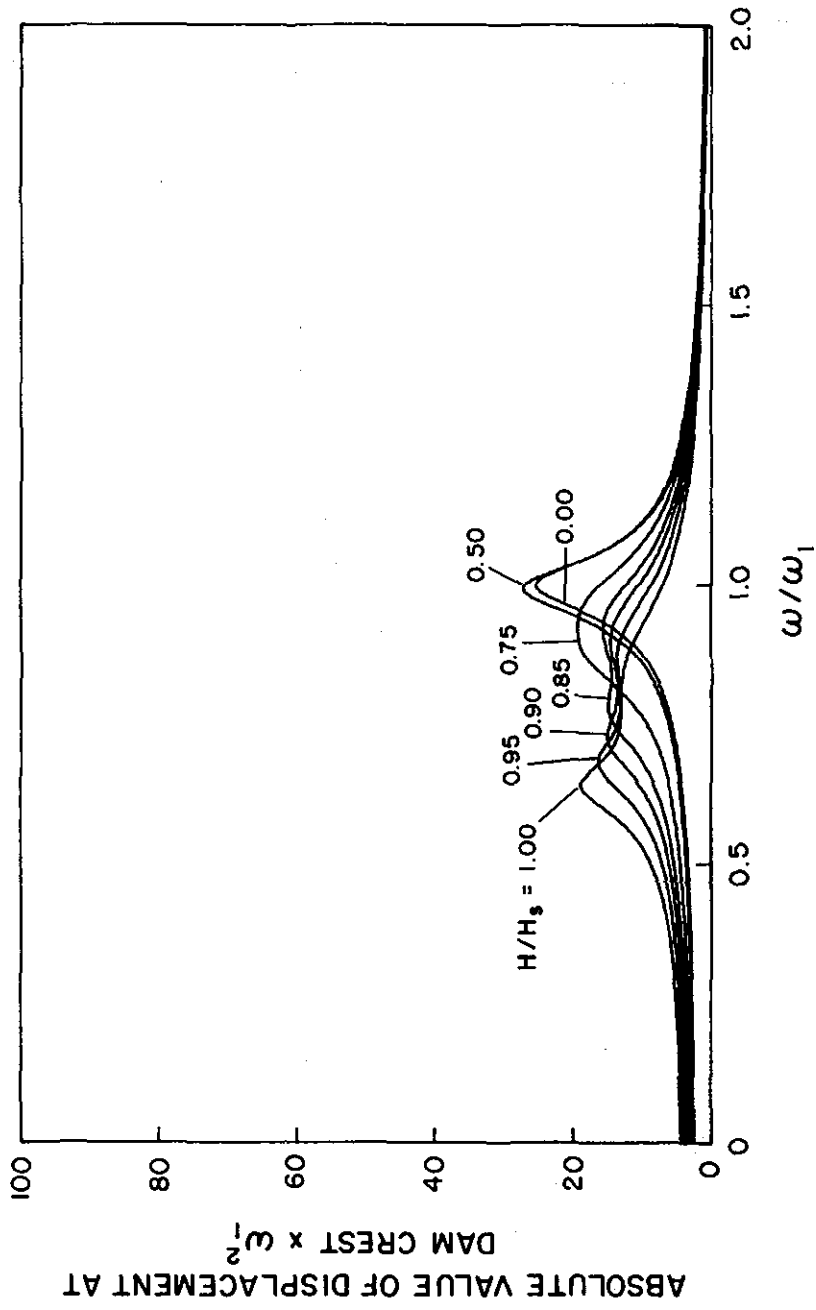


Figure A.7. Fundamental Mode Response of Dams on Rigid Foundation Rock due to Harmonic Horizontal Ground Motion;  $E_s = 6$  million psi,  $\alpha = 0.75$

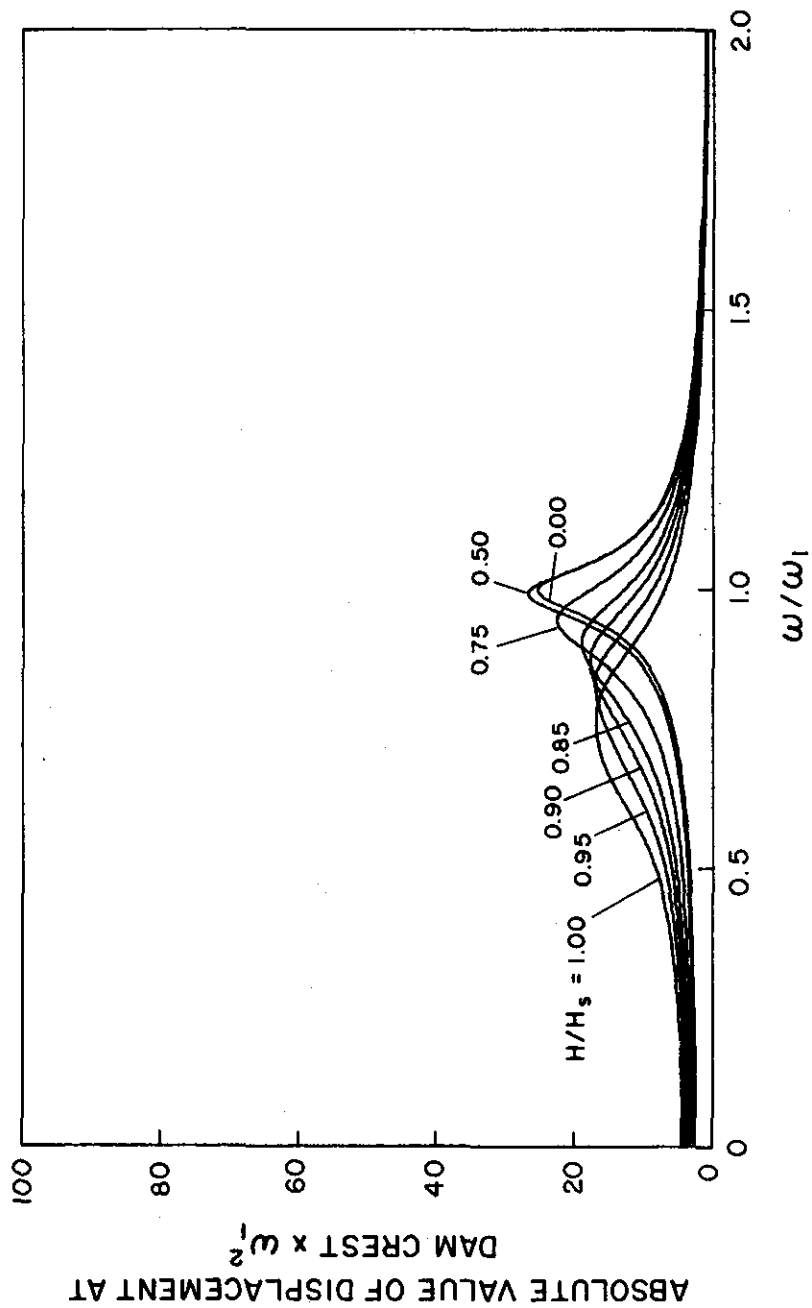


Figure A.8. Fundamental Mode Response of Dams on Rigid Foundation Rock due to Harmonic Horizontal Ground Motion;  $E_s = 6$  million psi,  $\alpha = 0.50$



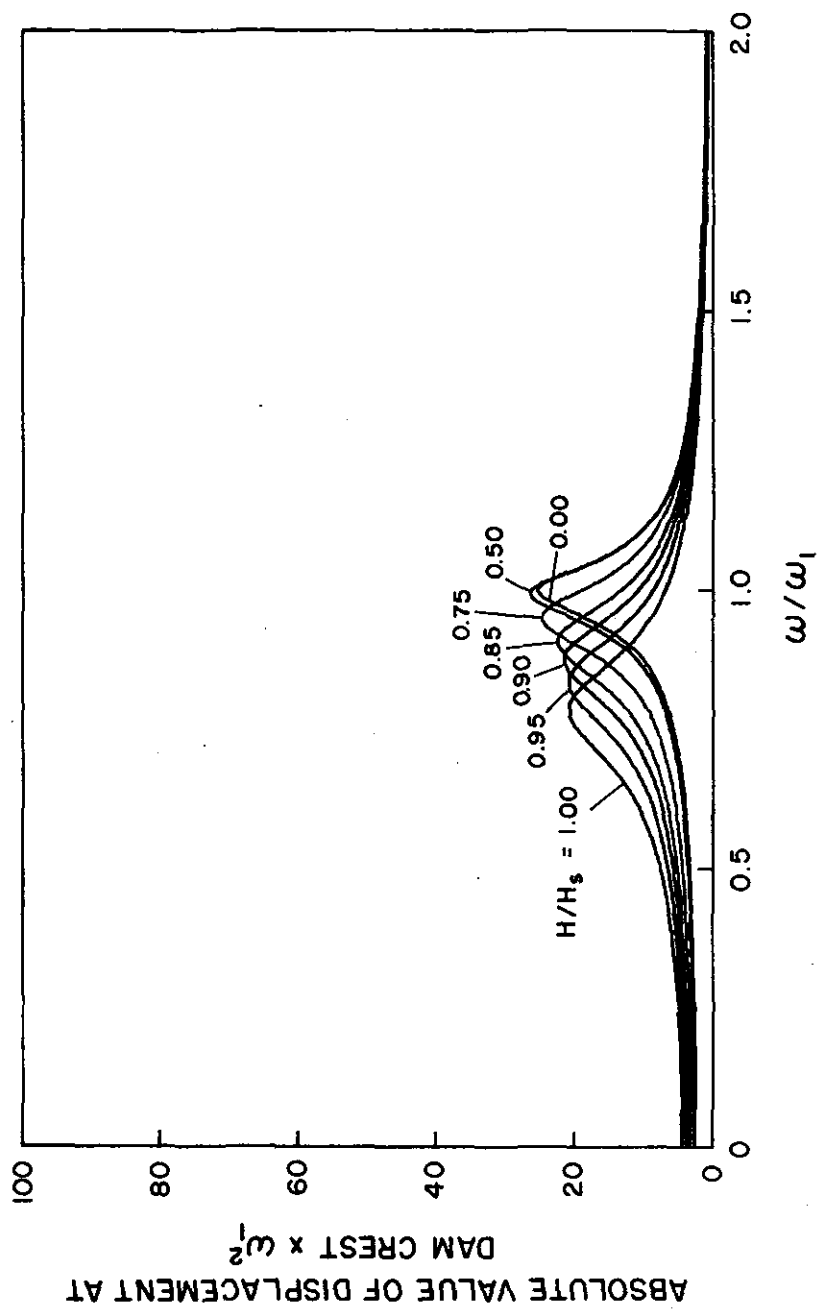


Figure A.9. Fundamental Mode Response of Dams on Rigid Foundation Rock due to Harmonic Horizontal Ground Motion;  $E_s = 6$  million psi,  $\alpha = 0.25$

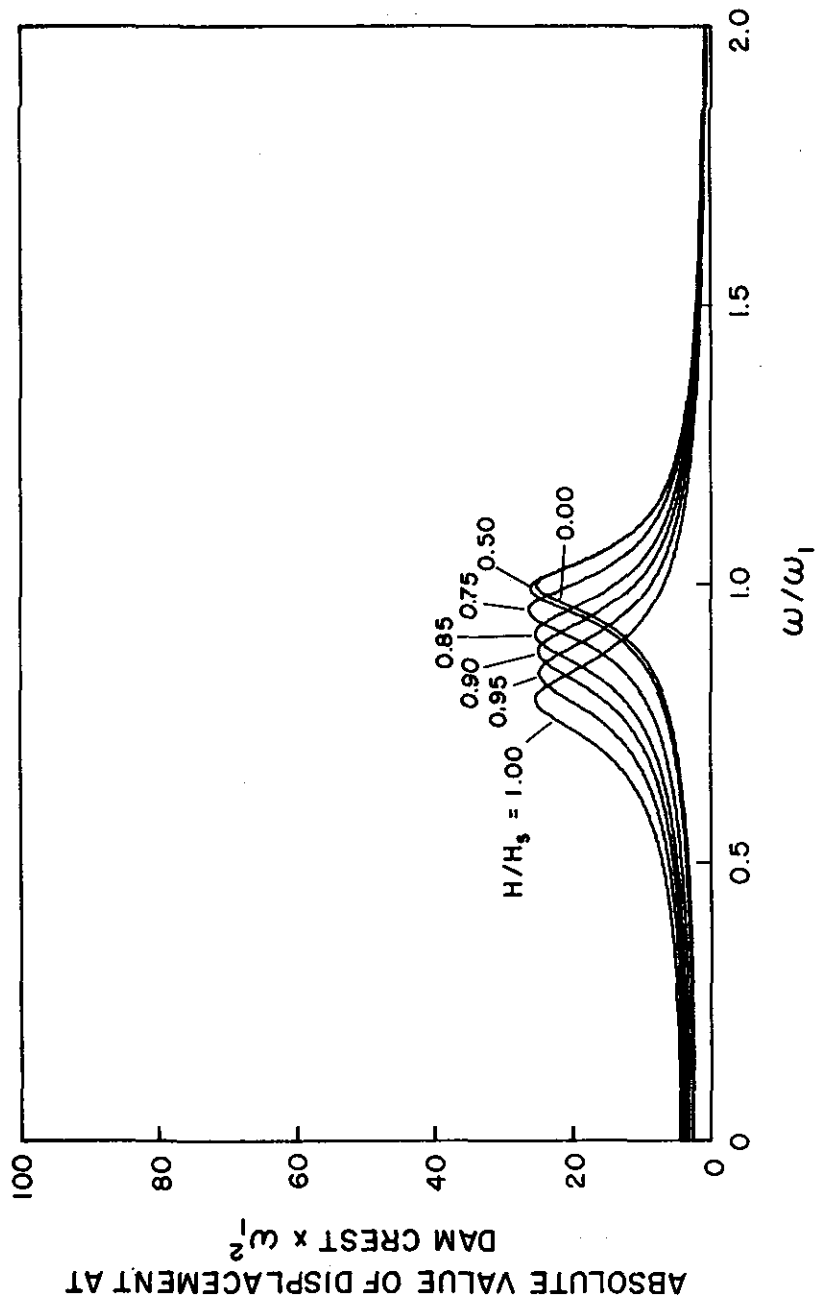


Figure A.10. Fundamental Mode Response of Dams on Rigid Foundation Rock due to Harmonic Horizontal Ground Motion;  $E_s = 6$  million psi,  $\alpha = 0$

## APPENDIX B: RESPONSE CONTRIBUTIONS OF HIGHER VIBRATION MODES

### Dams with Empty Reservoir

The maximum earthquake effects associated with the contribution of the  $n$ th mode of dam vibration to the response of the dam can be represented by equivalent lateral forces (2)

$$f_n(y) = m_s(y) \phi_n(y) \omega_n^2 \bar{Y}_n \quad (\text{B.1})$$

in which  $\bar{Y}_n$  is the maximum value of  $Y_n(t)$  which is governed by the  $n$ th modal equation

$$\ddot{Y}_n + 2\xi_n \omega_n \dot{Y}_n + \omega_n^2 Y_n = -\frac{L_n}{M_n} a_g(t) \quad (\text{B.2})$$

In Eqs. B.1 and B.2, the mass per unit height of the dam  $m_s(y) = w_s(y)/g$ ;  $\omega_n$  and  $\phi_n(y)$  are the natural frequency and the horizontal component of the shape of the  $n$ th mode of vibration;  $\xi_n$  is the damping ratio for this mode;  $a_g(t)$  is the ground acceleration; the generalized mass  $M_n$  and the generalized earthquake force coefficient  $L_n$  are:

$$M_n = \int_0^{H_s} m_s(y) \phi_n^2(y) dy \quad (\text{B.3a})$$

$$L_n = \int_0^{H_s} m_s(y) \phi_n(y) dy \quad (\text{B.3b})$$

Just as in the case of multistory buildings (14), soil-structure interaction effects may be neglected in a simplified procedure to compute the contributions of the higher vibration modes in the earthquake response of dams. Therefore these interaction effects have not been included in Eqs. B.1-B.3.

Because the periods of the higher vibration modes of concrete gravity dams are very short, an approximation to  $Y_n(t)$  is given by a "static" solution of Eq. B.2, i.e., by dropping the inertial and damping terms:

$$\omega_n^2 Y_n(t) = -\frac{L_n}{M_n} a_g(t), \quad n = 2, 3, \dots \quad (\text{B.4})$$

Thus,  $\bar{Y}_n$ , the maximum value of  $Y_n(t)$ , is given by

$$\omega_n^2 \bar{Y}_n = \frac{-L_n}{M_n} \bar{a}_g \quad (\text{B.5})$$

where  $\bar{a}_g$  is the maximum ground acceleration. Substitution of Eq. B.5 in Eq. B.1 gives

$$f_n(y) = \frac{-L_n}{M_n} m_s(y) \phi_n(y) \bar{a}_g \quad (\text{B.6})$$

This is the “static correction” method for representing the contributions of higher vibration modes (1, 12).

Alternatively we could start with the expression for the maximum equivalent lateral forces in terms of the earthquake response spectrum (2):

$$f_n(y) = \frac{L_n}{M_n} S_{an} m_s(y) \phi_n(y) \quad (\text{B.7})$$

in which  $S_{an} = S_a(T_n, \xi_n)$  is the ordinate of the pseudo-acceleration response spectrum for the ground motion evaluated at the  $n$ th mode vibration period  $T_n = 2\pi/\omega_n$  and damping ratio  $\xi_n$ . Because the periods of the higher vibration modes of concrete gravity dams are very short, the corresponding ordinates of the pseudo-acceleration response spectrum will be essentially equal to the maximum ground acceleration, i.e.  $S_{an} = \bar{a}_g$ . With little dynamic amplification, the higher vibration modes respond essentially in a “static” manner leading to:

$$f_n(y) = \frac{L_n}{M_n} m_s(y) \phi_n(y) \bar{a}_g \quad (\text{B.8})$$

which is the same as Eq. B.6, but for the negative sign which had been dropped in Eq. B.7 (2).

Thus the maximum response in each higher vibration mode is attained at the same instant of time, when the ground acceleration attains its maximum value  $\bar{a}_g$ . Based on this implication of the “static correction” concept, the maximum earthquake effects associated with all vibration modes higher than the fundamental are given by the equivalent lateral forces  $f_{sc}(y) = \sum_{n=2}^{\infty} f_n(y)$  which upon substitution of Eq. B.6 gives

$$f_{sc}(y) = - \sum_{n=2}^{\infty} \frac{L_n}{M_n} m_s(y) \phi_n(y) \bar{a}_g \quad (\text{B.9})$$

The deformation response of a dam to ground acceleration  $a_g(t)$  will be identical to the response of the structure on fixed base subjected to external forces equal to mass per unit height times the ground acceleration, acting opposite to the sense of ground acceleration. As shown in Ref. 2, the ground motion can therefore be replaced by effective forces  $= -m_s(y) a_g(t)$ . Corresponding to the maximum ground acceleration these forces are  $-m_s(y) \bar{a}_g$  which can be expressed as the summation of modal contributions:

$$-m_s(y) \bar{a}_g = -\sum_{n=1}^{\infty} \frac{L_n}{M_n} m_s(y) \phi_n(y) \bar{a}_g \quad (\text{B.10})$$

which can be utilized to rewrite Eq. B.9 as

$$f_{sc}(y) = -\frac{1}{g} w_s(y) \left[ 1 - \frac{L_1}{M_1} \phi_1(y) \right] \bar{a}_g \quad (\text{B.11})$$

Because the direction of the lateral earthquake forces is reversible, the sign of  $f_{sc}(y)$  is not relevant. Dropping the negative sign in Eq. B.11 and replacing  $\phi_1(y)$  by  $\phi(y)$  and  $\bar{a}_g$  by  $a_g$ , for convenience of notation, leads to Eq. 13.

### Dams with Impounded Water

The effects of dam-water interaction can be interpreted as introducing an added force and modifying the properties of the dam by an added mass and an added damping, which result in a modification of Eq. B.2 (10). Because the inertial and damping terms are dropped from Eq. B.2 in the "static correction" method of obtaining higher mode response, only the added hydrodynamic force (or pressure)  $-p_o(y)a_g(t)$  need be considered in representing hydrodynamic effects in Eq. B.2. Thus Eq. B.5 becomes

$$\omega_n^2 \bar{Y}_n = -\left[ \frac{L_n}{M_n} + \frac{1}{M_n} \int_0^H p_o(y) \phi_n(y) dy \right] \bar{a}_g \quad (\text{B.12})$$

in which  $p_o(y)$  is a real-valued, frequency-independent function describing the hydrodynamic pressure on a rigid dam, undergoing unit acceleration, with water compressibility neglected.

Substitution of Eq. B.12 into Eq. B.1 and summation over all vibration modes higher than the fundamental gives

$$f_{sc}(y) = - \sum_{n=2}^{\infty} \frac{L_n}{M_n} m_s(y) \phi_n(y) \bar{a}_g - \sum_{n=2}^{\infty} \frac{B_n}{M_n} m_s(y) \phi_n(y) \bar{a}_g \quad (\text{B.13})$$

in which

$$B_n = \int_0^H p_o(y) \phi_n(y) dy \quad (\text{B.14})$$

Representing the maximum value of the added hydrodynamic pressure as a summation of modal contributions leads to

$$-p_o(y) \bar{a}_g = - \sum_{n=1}^{\infty} \frac{B_n}{M_n} m_s(y) \phi_n(y) \bar{a}_g \quad (\text{B.15})$$

Equations B.10 and B.15 can be utilized to rewrite Eq. B.13 as

$$f_{sc}(y) = - \frac{1}{g} \left\{ w_s(y) \left[ 1 - \frac{L_1}{M_1} \phi_1(y) \right] + \left[ gp_o(y) - \frac{B_1}{M_1} w_s(y) \phi_1(y) \right] \right\} \bar{a}_g \quad (\text{B.16})$$

As before, dropping the negative sign in Eq. B.16 and replacing  $\phi_1(y)$  by  $\phi(y)$  and  $\bar{a}_g$  by  $a_g$  leads to Eq. 14.

For reasons mentioned earlier in this Appendix, dam-foundation rock interaction effects are neglected in the simplified analysis of higher mode response; thus Eq. B.16 is still applicable.

## APPENDIX C: DETAILED CALCULATIONS FOR PINE FLAT DAM

This appendix presents the detailed calculations required in the simplified analysis procedure as applied to the tallest, nonoverflow monolith of Pine Flat Dam. The simplified procedure is directly applicable because the upstream face of the dam is nearly vertical and the tail water effects are neglected. All computations are performed for a unit width of the dam monolith. Only the details for Case 4 in Table 7 (full reservoir and flexible foundation rock) are presented.

### Simplified Model of Monolith

The tallest, nonoverflow monolith of Pine Flat Dam is divided into ten blocks of equal height. Using a unit weight of 155 pcf for the concrete, the properties of the blocks are presented in Table C.1, from which the total weight is 9486 kips. Replacing the integrals in Eq. 7 by summations over the blocks gives:

$$M_1 \approx \frac{1}{g} \sum_{i=1}^{10} w_i \phi^2(y_i) = \frac{1}{g} (500 \text{ kip}) \quad (\text{C.1})$$

$$L_1 \approx \frac{1}{g} \sum_{i=1}^{10} w_i \phi(y_i) = \frac{1}{g} (1390 \text{ kip}) \quad (\text{C.2})$$

where  $w_i$  and  $y_i$  are the weight of block  $i$  and the elevation of its centroid, respectively. Additional properties of the simplified model are listed in Table C.2.

### Equivalent Lateral Forces -- Fundamental Mode

The equivalent lateral earthquake forces  $f_1(y)$  are given by Eq. 8, evaluated at each level using  $S_a(\tilde{T}_1, \tilde{\xi}_1)/g = 0.327$  (from Table 7) and  $\tilde{L}_1/\tilde{M}_1 = 3.41$  (from step 8 in the simplified procedure). The calculations are summarized in Table C.3.

### Stress Computation -- Fundamental Mode

The equivalent lateral earthquake forces  $f_1(y)$  consist of forces associated with the mass of the dam (the first term of Eq. 8) and the hydrodynamic pressure at the upstream face (the second term). For the purpose of computing bending stresses in the monolith, the forces associated with the mass are applied at the centroids of the blocks. The forces due to the hydrodynamic pressure are applied as a linearly distributed load to the upstream face of each block. Due to these two sets of lateral forces (Table C.3), the resultant bending moments in the monolith are computed at each level from the equations of equilibrium. The normal bending stresses are obtained from elementary beam theory. A computer program (described in Appendix D) was developed for computation of the normal bending stresses in a dam monolith due to equivalent lateral earthquake forces. Using this procedure, the normal bending stresses  $\sigma_{y1}$  at the two faces of Pine Flat Dam associated with the fundamental vibration mode response of the dam to the S69E component of Taft ground motion were computed (Table C.4).

The maximum principal stresses at the upstream and downstream faces due to the fundamental vibration mode response can be computed from the normal bending stresses  $\sigma_{y1}$  by an appropriate transformation (see Ref. 13, Figs. 4-2 and 4-3, pp. 41-42):

$$\sigma_1 = \sigma_{y1} \sec^2\theta + p_1 \tan^2\theta \quad (C.3)$$

where  $\theta$  is the angle of the face with respect to the vertical. Because no tail water is included in the analysis, the hydrodynamic pressure  $p_1 = 0$  for the downstream face. At the upstream face the hydrodynamic pressure  $p_1$  is given by the second term of Eq. 8:

$$p_1(y) = \frac{\tilde{L}_1}{\tilde{M}_1} S_a(\tilde{T}_1, \tilde{\xi}_1) p(y, \tilde{T}_r) \quad (C.4)$$

which was computed in Steps 1-9 of the simplified procedure. For the upstream face of Pine Flat Dam,  $\theta = 0^\circ$  near the top and  $\theta = 2.86^\circ$  at lower elevations. For such small values of  $\theta$ , the second term in Eq. C.3 turns out to be negligible.

The maximum principal stresses  $\sigma_1$  due to the fundamental vibration mode response are given in Table C.5. Note that Eq. C.3 is evaluated at each level with  $\theta$  for the block above that level.



### Equivalent Lateral Forces -- Higher Vibration Modes

The equivalent lateral earthquake forces  $f_{sc}(y)$  due to the higher vibration modes are given by Eq. 14, evaluated at each level using the maximum ground acceleration for the S69E component of the Taft Ground motion  $a_g = 0.18$  g, and  $L_1/M_1 = 2.78$  and  $B_1/M_1 = 0.425$ . The results are summarized in Table C.6. The calculation of bending moments due to the higher vibration modes is similar to the moment calculations for the fundamental vibration mode, as described previously.

### Stress Computation -- Higher Vibration Modes

The normal bending stresses at the faces of the monolith due to the equivalent lateral earthquake forces  $f_{sc}(y)$  are computed by the procedure described above for stresses due to forces  $f_1(y)$ . The resulting normal bending stresses  $\sigma_{y,sc}$  presented in Table C.7 are due to the response contributions of the higher vibration modes.

The maximum principal stresses at the upstream and downstream faces due to the higher vibration modes can be computed from the normal bending stresses  $\sigma_{y,sc}$  by a transformation similar to Eq. C.3:

$$\sigma_{sc} = \sigma_{y,sc} \sec^2\theta + p_{sc} \tan^2\theta \quad (\text{C.5})$$

Because no tail water is included in the analysis, the hydrodynamic pressure  $p_{sc} = 0$  for the downstream face. At the upstream face the hydrodynamic pressure  $p_{sc}$  is given by the second term of Eq. 14:

$$p_{sc}(y) = \left[ gp_o(y) - \frac{B_1}{M_1} w_s(y) \phi(y) \right] \frac{\bar{a}_g}{g} \quad (\text{C.6})$$

which was computed in step 11 of the simplified procedure. However, the contribution of the second term in Eq. C.5 is negligible because, as mentioned earlier,  $\theta$  is very small. The maximum principal stresses  $\sigma_{sc}$  due to the response contributions of the higher vibration modes are given in Table C.8.

### Initial Static Stresses

The maximum principal stresses at the upstream and downstream faces due to the initial forces on the dam -- self weight, hydrostatic pressure, thermal effects, etc. -- can be computed from the normal stresses  $\sigma_{y,st}$ , which include the effects of direct forces, and a transformation similar to Eqs. 35 and 37:

$$\sigma_{st} = \sigma_{y,st} \sec^2\theta + p_{st} \tan^2\theta \quad (C.7)$$

Because no tail water is included in the example analysis, the hydrostatic pressure  $p_{st} = 0$  for the downstream face. At the upstream face, the hydrostatic pressure  $p_{st}(y) = w(H-y)$ . However, the contribution of the second term in Eq. C.7 is negligible because, as mentioned earlier,  $\theta$  is very small for the upstream face. The maximum principal stresses  $\sigma_{st}$  due to the self weight of the dam and hydrostatic pressure are given in Table C.9.

### Response Combination: Maximum Principal Stresses

The SRSS or ABSUM combination rules (Eqs. 16-17) are applicable to the computation of any response quantity that is proportional to the generalized modal coordinate responses. Thus these combination rules are generally inappropriate to determine the principal stresses. However, as shown in the preceding sections, the second terms in Eqs. C.3, C.5 and C.7 are negligible in the analysis of Pine Flat Dam. Such would be the case for most gravity dams because the upstream face is usually almost vertical and the effects of tail water at the downstream face are small. Thus, the principal stresses in Eqs. C.3 and C.5 become proportional to the corresponding normal bending stresses (and hence to the modal coordinates) with the same proportionality constant  $\sec^2\theta$ . In this situation, the combination rules obviously apply to the principal stresses.

The maximum principal stresses  $\sigma_1$  due to the fundamental vibration mode (Table C.5) and  $\sigma_{sc}$  due to the higher vibration modes (Table C.8) are combined by the SRSS rule (Eq. 16) to obtain an estimate of the dynamic stress  $\sigma_d$ . The results at various levels in the dam are shown in Table C.9 and in Case 4 of Fig. 15.

The stresses  $\sigma_{st}$  at the faces of the monolith due to the initial static loads (weight of the dam and hydrostatic pressure), computed using elementary beam theory, are also shown in Table C.9. The total stresses, obtained by combining the static and dynamic stresses according to Eq. 18, are presented in Table C.9 and in Case 4 of Fig. 17.

Table C.1 - Properties of the Simplified Model

Block	Weight, w (k)	Elevation of centroid (ft)	$\phi$ at centroid	$w \phi$ (k)	$w \phi^2$ (k)
1	202.8	379.9	0.865	175.4	151.7
2	267.4	338.5	0.612	163.6	100.1
3	417.7	298.6	0.450	188.0	84.6
4	610.8	258.9	0.331	202.2	70.0
5	816.7	219.2	0.238	194.4	46.3
6	1022	179.3	0.164	167.6	27.5
7	1228	139.4	0.107	131.4	14.1
8	1434	99.5	0.065	93.2	6.1
9	1640	59.6	0.034	55.8	1.9
10	1846	19.6	0.010	18.5	0.2
Total	9486			1390	500

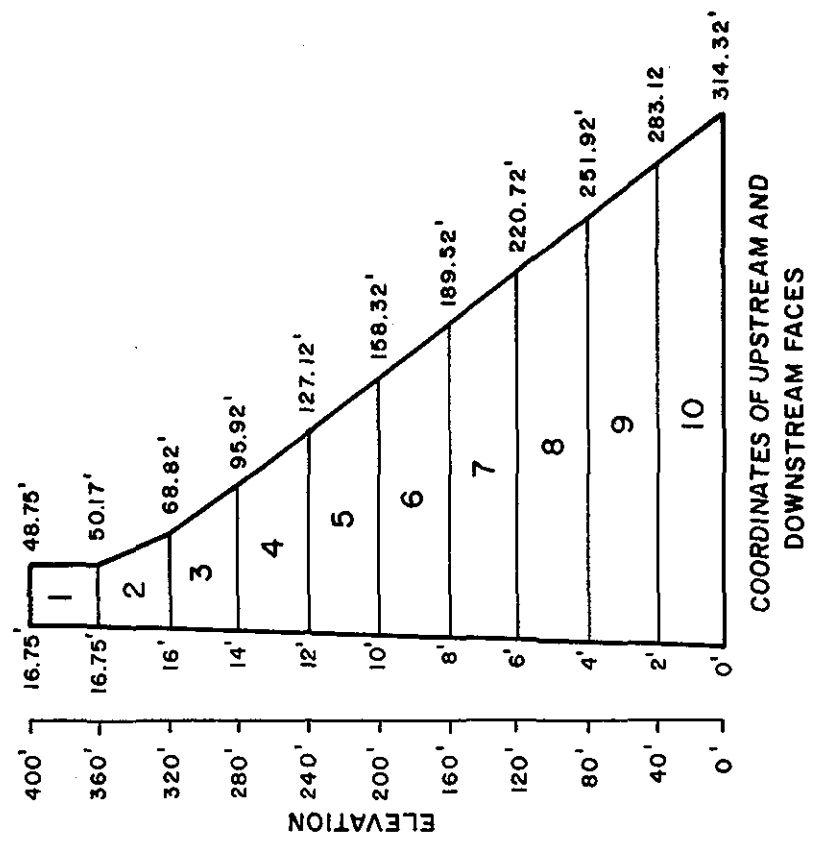


Table C.2 - Additional Properties of the Simplified Model

Level	Elevation $y$ (ft)	Width $b^{(1)}$ (ft)	Weight per Unit Height $w_s = 0.155b$ (k/ft)	Section Modulus $S = 1/6 b^2$ (ft <sup>3</sup> )
Top	400	32.0	4.96	170.1
1	360	33.4	5.18	185.9
2	320	52.8	8.19	464.6
3	280	81.9	12.7	1,118
4	240	115.1	17.8	2,209
5	200	148.3	23.0	3,666
6	160	181.5	28.1	5,492
7	120	214.7	33.3	7,684
8	80	247.9	38.4	10,240
9	40	281.1	43.6	13,170
10	0	314.3	48.7	16,470

<sup>(1)</sup>From Figure in Table C.1.

Table C.3 - Equivalent Lateral Earthquake Forces -- Fundamental Vibration Mode

Level	$y$ (ft)	$w_s^{(1)}$ (k/ft)	$\frac{y}{H_s}$	$\phi^{(2)}$	$w_s \phi$ (k/ft)	$\frac{y}{H}$	$\frac{gp}{wH}^{(3)}$	$gp$ (k/ft)	$f_1(y)^{(4)}$ (k/ft)
Top	400	4.96	1.00	1.00	4.96	1.05	0	0	5.52
1	360	5.18	0.90	0.73	3.80	0.94	0.079	1.68	6.11
2	320	8.19	0.80	0.53	4.35	0.84	0.137	2.96	8.15
3	280	12.7	0.70	0.39	4.95	0.73	0.159	3.39	9.30
4	240	17.8	0.60	0.28	4.98	0.63	0.163	3.50	9.46
5	200	23.0	0.50	0.20	4.60	0.52	0.159	3.43	8.95
6	160	28.1	0.40	0.13	3.65	0.42	0.150	3.24	7.69
7	120	33.3	0.30	0.084	2.80	0.31	0.144	3.09	6.57
8	80	38.4	0.20	0.047	1.80	0.21	0.132	2.85	5.19
9	40	43.6	0.10	0.021	0.92	0.10	0.125	2.68	4.01
10	0	48.7	0	0	0	0	0.117	2.51	2.80

(1) From Table C.2

(2) From Fig. 3 or Table 1

(3) From step 6, by linearly interpolating the data of Fig. 8 or Table 4.

(4) From Eq. 8.

Table C.4 - Normal Bending Stresses -- Fundamental Mode

Level	Section <sup>(1)</sup> Modulus (ft <sup>3</sup> )	Bending Moment (k-ft)	Bending Stress at Faces (psi)
Top	170.1	0	0
1	185.9	3,998	149
2	464.6	17,800	266
3	1,118	44,420	276
4	2,209	85,730	270
5	3,666	142,000	269
6	5,492	212,700	269
7	7,684	295,700	267
8	10,240	389,000	264
9	13,170	491,000	259
10	16,470	600,000	253

<sup>(1)</sup> From Table C.2

Table C.5 - Maximum Principal Stresses -- Fundamental Mode

Level	Bending Stress at Faces <sup>(1)</sup> (psi)	Upstream Face		Downstream Face	
		$\theta^{(2)}$ (°)	Max. Principal Stress, $\sigma_1$ , (psi)	$\theta^{(2)}$ (°)	Max. Principal Stress, $\sigma_1$ , (psi)
Top	0	0	0	0	0
1	149	0	149	2.06	149
2	266	1.09	266	25.2	324
3	276	2.86	276	34.4	403
4	270	2.86	270	38.0	434
5	269	2.86	269	38.0	433
6	269	2.86	269	38.0	433
7	267	2.86	267	38.0	429
8	264	2.86	264	38.0	425
9	259	2.86	259	38.0	417
10	253	2.86	253	38.0	407

<sup>(1)</sup> From Table C.4 with sign neglected

<sup>(2)</sup>  $\theta$  is for the block above each level



Table C.6 - Equivalent Lateral Earthquake Forces -- Higher Vibration Modes

Level	$y$ (ft)	$w_s [1 - \frac{L_1}{M_1} \phi]^{(1)}$ (k/ft)	$\frac{y}{H}$	$\frac{gp_0^{(2)}}{wH}$	$gp_0$ (k/ft)	$[gp_0 - \frac{B_1}{M_1} w_s \phi]^{(3)}$ (k/ft)	$f_{sc}(y)^{(4)}$ (k/ft)
Top	400	-8.83	1.05	0	0	-2.11	-1.98
1	360	-5.33	0.94	0.154	3.67	2.06	-0.59
2	320	-3.88	0.84	0.313	7.45	5.60	0.31
3	280	-1.07	0.73	0.437	10.3	8.20	1.29
4	240	3.94	0.63	0.523	12.5	10.4	2.58
5	200	10.2	0.52	0.598	14.1	12.1	4.03
6	160	17.9	0.42	0.650	15.5	14.0	5.74
7	120	25.5	0.31	0.693	16.4	15.2	7.33
8	80	33.4	0.21	0.720	17.1	16.3	8.96
9	40	41.1	0.10	0.737	17.5	17.1	10.5
10	0	48.7	0	0.742	17.6	17.6	11.9

(1)  $w_s$  and  $\phi$  from Table C.3

(2) From linear interpolation of data from Fig. 11 or Table 6

(3)  $w_s \phi$  from Table C.3

(4) From Eq. 14

Table C.7 - Normal Bending Stresses -- Higher Vibration Modes

Level	Section <sup>(1)</sup> Modulus (ft) <sup>3</sup>	Bending Moment (k-ft)	Normal Bending Stress at Faces (psi)
Top	170.1	0	0
1	185.9	-1,239	-46
2	464.6	-3,736	-56
3	1,118	-5,764	-36
4	2,209	-5,713	-18
5	3,666	-1,584	-3
6	5,492	9,024	11
7	7,684	28,680	26
8	10,240	60,000	41
9	13,170	105,600	56
10	16,470	168,000	71

<sup>(1)</sup> From Table C.2

Table C.8 - Maximum Principal Stresses -- Higher Vibration Modes

Level	Bending Stress at Faces <sup>(1)</sup> (psi)	Upstream Face		Downstream Face	
		$\theta^{(2)}$ (°)	Max. Principal Stress, $\sigma_{sc}$ , (psi)	$\theta^{(2)}$ (°)	Max. Principal Stress, $\sigma_{sc}$ , (psi)
Top	0	0	0	0	0
1	46	0	46	2.06	46
2	56	1.09	56	25.2	68
3	36	2.86	36	34.4	53
4	18	2.86	18	38.0	29
5	3	2.86	3	38.0	5
6	11	2.86	11	38.0	18
7	26	2.86	26	38.0	42
8	41	2.86	41	38.0	66
9	56	2.86	56	38.0	90
10	71	2.86	71	38.0	114

<sup>(1)</sup> From Table C.7, with sign neglected

<sup>(2)</sup>  $\theta$  is for the block above each level

Table C.9 - Response Combination of Maximum Principal Stresses (psi)

Level	Upstream Face					Downstream Face				
	$\sigma_1^{(1)}$	$\sigma_{sc}^{(2)}$	$\sigma_d$	$\sigma_{sf}$	$\sigma_{max}$	$\sigma_1^{(1)}$	$\sigma_{sc}^{(2)}$	$\sigma_d$	$\sigma_{sf}$	$\sigma_{max}$
Top	0	0	0	0	0	0	0	0	0	0
1	149	46	156	-41	115	149	46	156	-43	113
2	266	56	272	-72	200	324	68	332	-63	269
3	276	36	278	-83	195	403	53	406	-101	305
4	270	18	270	-95	175	434	29	434	-144	290
5	269	3	269	-106	163	433	5	433	-185	248
6	269	11	269	-119	150	433	18	433	-228	205
7	267	26	268	-133	135	429	42	432	-272	160
8	264	41	267	-148	119	425	66	430	-316	114
9	259	56	265	-163	102	417	90	426	-360	66
10	253	71	263	-178	85	407	114	423	-404	19

<sup>(1)</sup> From Table C.5<sup>(2)</sup> From Table C.8

## APPENDIX D: COMPUTER PROGRAM FOR STRESS COMPUTATION

This appendix describes a computer program for computing the stresses in a dam monolith using the results of the step-by-step simplified analysis procedure presented in this report. The program computes the bending stresses due to the equivalent lateral forces,  $f_1(y)$  and  $f_{sc}(y)$ , representing the maximum effects of the fundamental and higher vibration modes of the dam, respectively. The program also computes the direct and bending stresses due to the self-weight of the dam and hydrostatic pressure. Transformation to principal stresses and combination of stresses due to the three load cases are not performed.

The program is written in FORTRAN 77 for interactive execution.

### Simplified Model of Dam Monolith

A dam monolith is modeled as a series of blocks, numbered sequentially from the base to the crest. Increasing the number of blocks increases the accuracy of the computed stresses. The free surface of the impounded water may be at any elevation. The elevation of the reservoir bottom must be equal to the elevation of a block bottom. Figure D.1 shows the features of the simplified block model.

### Program Input

The program queries the user for all input data, which are entered free-format. The program assumes that the unit of length is feet, the unit of force and weight is kip, the unit of acceleration is g's, and the unit of stress is psi. The input data are as follows:

1.  $N$ , the number of blocks in the simplified model.
2. The default unit weight of concrete in the dam.
3. For the bottom of each block  $i$ , the x-coordinate  $u_i$  at the upstream face, the x-coordinate  $d_i$  at the downstream face, the elevation, and the unit weight of concrete in the block (enter zero if default unit weight).

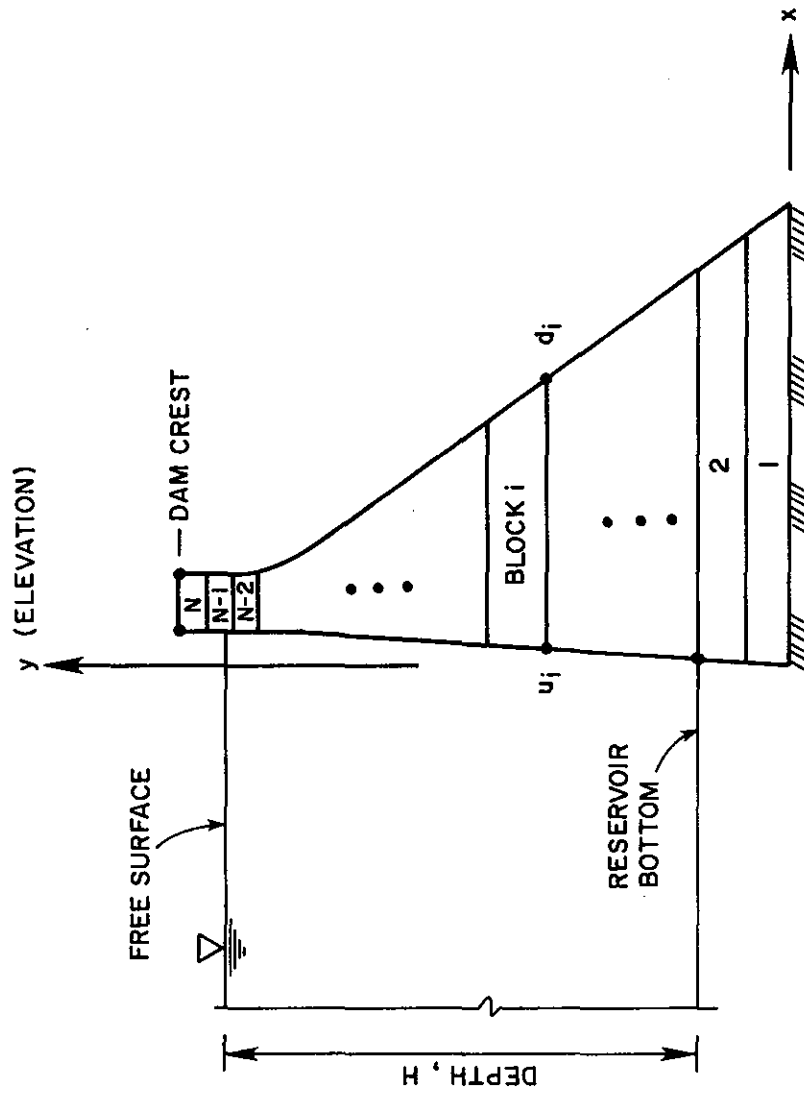


Figure D.1. Block Model of Dam Monolith

4. The x-coordinates of the upstream and downstream faces and the elevation of the dam crest.
5. An alternate value for the ratio  $L_1/M_1$ , if desired, where  $M_1$  and  $L_1$  are the generalized mass and earthquake force coefficient for the dam on rigid foundation rock with empty reservoir (Eq. 7). If not specified, the value of  $L_1/M_1$  computed from the block model (as in steps 7 and 8 of the step-by-step procedure) is used.

The remaining data are entered for each case:

6. The elevations of the free surface of water and reservoir bottom.
7. The ordinates of the hydrodynamic pressure function,  $gp/wH$ , at the  $y/H$  values indicated. The ordinates are obtained from Step 6 of the step-by-step procedure.
8. The pseudo-acceleration ordinate of the earthquake design spectrum evaluated at the fundamental vibration period and damping ratio of the dam as evaluated in Step 9 of the step-by-step procedure.
9. The ratio  $\tilde{L}_1/\tilde{M}_1$ , where  $\tilde{M}_1$  and  $\tilde{L}_1$  = generalized mass and earthquake force coefficient including hydrodynamic effects determined in Steps 7 and 8 of the step-by-step procedure. This ratio reduces to  $L_1/M_1$  for dam with empty reservoir.
10. An alternate value of  $B_1/M_1$ , if desired. If not specified the value computed in Step 11 of the step-by-step procedure is used.
11. The maximum ground acceleration of the design earthquake.

### Computed Response

The program computes the vertical, normal stresses at the bottom of each block at the upstream and downstream faces based on simple beam theory. Stresses are computed for three loading cases: (1) static forces (self-weight of the dam and hydrostatic pressure); (2) equivalent lateral forces associated with the fundamental vibration mode; and (3) the equivalent lateral forces associated with the higher vibration modes. The unit of stress is

pounds per square inch.

**Example**

The use of the computer program in the stress computation for Pine Flat Dam, detailed in Appendix C, is illustrated in the listing shown next wherein the computed vertical, normal stresses due to the three loading cases are also presented.



D&gt;

ENTER THE NUMBER OF BLOCKS IN THE DAM: 10

ENTER THE DEFAULT UNIT WEIGHT: 0.155

ENTER X1,X2,Y, AND UNIT WEIGHT OF BLOCK NO. 1: 0,314.32,0,0  
 ENTER X1,X2,Y, AND UNIT WEIGHT OF BLOCK NO. 2: 2,283.12,40,0  
 ENTER X1,X2,Y, AND UNIT WEIGHT OF BLOCK NO. 3: 4,251.92,80,0  
 ENTER X1,X2,Y, AND UNIT WEIGHT OF BLOCK NO. 4: 6,220.72,120,0  
 ENTER X1,X2,Y, AND UNIT WEIGHT OF BLOCK NO. 5: 8,189.52,160,0  
 ENTER X1,X2,Y, AND UNIT WEIGHT OF BLOCK NO. 6: 10,158.32,200,0  
 ENTER X1,X2,Y, AND UNIT WEIGHT OF BLOCK NO. 7: 12,127.12,240,0  
 ENTER X1,X2,Y, AND UNIT WEIGHT OF BLOCK NO. 8: 14,95.92,280,0  
 ENTER X1,X2,Y, AND UNIT WEIGHT OF BLOCK NO. 9: 16,68.82,320,0  
 ENTER X1,X2,Y, AND UNIT WEIGHT OF BLOCK NO. 10: 16.75,50.172,360,0

ENTER X1, X2 AND Y AT THE CREST: 16.75,48.75,400

## PROPERTIES OF THE DAM

BLOCK	CENTROID ELEV.	WEIGHT
10	379.855	202.808
9	338.500	267.350
8	298.560	417.694
7	258.877	610.824
6	219.160	816.664
5	179.329	1022.504
4	139.441	1228.344
3	99.522	1434.184
2	59.582	1640.024
1	19.628	1845.864
		9486.262

## FUNDAMENTAL VIBRATION PROPERTIES OF THE DAM

L1 = 1389.695      M1 = 499.738

THE FACTOR L1/M1 IS = 2.781

ENTER AN ALTERNATE VALUE FOR L1/M1:0

DO YOU WANT TO CONTINUE? (0=YES,1=NO):0

ENTER ELEVATION OF FREE - SURFACE: 381

ENTER ELEVATION OF RESERVOIR BOTTOM: 0

STATIC STRESSES IN DAM

BLOCK	UPSTREAM FACE	DOWNSTREAM FACE
10	-41.217	-43.062
9	-72.259	-51.872
8	-83.050	-69.518
7	-94.724	-89.360
6	-106.442	-114.791
5	-119.295	-141.630
4	-133.116	-168.865
3	-147.660	-196.191
2	-162.739	-223.509
1	-178.218	-250.787

ENTER THE HYDRODYNAMIC PRESSURE FOR THE  
FUNDAMENTAL VIBRATION MODE OF THE DAM

ENTER THE PRESSURE ORDINATE FOR Y/H = .945: 0.079

ENTER THE PRESSURE ORDINATE FOR Y/H = .840: 0.137

ENTER THE PRESSURE ORDINATE FOR Y/H = .735: 0.159

ENTER THE PRESSURE ORDINATE FOR Y/H = .630: 0.163

ENTER THE PRESSURE ORDINATE FOR Y/H = .525: 0.159

ENTER THE PRESSURE ORDINATE FOR Y/H = .420: 0.150

ENTER THE PRESSURE ORDINATE FOR Y/H = .315: 0.144

ENTER THE PRESSURE ORDINATE FOR Y/H = .210: 0.132

ENTER THE PRESSURE ORDINATE FOR Y/H = .105: 0.125

ENTER THE PRESSURE ORDINATE FOR Y/H = .000: 0.117

ENTER THE PSEUDO-ACCELERATION ORDINATE IN G: 0.327

ENTER L1(TILDE)/M1(TILDE) FACTOR:3.4

FUNDAMENTAL MODE STRESSES IN DAM

BLOCK	UPSTREAM FACE	DOWNSTREAM FACE
10	149.655	-149.655
9	266.785	-266.785
8	276.513	-276.513
7	270.140	-270.140
6	269.726	-269.726
5	269.447	-269.447
4	267.707	-267.707
3	264.298	-264.298
2	259.370	-259.370
1	253.233	-253.233

THE FACTOR B1/M1 IS = .428  
 ENTER AN ALTERNATE VALUE FOR B1/M1:0

ENTER MAX. GROUND ACCELERATION IN G: 0.18

HIGHER MODE STRESSES IN DAM

BLOCK	UPSTREAM FACE	DOWNSTREAM FACE
10	-46.290	46.290
9	-55.847	55.847
8	-35.803	35.803
7	-17.958	17.958
6	-2.985	2.985
5	11.409	-11.409
4	25.917	-25.917
3	40.693	-40.693
2	55.697	-55.697
1	70.840	-70.840

DO YOU WANT TO CONTINUE? (0=YES,1=NO):1  
 Stop - Program terminated.



C*****	SMPL	1
C	SMPL	2
C	SMPL	3
C	SMPL	4
C	SMPL	5
C	SMPL	6
C	SMPL	7
C	SMPL	8
C	SMPL	9
C	SMPL	10
C	SMPL	11
C	SMPL	12
C	SMPL	13
C*****	SMPL	14
C	SMPL	15
C	SMPL	16
C	SMPL	17
C	SMPL	18
C	SMPL	19
C	SMPL	20
C	SMPL	21
C	SMPL	22
C	SMPL	23
C	SMPL	24
C	SMPL	25
C	SMPL	26
C	SMPL	27
C	SMPL	28
C	SMPL	29
C	SMPL	30
C	SMPL	31
C	SMPL	32
C	SMPL	33
C	SMPL	34
C	SMPL	35
C	SMPL	36
C	SMPL	37
C	SMPL	38
C	SMPL	39
C	SMPL	40
C	SMPL	41
C	SMPL	42
C	SMPL	43
C	SMPL	44
C	SMPL	45
C	SMPL	46
C	SMPL	47
C	SMPL	48
C	SMPL	49
C	SMPL	50
C	SMPL	51
C	SMPL	52
C	SMPL	53
C	SMPL	54
C	SMPL	55

C	READ IN PROPERTIES OF THE IMPOUNDED WATER	SMPL 56
C	AND COMPUTE STRESSES DUE TO HYDROSTATIC PRESSURE	SMPL 57
C		SMPL 58
	CALL REDWAT (H,HB)	SMPL 59
	CALL DAMSTA (BLOCKS,NBLOCK,GAMMA,H,HB,PRESS,STRDUM)	SMPL 60
	STRFAC = 1.0/STRCON	SMPL 61
	CALL COMSTA (NBLOCK,STRWGT,STRDUM,STRSTA,STRFAC,TITSTA)	SMPL 62
C		SMPL 63
C	COMPUTE THE DYNAMIC STRESSES DUE TO THE FUNDAMENTAL	SMPL 64
C	MODE SHAPE	SMPL 65
C		SMPL 66
	CALL DAMDYN (BLOCKS,NBLOCK,GAMMA,H,HB,PRESS,STRDUM)	SMPL 67
	WRITE (*,97)	SMPL 68
	READ (*,*) SA	SMPL 69
	STRFAC = SA/STRCON	SMPL 70
	WRITE (*,95)	SMPL 71
	READ (*,*) SA	SMPL 72
	STRFAC = STRFAC*SA	SMPL 73
	CALL COMSTA (NBLOCK,STRFUN,STRDUM,STRDYN,STRFAC,TITFUN)	SMPL 74
C		SMPL 75
C	COMPUTE THE HIGHER MODE STRESSES	SMPL 76
C		SMPL 77
	CALL DAMCOR (BLOCKS,NBLOCK,GAMMA,H,HB,PARTFC(2),STRFUN,	SMPL 78
1	PRESS,STRDUM)	SMPL 79
	WRITE (*,94)	SMPL 80
	READ (*,*) SA	SMPL 81
	STRFAC = SA/STRCON	SMPL 82
	CALL COMSTA (NBLOCK,STRWCR,STRDUM,STRCOR,STRFAC,TITCOR)	SMPL 83
	GO TO 10	SMPL 84
C		SMPL 85
	20 RETURN	SMPL 86
C		SMPL 87
	99 FORMAT (///// ' DO YOU WANT TO CONTINUE? (0=YES,1=NO): ' )	SMPL 88
	97 FORMAT (// ' ENTER THE PSUEDO-ACCELERATION ORDINATE IN G: ' )	SMPL 89
	95 FORMAT (// ' ENTER L1(TILDE)/M1(TILDE) FACTOR: ' )	SMPL 90
	94 FORMAT (// ' ENTER MAX. GROUND ACCELERATION IN G: ' )	SMPL 91
C		SMPL 92
	END	SMPL 93
	SUBROUTINE DAMPRP (BLOCKS,NBLOCK,NMAX,WEIGHT,STRWGT,	SMPL 94
1	STRWCR,STRFUN,PARTFC)	SMPL 95
C		SMPL 96
C	INPUT THE PROPERTIES OF THE DAM, AND COMPUTE THE STATIC	SMPL 97
C	AND FUNDAMENTAL VIBRATION PROPERTIES OF THE DAM	SMPL 98
C		SMPL 99
	DIMENSION BLOCKS(5,1),WEIGHT(1),STRWGT(2,1),	SMPL 100
1	STRWCR(2,1),STRFUN(2,1),PARTFC(3)	SMPL 101
	EXTERNAL VALWGT,VALHOR	SMPL 102
C		SMPL 103
C	INPUT BLOCK PROPERTIES AND COMPUTE STATIC STRESSES	SMPL 104
C		SMPL 105
	CALL REDBLK (BLOCKS,NBLOCK,NMAX,WEIGHT)	SMPL 106
	CALL BLCKVL (BLOCKS,NBLOCK,WEIGHT,WEIGHT)	SMPL 107
	CALL STRLOD (BLOCKS,NBLOCK,WEIGHT,VALWGT,STRWGT)	SMPL 108
	CALL STRLOD (BLOCKS,NBLOCK,WEIGHT,VALHOR,STRWCR)	SMPL 109
C		SMPL 110

	WRITE (*,99)	SMPL 111
	DO 10 J=1,NBLOCK	SMPL 112
	I = NBLOCK + 1 - J	SMPL 113
	WRITE (*,98) I, BLOCKS(5,I),WEIGHT(I)	SMPL 114
10	CONTINUE	SMPL 115
C		SMPL 116
C	COMPUTE THE FUNDAMENTAL VIBRATION PROPERTIES AND STRESSES	SMPL 117
C	DUE TO THE EFFECTIVE EARTHQUAKE FORCE	SMPL 118
C		SMPL 119
	CALL FUNMOD (BLOCKS,NBLOCK,WEIGHT,WEIGHT,XTOT,PARTFC(1),	SMPL 120
1	PARTFC(2))	SMPL 121
	CALL STRLOD (BLOCKS,NBLOCK,WEIGHT,VALHOR,STRFUN)	SMPL 122
C		SMPL 123
	PARTFC(3) = PARTFC(1)/PARTFC(2)	SMPL 124
	WRITE (*,97) XTOT,(PARTFC(I),I=1,3)	SMPL 125
	READ (*,*) DUM	SMPL 126
	IF (DUM.GT.0.0) PARTFC(3) = DUM	SMPL 127
C		SMPL 128
C	COMPUTE THE HIGHER MODE STRESSES DUE TO THE	SMPL 129
C	WEIGHT OF THE DAM	SMPL 130
C		SMPL 131
	DO 20 J=1,NBLOCK	SMPL 132
	STRWCR(1,J) = STRWCR(1,J) - PARTFC(3)*STRFUN(1,J)	SMPL 133
	STRWCR(2,J) = STRWCR(2,J) - PARTFC(3)*STRFUN(2,J)	SMPL 134
20	CONTINUE	SMPL 135
C		SMPL 136
	RETURN	SMPL 137
C		SMPL 138
	99 FORMAT (////3X,'PROPERTIES OF THE DAM'///' BLOCK',2X,'CENTROID',	SMPL 139
1	4X,'WEIGHT'/10X,'ELEV.'/1X,27('-')//)	SMPL 140
	98 FORMAT (3X,I2,3X,F8.3,3X,F8.3)	SMPL 141
	97 FORMAT (19X,'-----'/19X,F8.3//	SMPL 142
1	' FUNDAMENTAL VIBRATION PROPERTIES OF THE DAM'//	SMPL 143
2	5X,' L1 =',F9.3,5X,' M1 =',F9.3//	SMPL 144
3	5X,' THE FACTOR L1/M1 IS =',F9.3//	SMPL 145
4	' ENTER AN ALTERNATE VALUE FOR L1/M1:' )	SMPL 146
C		SMPL 147
	END	SMPL 148
	SUBROUTINE DAMSTA (BLOCKS,NBLOCK,GAMMA,H,HB,PRESS,STRDUM)	SMPL 149
C		SMPL 150
C	COMPUTE THE STATIC STRESSES IN THE DAM DUE TO IMPOUNDED WATER	SMPL 151
C		SMPL 152
	DIMENSION BLOCKS(5,1),PRESS(1),STRDUM(2,1)	SMPL 153
	EXTERNAL VALHST	SMPL 154
C		SMPL 155
C	COMPUTE STATIC STRESSES DUE TO IMPOUNDED WATER	SMPL 156
C		SMPL 157
	CALL CALHST (BLOCKS,NBLOCK,H,HB,GAMMA,PRESS)	SMPL 158
	CALL STRPRS (BLOCKS,NBLOCK,PRESS,1,H,HB,VALHST,STRDUM)	SMPL 159
C		SMPL 160
C	COMPUTE STATIC STRESSES DUE TO TAILWATER -- NOT	SMPL 161
C	IMPLEMENTED IN THIS VERSION OF THE PROGRAM	SMPL 162
C		SMPL 163
	RETURN	SMPL 164
	END	SMPL 165

	SUBROUTINE DAMDYN (BLOCKS,NBLOCK,GAMMA,H,HB,PRESS,STRDUM)	SMPL 166
C		SMPL 167
C	READ HYDRODYNAMIC PRESSURE AND COMPUTE STRESSES	SMPL 168
C	DUE TO THE HYDRODYNAMIC PRESSURE	SMPL 169
C		SMPL 170
	DIMENSION BLOCKS(5,1),PRESS(1),STRDUM(2,1)	SMPL 171
	EXTERNAL VALHDY	SMPL 172
C		SMPL 173
	CALL REDHDY (BLOCKS,NBLOCK,H,HB,GAMMA,PRESS)	SMPL 174
	CALL STRPRS (BLOCKS,NBLOCK,PRESS,1,H,HB,VALHDY,STRDUM)	SMPL 175
C		SMPL 176
	RETURN	SMPL 177
	END	SMPL 178
	SUBROUTINE DAMCOR (BLOCKS,NBLOCK,GAMMA,H,HB,XM1,STRFUN,	SMPL 179
1	PRESS,STRDUM)	SMPL 180
C		SMPL 181
	DIMENSION BLOCKS(5,1),PRESS(1),STRFUN(2,1),STRDUM(2,1)	SMPL 182
	EXTERNAL VALHDY	SMPL 183
	DATA BFACT/0.052/	SMPL 184
C		SMPL 185
	CALL CORPRS (BLOCKS,NBLOCK,H,HB,GAMMA,PRESS)	SMPL 186
	CALL STRPRS (BLOCKS,NBLOCK,PRESS,1,H,HB,VALHDY,STRDUM)	SMPL 187
C		SMPL 188
	D = H - HB	SMPL 189
	HS = BLOCKS(3,NBLOCK+1) - BLOCKS(3,1)	SMPL 190
	B01M1 = 0.5*BFACT*GAMMA*D*D*D*D/(HS*HS*XM1)	SMPL 191
	WRITE (*,99) B01M1	SMPL 192
	READ (*,*) D	SMPL 193
	IF (D.GT.0.0) B01M1 = D	SMPL 194
C		SMPL 195
	DO 10 J = 1,NBLOCK	SMPL 196
	STRDUM(1,J) = STRDUM(1,J) - B01M1*STRFUN(1,J)	SMPL 197
	STRDUM(2,J) = STRDUM(2,J) - B01M1*STRFUN(2,J)	SMPL 198
10	CONTINUE	SMPL 199
C		SMPL 200
	RETURN	SMPL 201
C		SMPL 202
	99 FORMAT (/' THE FACTOR B1/M1 IS = ',F9.3/	SMPL 203
1	' ENTER AN ALTERNATE VALUE FOR B1/M1: ' )	SMPL 204
	END	SMPL 205
	SUBROUTINE REDBLK (BLOCKS,NBLOCK,NMAX,UNITWT)	SMPL 206
C		SMPL 207
C	READ THE PROPERTIES OF THE BLOCKS IN THE DAM	SMPL 208
C		SMPL 209
	DIMENSION BLOCKS(5,1),UNITWT(1)	SMPL 210
C		SMPL 211
	WRITE (*,99)	SMPL 212
	READ (*,*) NBLOCK	SMPL 213
	IF (NBLOCK.GT.NMAX) GO TO 20	SMPL 214
C		SMPL 215
	WRITE (*,97)	SMPL 216
	READ (*,*) DEFWGT	SMPL 217
C		SMPL 218
	DO 10 I=1,NBLOCK	SMPL 219
	WRITE (*,95) I	SMPL 220



	READ (*,*) (BLOCKS(J,I),J=1,3),UNT	SMPL 221
	IF (UNT.LE.0.0) UNT = DEFWGT	SMPL 222
	UNITWT(I) = UNT	SMPL 223
10	CONTINUE	SMPL 224
C		SMPL 225
	WRITE (*,93)	SMPL 226
	READ (*,*) (BLOCKS(J,NBLOCK+1),J=1,3)	SMPL 227
C		SMPL 228
	RETURN	SMPL 229
C		SMPL 230
C	TOO MANY BLOCKS REQUESTED FOR STORAGE ALLOCATED	SMPL 231
C		SMPL 232
20	STOP	SMPL 233
C		SMPL 234
	99 FORMAT (/' ENTER THE NUMBER OF BLOCKS IN THE DAM: ' )	SMPL 235
	97 FORMAT (/' ENTER THE DEFAULT UNIT WEIGHT: ' )	SMPL 236
	95 FORMAT (5X, ' ENTER X1,X2,Y, AND UNIT WEIGHT OF BLOCK NO. ',	SMPL 237
	1 I2, ': ' )	SMPL 238
	93 FORMAT (/'5X, ' ENTER X1, X2 AND Y AT THE CREST: ' )	SMPL 239
C		SMPL 240
	END	SMPL 241
	SUBROUTINE CORPRS (BLOCKS,NBLOCK,H,HB,GAMMA,PRESS)	SMPL 242
C		SMPL 243
C	COMPUTE THE HYDRODYNAMIC PRESSURE ON THE UPSTREAM FACE OF A	SMPL 244
C	RIGID DAM WITH INCOMPRESSIBLE WATER. USED FOR THE	SMPL 245
C	COMPUTATION OF HIGHER MODE STRESSES.	SMPL 246
C		SMPL 247
	DIMENSION BLOCKS(5,1),PRESS(1)	SMPL 248
C		SMPL 249
	DEPTH = H - HB	SMPL 250
	IF (DEPTH.LE.0.0) RETURN	SMPL 251
	NBL1 = NBLOCK + 1	SMPL 252
	HS = BLOCKS(3,NBL1) - BLOCKS(3,1)	SMPL 253
C		SMPL 254
	DO 10 I = 1,NBL1	SMPL 255
	PRESS(I) = 0.0	SMPL 256
	Y = (BLOCKS(3,I) - HB)/DEPTH	SMPL 257
	IF (Y.GT.1.0.OR.Y.LT.0.0) GO TO 10	SMPL 258
	CALL POYFUN (Y,P0)	SMPL 259
	PRESS(I) = GAMMA*DEPTH*P0	SMPL 260
10	CONTINUE	SMPL 261
C		SMPL 262
	RETURN	SMPL 263
	END	SMPL 264
	SUBROUTINE BLCKVL (BLOCKS,NBLOCK,UNITWT,WEIGHT)	SMPL 265
C		SMPL 266
C	COMPUTE THE LOCATIONS OF THE CENTROIDS AND	SMPL 267
C	WEIGHTS OF THE BLOCKS	SMPL 268
C		SMPL 269
	DIMENSION BLOCKS(5,1),UNITWT(1),WEIGHT(1)	SMPL 270
C		SMPL 271
C	LOOP OVER THE BLOCKS, ONE AT A TIME, TOP TO BOTTOM	SMPL 272
C		SMPL 273
	DO 10 J=1,NBLOCK	SMPL 274
	I = NBLOCK + 1 - J	SMPL 275

C		SMPL 276
	TOP = BLOCKS(2,I+1) - BLOCKS(1,I+1)	SMPL 277
	BOT = BLOCKS(2,I ) - BLOCKS(1,I )	SMPL 278
	DX = BLOCKS(1,I+1) - BLOCKS(1,I )	SMPL 279
	DY = BLOCKS(3,I+1) - BLOCKS(3,I )	SMPL 280
C		SMPL 281
	CALL CENTRD (TOP,BOT,0.0,DY,AREA,DUM,DUM,RY)	SMPL 282
	BLOCKS(4,I) = BLOCKS(1,I) +	SMPL 283
1	(2.0*DX*TOP + DX*BOT + TOP*BOT	SMPL 284
2	+ TOP*TOP + BOT*BOT)/	SMPL 285
3	(3.0*(TOP + BOT))	SMPL 286
	BLOCKS(5,I) = BLOCKS(3,I) + RY	SMPL 287
C		SMPL 288
	WEIGHT(I) = AREA*UNITWT(I)	SMPL 289
10	CONTINUE	SMPL 290
C		SMPL 291
	RETURN	SMPL 292
	END	SMPL 293
	SUBROUTINE FUNMOD (BLOCKS,NBLOCK,WEIGHT,WPHI,W1,W2,W3)	SMPL 294
C		SMPL 295
C	COMPUTE THE EFFECTIVE LATERAL LOAD FOR EACH BLOCK	SMPL 296
C	AND THE TOTAL WEIGHT, EFFECTIVE EARTHQUAKE FORCE,	SMPL 297
C	AND GENERALIZED WEIGHT OF THE DAM	SMPL 298
C		SMPL 299
	DIMENSION BLOCKS(5,1),WEIGHT(1),WPHI(1)	SMPL 300
C		SMPL 301
	HS = BLOCKS(3,NBLOCK+1) - BLOCKS(3,1)	SMPL 302
	W1 = 0.0	SMPL 303
	W2 = 0.0	SMPL 304
	W3 = 0.0	SMPL 305
C		SMPL 306
C	LOOP OVER BLOCKS, ONE AT A TIME, BOTTOM TO TOP	SMPL 307
C		SMPL 308
	DO 10 I=1,NBLOCK	SMPL 309
	Y = (BLOCKS(5,I) - BLOCKS(3,1))/HS	SMPL 310
	CALL PHIONE (Y,PHI)	SMPL 311
	W = WEIGHT(I)	SMPL 312
	WP = W*PHI	SMPL 313
	WPHI(I) = WP	SMPL 314
	W1 = W1 + W	SMPL 315
	W2 = W2 + WP	SMPL 316
	W3 = W3 + WP*PHI	SMPL 317
10	CONTINUE	SMPL 318
C		SMPL 319
	RETURN	SMPL 320
	END	SMPL 321
	SUBROUTINE PHIONE (Y,PHI)	SMPL 322
C		SMPL 323
C	OBTAIN THE ORDINATE OF THE FUNDAMENTAL VIBRATION MODE	SMPL 324
C	OF THE DAM, USE THE STANDARD MODE SHAPE	SMPL 325
C		SMPL 326
	DIMENSION PHI1(22)	SMPL 327
	DATA DY/0.05/,PHI1/0.000 , 0.010 , 0.021 , 0.034 , 0.047 ,	SMPL 328
1	0.065 , 0.084 , 0.108 , 0.135 , 0.165 ,	SMPL 329
2	0.200 , 0.240 , 0.284 , 0.334 , 0.389 ,	SMPL 330

```

3          0.455 , 0.530 , 0.619 , 0.735 , 0.866 ,      SMPL 331
4          1.000 , 1.000 /                                SMPL 332
C                                                    SMPL 333
  A = Y/DY                                              SMPL 334
  I = IFIX(A) + 1                                       SMPL 335
  A = FLOAT(I) - A                                       SMPL 336
  PHI = A*PHI1(I) + (1.0-A)*PHI1(I+1)                 SMPL 337
C                                                    SMPL 338
  RETURN                                               SMPL 339
  END                                                 SMPL 340
  SUBROUTINE POYFUN (Y,PO)                               SMPL 341
C                                                    SMPL 342
C          OBTAIN THE HYDRODYNAIC PRESSURE ON A RIGID DAM WITH SMPL 343
C          INCOMPRESSIBLE WATER.                       SMPL 344
C                                                    SMPL 345
  DIMENSION POY(22)                                     SMPL 346
  DATA DY/0.05/,POY/0.742 , 0.741 , 0.737 , 0.731 , 0.722 , 0.711 , SMPL 347
1          0.696 , 0.680 , 0.659 , 0.637 , 0.610 , 0.580 , SMPL 348
2          0.546 , 0.509 , 0.465 , 0.418 , 0.362 , 0.301 , SMPL 349
3          0.224 , 0.137 , 0.000 , 0.000 /            SMPL 350
C                                                    SMPL 351
  A = Y/DY                                              SMPL 352
  I = IFIX(A) + 1                                       SMPL 353
  A = FLOAT(I) - A                                       SMPL 354
  PO = A*POY(I) + (1.0-A)*POY(I+1)                   SMPL 355
  RETURN                                               SMPL 356
  END                                                 SMPL 357
  SUBROUTINE REDWAT (H,HB)                               SMPL 358
C                                                    SMPL 359
C          READ THE ELEVATIONS OF THE RESERVOIR        SMPL 360
C                                                    SMPL 361
  WRITE (*,99)                                          SMPL 362
  READ (*,*) H                                          SMPL 363
  WRITE (*,98)                                          SMPL 364
  READ (*,*) HB                                         SMPL 365
C                                                    SMPL 366
  RETURN                                               SMPL 367
C                                                    SMPL 368
99 FORMAT (///' ENTER ELEVATION OF FREE - SURFACE: ' ) SMPL 369
98 FORMAT (/ ' ENTER ELEVATION OF RESERVOIR BOTTOM: ' ) SMPL 370
  END                                                 SMPL 371
  SUBROUTINE CALHST (BLOCKS,NBLOCK,H,HB,GAMMA,PRESS)   SMPL 372
C                                                    SMPL 373
C          COMPUTE THE HYDROSTATIC PRESSURE ON THE FACE OF THE DAM SMPL 374
C                                                    SMPL 375
  DIMENSION BLOCKS(5,1),PRESS(1)                     SMPL 376
C                                                    SMPL 377
C          LOOP OVER THE BLOCK LEVELS, ONE AT A TIME, BOTTOM TO TOP SMPL 378
C                                                    SMPL 379
  NBL1 = NBLOCK + 1                                    SMPL 380
  DO 10 I=1,NBL1                                       SMPL 381
    PRESS(I) = 0.0                                       SMPL 382
    Y = BLOCKS(3,I)                                       SMPL 383
    IF (Y.LT.H.AND.Y.GE.HB) PRESS(I) = GAMMA*(H-Y)     SMPL 384
10  CONTINUE                                           SMPL 385

```

```

C                                     SMPL 386
RETURN                               SMPL 387
END                                  SMPL 388
SUBROUTINE REDHDY (BLOCKS,NBLOCK,H,HB,GAMMA,PRESS) SMPL 389
C                                     SMPL 390
C      READ AND COMPUTE THE HYDRODYNAMIC PRESSURE AT THE SMPL 391
C      BLOCK LEVELS ON THE UPSTREAM FACE OF THE DAM SMPL 392
C                                     SMPL 393
C      DIMENSION BLOCKS(5,1),PRESS(1) SMPL 394
C                                     SMPL 395
C      DEPTH = H - HB SMPL 396
C      IF (DEPTH.EQ.0.0) RETURN SMPL 397
C                                     SMPL 398
C      NBL1 = NBLOCK + 1 SMPL 399
C      HHS = DEPTH/(BLOCKS(3,NBL1) - BLOCKS(3,1)) SMPL 400
C      HHS2 = HHS*HHS SMPL 401
C                                     SMPL 402
C      LOOP OVER BLOCK LEVELS, ONE AT A TIME, TOP TO BOTTOM SMPL 403
C                                     SMPL 404
C      WRITE (*,99) SMPL 405
C      DO 10 J=1,NBL1 SMPL 406
C          I = NBLOCK + 2 - J SMPL 407
C          PRESS(I) = 0.0 SMPL 408
C          Y = (BLOCKS(3,I) - HB)/DEPTH SMPL 409
C          IF (Y.GT.1.0.OR.Y.LT.0.0) GO TO 10 SMPL 410
C                                     SMPL 411
C          READ PRESSURE COEFFICIENT AND COMPUTE HYDRODYNAMIC SMPL 412
C          PRESSURE AT THE BLOCK LEVEL SMPL 413
C                                     SMPL 414
C          WRITE (*,98) Y SMPL 415
C          READ (*,*) P SMPL 416
C          PRESS(I) = GAMMA*DEPTH*HHS2*P SMPL 417
C                                     SMPL 418
C      10 CONTINUE SMPL 419
C      RETURN SMPL 420
C                                     SMPL 421
C      99 FORMAT (// ' ENTER THE HYDRODYNAMIC PRESSURE FOR THE ' / SMPL 422
C      1 ' FUNDAMENTAL VIBRATION MODE OF THE DAM ' ) SMPL 423
C      98 FORMAT (/5X, ' ENTER THE PRESSURE ORDINATE FOR Y/H = ', SMPL 424
C      1 F5.3, ': ' ) SMPL 425
C      end SMPL 426
SUBROUTINE STRLOD (BLOCKS,NBLOCK,LOADS,VALUES,STRESS) SMPL 427
C                                     SMPL 428
C      COMPUTE THE NORMAL STRESSES DUE TO LOADS APPLIED AT THE SMPL 429
C      CENTROID OF THE BLOCKS SMPL 430
C                                     SMPL 431
C      DIMENSION BLOCKS(5,1),LOADS(1),STRESS(2,1) SMPL 432
C      REAL LOADS,M SMPL 433
C                                     SMPL 434
C      HSUM = 0.0 SMPL 435
C      HYSUM = 0.0 SMPL 436
C      VSUM = 0.0 SMPL 437
C      VXSUM = 0.0 SMPL 438
C                                     SMPL 439
C      LOOP OVER BLOCKS, ONE AT A TIME, TOP TO BOTTOM SMPL 440

```

C		SMPL 441
	DO 10 J=1,NBLOCK	SMPL 442
	I = NBLOCK + 1 - J	SMPL 443
C		SMPL 444
C	OBTAIN THE LOADS AT THE CENTROID OF BLOCK I	SMPL 445
C		SMPL 446
	CALL VALUES (I,LOADS,V,H)	SMPL 447
	HSUM = HSUM + H	SMPL 448
	HYSUM = HYSUM + H*BLOCKS(5,I)	SMPL 449
	VSUM = VSUM + V	SMPL 450
	VXSUM = VXSUM + V*BLOCKS(4,I)	SMPL 451
C		SMPL 452
C	COMPUTE THE BENDING MOMENT AND STRESSES AT THE	SMPL 453
C	BOTTOM OF BLOCK I	SMPL 454
C		SMPL 455
	M = HYSUM - VXSUM - BLOCKS(3,I)*HSUM	SMPL 456
1	+ 0.5*(BLOCKS(2,I)+BLOCKS(1,I))*VSUM	SMPL 457
C		SMPL 458
	T = BLOCKS(2,I) - BLOCKS(1,I)	SMPL 459
	M = 6.0*M/(T*T)	SMPL 460
	STRESS(1,I) = VSUM/T + M	SMPL 461
	STRESS(2,I) = VSUM/T - M	SMPL 462
C		SMPL 463
10	CONTINUE	SMPL 464
	RETURN	SMPL 465
	END	SMPL 466
	SUBROUTINE STRPRS (BLOCKS,NBLOCK,PRESS,IUPDN,H,HB,VALUES,STRESS)	SMPL 467
C		SMPL 468
C	COMPUTE THE NORMAL STRESSES DUE TO PRESSURE APPLIED	SMPL 469
C	AT THE FACE, UPSTREAM (IUPDN=1) OR DOWNSTREAM (IUPDN=2),	SMPL 470
C	OF THE BLOCKS	SMPL 471
C		SMPL 472
	DIMENSION BLOCKS(5,1),PRESS(1),STRESS(2,1)	SMPL 473
	REAL M	SMPL 474
	LOGICAL YCOMP	SMPL 475
C		SMPL 476
	HSUM = 0.0	SMPL 477
	HYSUM = 0.0	SMPL 478
	VSUM = 0.0	SMPL 479
	VXSUM = 0.0	SMPL 480
C		SMPL 481
	YB = BLOCKS(3,NBLOCK+1)	SMPL 482
C		SMPL 483
C	LOOP OVER BLOCKS, ONE AT A TIME, TOP TO BOTTOM	SMPL 484
C		SMPL 485
	DO 40 J=1,NBLOCK	SMPL 486
C		SMPL 487
	I = NBLOCK + 1 - J	SMPL 488
	YBT = YB	SMPL 489
	YB = BLOCKS(3,I)	SMPL 490
C		SMPL 491
	IF (YB.GE.H.OR.YBT.LE.HB) GO TO 30	SMPL 492
C		SMPL 493
C	THE BLOCK TOUCHS WATER, OBTAIN THE WATER PRESSURE	SMPL 494
C	AT THE TOP AND BOTTOM OF THE BLOCK	SMPL 495

C		SMPL 496
	CALL VALUES (I,PRESS,P1,P2,YCOMP)	SMPL 497
	DX = 0.0	SMPL 498
	IF (YCOMP) DX = BLOCKS(IUPDN,I+1) - BLOCKS(IUPDN,I)	SMPL 499
	DY = BLOCKS(3,I+1) - BLOCKS(3,I)	SMPL 500
	IF (YBT.LE.H) GO TO 10	SMPL 501
C		SMPL 502
C	TOP OF WATER IS IN BLOCK, MODIFY TOP PRESSURE POINT	SMPL 503
C		SMPL 504
	DUM = H - YB	SMPL 505
	DX = DX*DUM/DY	SMPL 506
	DY = DUM	SMPL 507
	P1 = 0.0	SMPL 508
	GO TO 20	SMPL 509
C		SMPL 510
C	CHECK THAT BOTTOM OF WATER CORRESPONDS TO A BLOCK	SMPL 511
C		SMPL 512
10	IF (YB.LT.HB) WRITE (*,99)	SMPL 513
C		SMPL 514
C	COMPUTE PRESSURE AND FORCES ACTING ON BLOCK I	SMPL 515
C		SMPL 516
20	CALL CENTRD (P1,P2,DX,DY,H1,V,RX,RY)	SMPL 517
C		SMPL 518
C	COMPUTE THE STRESS RESULTANTS AT THE BOTTOM OF BLOCK	SMPL 519
C		SMPL 520
	HSUM = HSUM + H1	SMPL 521
	HYSUM = HYSUM + H1*(YB+RY)	SMPL 522
	VSUM = VSUM + V	SMPL 523
	VXSUM = VXSUM + V*(BLOCKS(IUPDN,I)+RX)	SMPL 524
C		SMPL 525
C	COMPUTE THE BENDING MOMENTS AND STRESSES AT THE	SMPL 526
C	BOTTOM OF BLOCK I	SMPL 527
C		SMPL 528
30	M = HYSUM - VXSUM - BLOCKS(3,I)*HSUM	SMPL 529
1	+ 0.5*(BLOCKS(2,I)+BLOCKS(1,I))*VSUM	SMPL 530
C		SMPL 531
	T = BLOCKS(2,I) - BLOCKS(1,I)	SMPL 532
	M = 6.0*M/(T*T)	SMPL 533
	STRESS(1,I) = VSUM/T + M	SMPL 534
	STRESS(2,I) = VSUM/T - M	SMPL 535
C		SMPL 536
40	CONTINUE	SMPL 537
	RETURN	SMPL 538
C		SMPL 539
99	FORMAT (//' ERROR IN MODEL - RESERVOIR BOTTOM DOES NOT'/	SMPL 540
1	' COINCIDE WITH THE BOTTOM OF A BLOCK'/)	SMPL 541
C		SMPL 542
	END	SMPL 543
	SUBROUTINE VALWGT (I,LOADS,V,H)	SMPL 544
C		SMPL 545
C	OBTAIN THE WEIGHT OF BLOCK I	SMPL 546
C		SMPL 547
	DIMENSION LOADS(1)	SMPL 548
	REAL LOADS	SMPL 549
C		SMPL 550

	H = 0.0	SMPL 551
	V = - LOADS(I)	SMPL 552
C		SMPL 553
	RETURN	SMPL 554
	END	SMPL 555
	SUBROUTINE VALHOR (I,LOADS,V,H)	SMPL 556
C		SMPL 557
C	OBTAIN THE EFFECTIVE LATERAL FORCE ON BLOCK I	SMPL 558
C		SMPL 559
	DIMENSION LOADS(1)	SMPL 560
	REAL LOADS	SMPL 561
C		SMPL 562
	H = LOADS(I)	SMPL 563
	V = 0.0	SMPL 564
C		SMPL 565
	RETURN	SMPL 566
	END	SMPL 567
	SUBROUTINE VALHST (I,PRESS,P1,P2,YCOMP)	SMPL 568
C		SMPL 569
C	OBTAIN THE HYDROSTATIC PRESSURE ON BLOCK I	SMPL 570
C		SMPL 571
	DIMENSION PRESS(1)	SMPL 572
	LOGICAL YCOMP	SMPL 573
C		SMPL 574
	P1 = PRESS(I+1)	SMPL 575
	P2 = PRESS(I )	SMPL 576
	YCOMP = .TRUE.	SMPL 577
C		SMPL 578
	RETURN	SMPL 579
	END	SMPL 580
	SUBROUTINE VALHDY (I,PRESS,P1,P2,YCOMP)	SMPL 581
C		SMPL 582
C	OBTAIN THE HYDRODYNAMIC PRESSURE ON BLOCK I	SMPL 583
C		SMPL 584
	DIMENSION PRESS(1)	SMPL 585
	LOGICAL YCOMP	SMPL 586
C		SMPL 587
	P1 = PRESS(I+1)	SMPL 588
	P2 = PRESS(I )	SMPL 589
	YCOMP = .FALSE.	SMPL 590
C		SMPL 591
	RETURN	SMPL 592
	END	SMPL 593
	SUBROUTINE CENTRD (P1,P2,DX,DY,PX,PY,RX,RY)	SMPL 594
C		SMPL 595
C	COMPUTE THE RESULTANT PRESSURE FORCE ON A SURFACE,	SMPL 596
C	ALSO LOCATES THE VERTICAL CENTROID OF A BLOCK	SMPL 597
C		SMPL 598
	A = 0.5*(P1+P2)	SMPL 599
	PX = A*DY	SMPL 600
	PY = - A*DX	SMPL 601
C		SMPL 602
	RX = 0.0	SMPL 603
	RY = 0.0	SMPL 604
	IF (A.EQ.0.0) RETURN	SMPL 605

C		SMPL 606
	A = (2.0*P1+P2)/(6.0*A)	SMPL 607
	RX = A*DX	SMPL 608
	RY = A*DY	SMPL 609
C		SMPL 610
	RETURN	SMPL 611
	END	SMPL 612
	SUBROUTINE COMSTA (NBLOCK,STR1,STR2,STR3,STRFAC,TITLE)	SMPL 613
C		SMPL 614
C	ADD STRESSES STR2 TO STR1 AND PUT IN STR3	SMPL 615
C		SMPL 616
	DIMENSION STR1(2,1),STR2(2,1),STR3(2,1)	SMPL 617
	CHARACTER*40 TITLE	SMPL 618
C		SMPL 619
	WRITE (*,99) TITLE	SMPL 620
C		SMPL 621
	DO 10 J=1,NBLOCK	SMPL 622
	I = NBLOCK + 1 - J	SMPL 623
	STR3(1,I) = (STR1(1,I) + STR2(1,I))*STRFAC	SMPL 624
	STR3(2,I) = (STR1(2,I) + STR2(2,I))*STRFAC	SMPL 625
	WRITE (*,98) I,STR3(1,I),STR3(2,I)	SMPL 626
C		SMPL 627
	10 CONTINUE	SMPL 628
C		SMPL 629
	RETURN	SMPL 630
C		SMPL 631
	99 FORMAT (//2X,A40// ' BLOCK',5X, 'UPSTREAM FACE',2X, 'DOWNSTREAM FACE'	SMPL 632
	1        /1X,40('-')//	SMPL 633
	98 FORMAT (3X,I2,10X,F8.3,9X,F8.3)	SMPL 634
C		SMPL 635
	END	SMPL 636



## EARTHQUAKE ENGINEERING RESEARCH CENTER REPORTS

NOTE: Numbers in parentheses are Accession Numbers assigned by the National Technical Information Service; these are followed by a price code. Copies of the reports may be ordered from the National Technical Information Service, 5285 Port Royal Road, Springfield, Virginia, 22161. Accession Numbers should be quoted on orders for reports (PB --- ---) and remittance must accompany each order. Reports without this information were not available at time of printing. The complete list of EERC reports (from EERC 67-1) is available upon request from the Earthquake Engineering Research Center, University of California, Berkeley, 47th Street and Hoffman Boulevard, Richmond, California 94804.

- UCB/EERC-79/01 "Hysteretic Behavior of Lightweight Reinforced Concrete Beam-Column Subassemblages," by B. Forzani, E.P. Popov and V.V. Bertero - April 1979 (PB 298 267)A06
- UCB/EERC-79/02 "The Development of a Mathematical Model to Predict the Flexural Response of Reinforced Concrete Beams to Cyclic Loads, Using System Identification," by J. Stanton & H. McNiven - Jan. 1979 (PB 295 875)A10
- UCB/EERC-79/03 "Linear and Nonlinear Earthquake Response of Simple Torsionally Coupled Systems," by C.L. Kan and A.K. Chopra - Feb. 1979 (PB 298 262)A06
- UCB/EERC-79/04 "A Mathematical Model of Masonry for Predicting its Linear Seismic Response Characteristics," by Y. Mengi and H.D. McNiven - Feb. 1979 (PB 298 266)A06
- UCB/EERC-79/05 "Mechanical Behavior of Lightweight Concrete Confined by Different Types of Lateral Reinforcement," by M.A. Manrique, V.V. Bertero and E.P. Popov - May 1979 (PB 301 114)A06
- UCB/EERC-79/06 "Static Tilt Tests of a Tall Cylindrical Liquid Storage Tank," by R.W. Clough and A. Niwa - Feb. 1979 (PB 301 167)A06
- UCB/EERC-79/07 "The Design of Steel Energy Absorbing Restrainers and Their Incorporation into Nuclear Power Plants for Enhanced Safety: Volume 1 - Summary Report," by P.N. Spencer, V.F. Zackay, and E.R. Parker - Feb. 1979 (UCB/EERC-79/07)A09
- UCB/EERC-79/08 "The Design of Steel Energy Absorbing Restrainers and Their Incorporation into Nuclear Power Plants for Enhanced Safety: Volume 2 - The Development of Analyses for Reactor System Piping," "Simple Systems" by M.C. Lee, J. Penzien, A.K. Chopra and K. Suzuki "Complex Systems" by G.H. Powell, E.L. Wilson, R.W. Clough and D.G. Row - Feb. 1979 (UCB/EERC-79/08)A10
- UCB/EERC-79/09 "The Design of Steel Energy Absorbing Restrainers and Their Incorporation into Nuclear Power Plants for Enhanced Safety: Volume 3 - Evaluation of Commercial Steels," by W.S. Owen, R.M.N. Pelloux, R.O. Ritchie, M. Faral, T. Ohhashi, J. Toplosky, S.J. Hartman, V.F. Zackay and E.R. Parker - Feb. 1979 (UCB/EERC-79/09)A04
- UCB/EERC-79/10 "The Design of Steel Energy Absorbing Restrainers and Their Incorporation into Nuclear Power Plants for Enhanced Safety: Volume 4 - A Review of Energy-Absorbing Devices," by J.M. Kelly and M.S. Skinner - Feb. 1979 (UCB/EERC-79/10)A04
- UCB/EERC-79/11 "Conservatism In Summation Rules for Closely Spaced Modes," by J.M. Kelly and J.L. Sackman - May 1979 (PB 301 328)A03
- UCB/EERC-79/12 "Cyclic Loading Tests of Masonry Single Piers; Volume 3 - Height to Width Ratio of 0.5," by P.A. Hidalgo, R.L. Mayes, H.D. McNiven and R.W. Clough - May 1979 (PB 301 321)A08
- UCB/EERC-79/13 "Cyclic Behavior of Dense Course-Grained Materials in Relation to the Seismic Stability of Dams," by N.G. Banerjee, H.B. Seed and C.K. Chan - June 1979 (PB 301 373)A13
- UCB/EERC-79/14 "Seismic Behavior of Reinforced Concrete Interior Beam-Column Subassemblages," by S. Viwathanatepa, E.P. Popov and V.V. Bertero - June 1979 (PB 301 326)A10
- UCB/EERC-79/15 "Optimal Design of Localized Nonlinear Systems with Dual Performance Criteria Under Earthquake Excitations," by M.A. Bhatti - July 1979 (PB 80 167 109)A06
- UCB/EERC-79/16 "OPTDYN - A General Purpose Optimization Program for Problems with or without Dynamic Constraints," by M.A. Bhatti, E. Polak and K.S. Pister - July 1979 (PB 80 167 091)A05
- UCB/EERC-79/17 "ANSR-II, Analysis of Nonlinear Structural Response, Users Manual," by D.P. Mondkar and G.H. Powell July 1979 (PB 80 113 301)A05
- UCB/EERC-79/18 "Soil Structure Interaction in Different Seismic Environments," A. Gomez-Masso, J. Lysmer, J.-C. Chen and H.B. Seed - August 1979 (PB 80 101 520)A04
- UCB/EERC-79/19 "ARMA Models for Earthquake Ground Motions," by M.K. Chang, J.W. Kwiatkowski, R.F. Nau, R.M. Oliver and K.S. Pister - July 1979 (PB 301 166)A05
- UCB/EERC-79/20 "Hysteretic Behavior of Reinforced Concrete Structural Walls," by J.M. Vallenias, V.V. Bertero and E.P. Popov - August 1979 (PB 80 165 905)A12
- UCB/EERC-79/21 "Studies on High-Frequency Vibrations of Buildings - 1: The Column Effect," by J. Lubliner - August 1979 (PB 80 158 553)A03
- UCB/EERC-79/22 "Effects of Generalized Loadings on Bond Reinforcing Bars Embedded in Confined Concrete Blocks," by S. Viwathanatepa, E.P. Popov and V.V. Bertero - August 1979 (PB 81 124 018)A14
- UCB/EERC-79/23 "Shaking Table Study of Single-Story Masonry Houses, Volume 1: Test Structures 1 and 2," by P. Gülkan, R.L. Mayes and R.W. Clough - Sept. 1979 (HUD-000 1763)A12
- UCB/EERC-79/24 "Shaking Table Study of Single-Story Masonry Houses, Volume 2: Test Structures 3 and 4," by P. Gülkan, R.L. Mayes and R.W. Clough - Sept. 1979 (HUD-000 1836)A12
- UCB/EERC-79/25 "Shaking Table Study of Single-Story Masonry Houses, Volume 3: Summary, Conclusions and Recommendations," by R.W. Clough, R.L. Mayes and P. Gülkan - Sept. 1979 (HUD-000 1837)A06

- UCB/EERC-79/26 "Recommendations for a U.S.-Japan Cooperative Research Program Utilizing Large-Scale Testing Facilities," by U.S.-Japan Planning Group - Sept. 1979(PB 301 407)A06
- UCB/EERC-79/27 "Earthquake-Induced Liquefaction Near Lake Amatitlan, Guatemala," by H.B. Seed, I. Arango, C.K. Chan, A. Gomez-Masso and R. Grant de Ascoli - Sept. 1979(NUREG-CR1341)A03
- UCB/EERC-79/28 "Infill Panels: Their Influence on Seismic Response of Buildings," by J.W. Axley and V.V. Bertero Sept. 1979(PB 80 163 371)A10
- UCB/EERC-79/29 "3D Truss Bar Element (Type 1) for the ANSR-II Program," by D.P. Mondkar and G.H. Powell - Nov. 1979 (PB 80 169 709)A02
- UCB/EERC-79/30 "2D Beam-Column Element (Type 5 - Parallel Element Theory) for the ANSR-II Program," by D.G. Row, G.H. Powell and D.P. Mondkar - Dec. 1979(PB 80 167 224)A03
- UCB/EERC-79/31 "3D Beam-Column Element (Type 2 - Parallel Element Theory) for the ANSR-II Program," by A. Riahi, G.H. Powell and D.P. Mondkar - Dec. 1979(PB 80 167 216)A03
- UCB/EERC-79/32 "On Response of Structures to Stationary Excitation," by A. Der Kiureghian - Dec. 1979(PB 80166 929)A03
- UCB/EERC-79/33 "Undisturbed Sampling and Cyclic Load Testing of Sands," by S. Singh, H.B. Seed and C.K. Chan Dec. 1979(ADA 087 298)A07
- UCB/EERC-79/34 "Interaction Effects of Simultaneous Torsional and Compressional Cyclic Loading of Sand," by P.M. Griffin and W.N. Houston - Dec. 1979(ADA 092 352)A15
- UCB/EERC-80/01 "Earthquake Response of Concrete Gravity Dams Including Hydrodynamic and Foundation Interaction Effects," by A.K. Chopra, P. Chakrabarti and S. Gupta - Jan. 1980(AD-A087297)A10
- UCB/EERC-80/02 "Rocking Response of Rigid Blocks to Earthquakes," by C.S. Yim, A.K. Chopra and J. Penzien - Jan. 1980 (PB80 166 002)A04
- UCB/EERC-80/03 "Optimum Inelastic Design of Seismic-Resistant Reinforced Concrete Frame Structures," by S.W. Zagajeski and V.V. Bertero - Jan. 1980(PB80 164 635)A06
- UCB/EERC-80/04 "Effects of Amount and Arrangement of Wall-Panel Reinforcement on Hysteretic Behavior of Reinforced Concrete Walls," by R. Iliya and V.V. Bertero - Feb. 1980(PB81 122 525)A09
- UCB/EERC-80/05 "Shaking Table Research on Concrete Dam Models," by A. Niwa and R.W. Clough - Sept. 1980(PB81 122 368)A06
- UCB/EERC-80/06 "The Design of Steel Energy-Absorbing Restrainers and their Incorporation into Nuclear Power Plants for Enhanced Safety (Vol 1A): Piping with Energy Absorbing Restrainers: Parameter Study on Small Systems," by G.H. Powell, C. Oughourlian and J. Simons - June 1980
- UCB/EERC-80/07 "Inelastic Torsional Response of Structures Subjected to Earthquake Ground Motions," by Y. Yamazaki April 1980(PB81 122 327)A08
- UCB/EERC-80/08 "Study of X-Braced Steel Frame Structures Under Earthquake Simulation," by Y. Ghanaat - April 1980 (PB81 122 335)A11
- UCB/EERC-80/09 "Hybrid Modelling of Soil-Structure Interaction," by S. Gupta, T.W. Lin, J. Penzien and C.S. Yeh May 1980(PB81 122 319)A07
- UCB/EERC-80/10 "General Applicability of a Nonlinear Model of a One Story Steel Frame," by B.I. Sveinsson and H.D. McNiven - May 1980(PB81 124 877)A06
- UCB/EERC-80/11 "A Green-Function Method for Wave Interaction with a Submerged Body," by W. Kioka - April 1980 (PB81 122 269)A07
- UCB/EERC-80/12 "Hydrodynamic Pressure and Added Mass for Axisymmetric Bodies," by F. Nilrat - May 1980(PB81 122 343)A08
- UCB/EERC-80/13 "Treatment of Non-Linear Drag Forces Acting on Offshore Platforms," by B.V. Dao and J. Penzien May 1980(PB81 153 413)A07
- UCB/EERC-80/14 "2D Plane/Axisymmetric Solid Element (Type 3 - Elastic or Elastic-Perfectly Plastic) for the ANSR-II Program," by D.P. Mondkar and G.H. Powell - July 1980(PB81 122 350)A03
- UCB/EERC-80/15 "A Response Spectrum Method for Random Vibrations," by A. Der Kiureghian - June 1980(PB81 122 301)A03
- UCB/EERC-80/16 "Cyclic Inelastic Buckling of Tubular Steel Braces," by V.A. Zayas, E.P. Popov and S.A. Mahin June 1980(PB81 124 885)A10
- UCB/EERC-80/17 "Dynamic Response of Simple Arch Dams Including Hydrodynamic Interaction," by C.S. Porter and A.K. Chopra - July 1980(PB81 124 000)A13
- UCB/EERC-80/18 "Experimental Testing of a Friction Damped Aseismic Base Isolation System with Fail-Safe Characteristics," by J.M. Kelly, K.E. Beucke and M.S. Skinner - July 1980(PB81 148 595)A04
- UCB/EERC-80/19 "The Design of Steel Energy-Absorbing Restrainers and their Incorporation into Nuclear Power Plants for Enhanced Safety (Vol 1B): Stochastic Seismic Analyses of Nuclear Power Plant Structures and Piping Systems Subjected to Multiple Support Excitations," by M.C. Lee and J. Penzien - June 1980
- UCB/EERC-80/20 "The Design of Steel Energy-Absorbing Restrainers and their Incorporation into Nuclear Power Plants for Enhanced Safety (Vol 1C): Numerical Method for Dynamic Substructure Analysis," by J.M. Dickens and E.L. Wilson - June 1980
- UCB/EERC-80/21 "The Design of Steel Energy-Absorbing Restrainers and their Incorporation into Nuclear Power Plants for Enhanced Safety (Vol 2): Development and Testing of Restraints for Nuclear Piping Systems," by J.M. Kelly and M.S. Skinner - June 1980
- UCB/EERC-80/22 "3D Solid Element (Type 4-Elastic or Elastic-Perfectly-Plastic) for the ANSR-II Program," by D.P. Mondkar and G.H. Powell - July 1980(PB81 123 242)A03
- UCB/EERC-80/23 "Gap-Friction Element (Type 5) for the ANSR-II Program," by D.P. Mondkar and G.H. Powell - July 1980 (PB81 122 285)A03

- UCB/EERC-80/24 "U-Bar Restraint Element (Type 11) for the ANSR-II Program," by C. Oughourlian and G.H. Powell July 1980(PB81 122 293)A03
- UCB/EERC-80/25 "Testing of a Natural Rubber Base Isolation System by an Explosively Simulated Earthquake," by J.M. Kelly - August 1980(PB81 201 360)A04
- UCB/EERC-80/26 "Input Identification from Structural Vibrational Response," by Y. Hu - August 1980(PB81 152 308)A05
- UCB/EERC-80/27 "Cyclic Inelastic Behavior of Steel Offshore Structures," by V.A. Zayas, S.A. Mahin and E.P. Popov August 1980(PB81 196 180)A15
- UCB/EERC-80/28 "Shaking Table Testing of a Reinforced Concrete Frame with Biaxial Response," by M.G. Oliva October 1980(PB81 154 304)A10
- UCB/EERC-80/29 "Dynamic Properties of a Twelve-Story Prefabricated Panel Building," by J.G. Bouwkamp, J.P. Kollegger and R.M. Stephen - October 1980(PB82 117 128)A06
- UCB/EERC-80/30 "Dynamic Properties of an Eight-Story Prefabricated Panel Building," by J.G. Bouwkamp, J.P. Kollegger and R.M. Stephen - October 1980(PB81 200 313)A05
- UCB/EERC-80/31 "Predictive Dynamic Response of Panel Type Structures Under Earthquakes," by J.P. Kollegger and J.G. Bouwkamp - October 1980(PB81 152 316)A04
- UCB/EERC-80/32 "The Design of Steel Energy-Absorbing Restrainers and their Incorporation into Nuclear Power Plants for Enhanced Safety (Vol 3): Testing of Commercial Steels in Low-Cycle Torsional Fatigue," by P. Spencer, E.R. Parker, E. Jongewaard and M. Drory
- UCB/EERC-80/33 "The Design of Steel Energy-Absorbing Restrainers and their Incorporation into Nuclear Power Plants for Enhanced Safety (Vol 4): Shaking Table Tests of Piping Systems with Energy-Absorbing Restrainers," by S.F. Stiemer and W.G. Godden - Sept. 1980
- UCB/EERC-80/34 "The Design of Steel Energy-Absorbing Restrainers and their Incorporation into Nuclear Power Plants for Enhanced Safety (Vol 5): Summary Report," by P. Spencer
- UCB/EERC-80/35 "Experimental Testing of an Energy-Absorbing Base Isolation System," by J.M. Kelly, M.S. Skinner and K.E. Beucke - October 1980(PB81 154 072)A04
- UCB/EERC-80/36 "Simulating and Analyzing Artificial Non-Stationary Earthquake Ground Motions," by R.F. Nau, R.M. Oliver and K.S. Pister - October 1980(PB81 153 397)A04
- UCB/EERC-80/37 "Earthquake Engineering at Berkeley - 1980," - Sept. 1980(PB81 205 874)A09
- UCB/EERC-80/38 "Inelastic Seismic Analysis of Large Panel Buildings," by V. Schricker and G.H. Powell - Sept. 1980 (PB81 154 338)A13
- UCB/EERC-80/39 "Dynamic Response of Embankment, Concrete-Gravity and Arch Dams Including Hydrodynamic Interaction," by J.F. Hall and A.K. Chopra - October 1980(PB81 152 324)A11
- UCB/EERC-80/40 "Inelastic Buckling of Steel Struts Under Cyclic Load Reversal," by R.G. Black, W.A. Wenger and E.P. Popov - October 1980(PB81 154 312)A08
- UCB/EERC-80/41 "Influence of Site Characteristics on Building Damage During the October 3, 1974 Lima Earthquake," by P. Repetto, I. Arango and H.B. Seed - Sept. 1980(PB81 161 739)A05
- UCB/EERC-80/42 "Evaluation of a Shaking Table Test Program on Response Behavior of a Two Story Reinforced Concrete Frame," by J.M. Blondet, R.W. Clough and S.A. Mahin
- UCB/EERC-80/43 "Modelling of Soil-Structure Interaction by Finite and Infinite Elements," by F. Medina - December 1980(PB81 229 270)A04
- UCB/EERC-81/01 "Control of Seismic Response of Piping Systems and Other Structures by Base Isolation," edited by J.M. Kelly - January 1981 (PB81 200 735)A05
- UCB/EERC-81/02 "OPTNSR - An Interactive Software System for Optimal Design of Statically and Dynamically Loaded Structures with Nonlinear Response," by M.A. Bhatti, V. Ciampi and K.S. Pister - January 1981 (PB81 218 851)A09
- UCB/EERC-81/03 "Analysis of Local Variations in Free Field Seismic Ground Motions," by J.-C. Chen, J. Lysmer and H.B. Seed - January 1981 (AD-A099508)A13
- UCB/EERC-81/04 "Inelastic Structural Modeling of Braced Offshore Platforms for Seismic Loading," by V.A. Zayas, P.-S.B. Shing, S.A. Mahin and E.P. Popov - January 1981(PB82 138 777)A07
- UCB/EERC-81/05 "Dynamic Response of Light Equipment in Structures," by A. Der Kiureghian, J.L. Sackman and B. Nour-Omid - April 1981 (PB81 218 497)A04
- UCB/EERC-81/06 "Preliminary Experimental Investigation of a Broad Base Liquid Storage Tank," by J.G. Bouwkamp, J.P. Kollegger and R.M. Stephen - May 1981(PB82 140 385)A03
- UCB/EERC-81/07 "The Seismic Resistant Design of Reinforced Concrete Coupled Structural Walls," by A.E. Aktan and V.V. Bertero - June 1981(PB82 113 358)A11
- UCB/EERC-81/08 "The Undrained Shearing Resistance of Cohesive Soils at Large Deformations," by M.R. Pyles and H.B. Seed - August 1981
- UCB/EERC-81/09 "Experimental Behavior of a Spatial Piping System with Steel Energy Absorbers Subjected to a Simulated Differential Seismic Input," by S.F. Stiemer, W.G. Godden and J.M. Kelly - July 1981

- UCB/EERC-81/10 "Evaluation of Seismic Design Provisions for Masonry in the United States," by B.I. Sveinsson, R.L. Mayes and H.D. McNiven - August 1981 (PB82 166 075)A08
- UCB/EERC-81/11 "Two-Dimensional Hybrid Modelling of Soil-Structure Interaction," by T.-J. Tzong, S. Gupta and J. Penzien - August 1981 (PB82 142 118)A04
- UCB/EERC-81/12 "Studies on Effects of Infills in Seismic Resistant R/C Construction," by S. Brokken and V.V. Bertero - September 1981 (PB82 166 190)A09
- UCB/EERC-81/13 "Linear Models to Predict the Nonlinear Seismic Behavior of a One-Story Steel Frame," by H. Valdimarsson, A.H. Shah and H.D. McNiven - September 1981 (PB82 138 793)A07
- UCB/EERC-81/14 "TLUSH: A Computer Program for the Three-Dimensional Dynamic Analysis of Earth Dams," by T. Kagawa, L.H. Mejia, H.B. Seed and J. Lysmer - September 1981 (PB82 139 940)A06
- UCB/EERC-81/15 "Three Dimensional Dynamic Response Analysis of Earth Dams," by L.H. Mejia and H.B. Seed - September 1981 (PB82 137 274)A12
- UCB/EERC-81/16 "Experimental Study of Lead and Elastomeric Dampers for Base Isolation Systems," by J.M. Kelly and S.B. Hodder - October 1981 (PB82 166 182)A05
- UCB/EERC-81/17 "The Influence of Base Isolation on the Seismic Response of Light Secondary Equipment," by J.M. Kelly - April 1981 (PB82 255 266)A04
- UCB/EERC-81/18 "Studies on Evaluation of Shaking Table Response Analysis Procedures," by J. Marcial Blondet - November 1981 (PB82 197 278)A10
- UCB/EERC-81/19 "DELIGHT.STRUCT: A Computer-Aided Design Environment for Structural Engineering," by R.J. Balling, K.S. Pister and E. Polak - December 1981 (PB82 218 496)A07
- UCB/EERC-81/20 "Optimal Design of Seismic-Resistant Planar Steel Frames," by R.J. Balling, V. Ciampi, K.S. Pister and E. Polak - December 1981 (PB82 220 179)A07
- UCB/EERC-82/01 "Dynamic Behavior of Ground for Seismic Analysis of Lifeline Systems," by T. Sato and A. Der Kiureghian - January 1982 (PB82 218 926)A05
- UCB/EERC-82/02 "Shaking Table Tests of a Tubular Steel Frame Model," by Y. Ghanaat and R. W. Clough - January 1982 (PB82 220 161)A07
- UCB/EERC-82/03 "Behavior of a Piping System under Seismic Excitation: Experimental Investigations of a Spatial Piping System supported by Mechanical Shock Arrestors and Steel Energy Absorbing Devices under Seismic Excitation," by S. Schneider, H.-M. Lee and W. G. Godden - May 1982 (PB83 172 544)A09
- UCB/EERC-82/04 "New Approaches for the Dynamic Analysis of Large Structural Systems," by E. L. Wilson - June 1982 (PB83 148 080)A05
- UCB/EERC-82/05 "Model Study of Effects of Damage on the Vibration Properties of Steel Offshore Platforms," by F. Shahrivar and J. G. Bouwkamp - June 1982 (PB83 148 742)A10
- UCB/EERC-82/06 "States of the Art and Practice in the Optimum Seismic Design and Analytical Response Prediction of R/C Frame-Wall Structures," by A. E. Aktan and V. V. Bertero - July 1982 (PB83 147 736)A05
- UCB/EERC-82/07 "Further Study of the Earthquake Response of a Broad Cylindrical Liquid-Storage Tank Model," by G. C. Manos and R. W. Clough - July 1982 (PB83 147 744)A11
- UCB/EERC-82/08 "An Evaluation of the Design and Analytical Seismic Response of a Seven Story Reinforced Concrete Frame - Wall Structure," by F. A. Charney and V. V. Bertero - July 1982 (PB83 157 628)A09
- UCB/EERC-82/09 "Fluid-Structure Interactions: Added Mass Computations for Incompressible Fluid," by J. S.-H. Kuo - August 1982 (PB83 156 281)A07
- UCB/EERC-82/10 "Joint-Opening Nonlinear Mechanism: Interface Smeared Crack Model," by J. S.-H. Kuo - August 1982 (PB83 149 195)A05
- UCB/EERC-82/11 "Dynamic Response Analysis of Teché Dam," by R. W. Clough, R. M. Stephen and J. S.-H. Kuo - August 1982 (PB83 147 496)A06
- UCB/EERC-82/12 "Prediction of the Seismic Responses of R/C Frame-Coupled Wall Structures," by A. E. Aktan, V. V. Bertero and M. Piazza - August 1982 (PB83 149 203)A09
- UCB/EERC-82/13 "Preliminary Report on the SMART 1 Strong Motion Array in Taiwan," by B. A. Bolt, C. H. Loh, J. Penzien, Y. B. Tsai and Y. T. Yeh - August 1982 (PB83 159 400)A10
- UCB/EERC-82/14 "Shaking-Table Studies of an Eccentrically X-Braced Steel Structure," by M. S. Yang - September 1982 (PB83 260 778)A12
- UCB/EERC-82/15 "The Performance of Stairways in Earthquakes," by C. Roha, J. W. Axley and V. V. Bertero - September 1982 (PB83 157 693)A07
- UCB/EERC-82/16 "The Behavior of Submerged Multiple Bodies in Earthquakes," by W.-G. Liao - Sept. 1982 (PB83 158 709)A27
- UCB/EERC-82/17 "Effects of Concrete Types and Loading Conditions on Local Bond-Slip Relationships," by A. D. Cowell, E. P. Popov and V. V. Bertero - September 1982 (PB83 153 577)A04

- UCB/EERC-82/18 "Mechanical Behavior of Shear Wall Vertical Boundary Members: An Experimental Investigation," by M. T. Wagner and V. V. Bertero - October 1982 (PB83 159 764)A05
- UCB/EERC-82/19 "Experimental Studies of Multi-support Seismic Loading on Piping Systems," by J. M. Kelly and A. D. Cowell - November 1982
- UCB/EERC-82/20 "Generalized Plastic Hinge Concepts for 3D Beam-Column Elements," by P. F.-S. Chen and G. H. Powell - November 1982 (PB83 247 981)A13
- UCB/EERC-82/21 "ANSR-III: General Purpose Computer Program for Nonlinear Structural Analysis," by C. V. Oughourlian and G. H. Powell - November 1982 (PB83 251 330)A12
- UCB/EERC-82/22 "Solution Strategies for Statically Loaded Nonlinear Structures," by J. W. Simons and G. H. Powell - November 1982 (PB83 197 970)A06
- UCB/EERC-82/23 "Analytical Model of Deformed Bar Anchorages under Generalized Excitations," by V. Ciampi, R. Eligehausen, V. V. Bertero and E. P. Popov - November 1982 (PB83 169 532)A06
- UCB/EERC-82/24 "A Mathematical Model for the Response of Masonry Walls to Dynamic Excitations," by H. Sucuođlu, Y. Mengi and H. D. McNiven - November 1982 (PB83 169 011)A07
- UCB/EERC-82/25 "Earthquake Response Considerations of Broad Liquid Storage Tanks," by F. J. Cambra - November 1982 (PB83 251 215)A09
- UCB/EERC-82/26 "Computational Models for Cyclic Plasticity, Rate Dependence and Creep," by B. Mosaddad and G. H. Powell - November 1982 (PB83 245 829)A08
- UCB/EERC-82/27 "Inelastic Analysis of Piping and Tubular Structures," by M. Mahasuverachai and G. H. Powell - November 1982 (PB83 249 987)A07
- UCB/EERC-83/01 "The Economic Feasibility of Seismic Rehabilitation of Buildings by Base Isolation," by J. M. Kelly - January 1983 (PB83 197 988)A05
- UCB/EERC-83/02 "Seismic Moment Connections for Moment-Resisting Steel Frames," by E. P. Popov - January 1983 (PB83 195 412)A04
- UCB/EERC-83/03 "Design of Links and Beam-to-Column Connections for Eccentrically Braced Steel Frames," by E. P. Popov and J. O. Malley - January 1983 (PB83 194 811)A04
- UCB/EERC-83/04 "Numerical Techniques for the Evaluation of Soil-Structure Interaction Effects in the Time Domain," by E. Bayo and E. L. Wilson - February 1983 (PB83 245 605)A09
- UCB/EERC-83/05 "A Transducer for Measuring the Internal Forces in the Columns of a Frame-Wall Reinforced Concrete Structure," by R. Sause and V. V. Bertero - May 1983 (PB84 119 494)A06
- UCB/EERC-83/06 "Dynamic Interactions between Floating Ice and Offshore Structures," by P. Croteau - May 1983 (PB84 119 486)A16
- UCB/EERC-83/07 "Dynamic Analysis of Multiply Tuned and Arbitrarily Supported Secondary Systems," by T. Igusa and A. Der Kiureghian - June 1983 (PB84 118 272)A11
- UCB/EERC-83/08 "A Laboratory Study of Submerged Multi-body Systems in Earthquakes," by G. R. Ansari - June 1983 (PB83 261 842)A17
- UCB/EERC-83/09 "Effects of Transient Foundation Uplift on Earthquake Response of Structures," by C.-S. Yim and A. K. Chopra - June 1983 (PB83 261 396)A07
- UCB/EERC-83/10 "Optimal Design of Friction-Braced Frames under Seismic Loading," by M. A. Austin and K. S. Pister - June 1983 (PB84 119 288)A06
- UCB/EERC-83/11 "Shaking Table Study of Single-Story Masonry Houses: Dynamic Performance under Three Component Seismic Input and Recommendations," by G. C. Manos, R. W. Clough and R. L. Mayes - June 1983
- UCB/EERC-83/12 "Experimental Error Propagation in Pseudodynamic Testing," by P. B. Shing and S. A. Mahin - June 1983 (PB84 119 270)A09
- UCB/EERC-83/13 "Experimental and Analytical Predictions of the Mechanical Characteristics of a 1/5-scale Model of a 7-story R/C Frame-Wall Building Structure," by A. E. Aktan, V. V. Bertero, A. A. Chowdhury and T. Nagashima - August 1983 (PB84 119 213)A07
- UCB/EERC-83/14 "Shaking Table Tests of Large-Panel Precast Concrete Building System Assemblages," by M. G. Oliva and R. W. Clough - August 1983
- UCB/EERC-83/15 "Seismic Behavior of Active Beam Links in Eccentrically Braced Frames," by K. D. Hjelmstad and E. P. Popov - July 1983 (PB84 119 676)A09
- UCB/EERC-83/16 "System Identification of Structures with Joint Rotation," by J. S. Dimsdale and H. D. McNiven - July 1983
- UCB/EERC-83/17 "Construction of Inelastic Response Spectra for Single-Degree-of-Freedom Systems," by S. Mahin and J. Lin - July 1983

- UCB/EERC-83/18 "Interactive Computer Analysis Methods for Predicting the Inelastic Cyclic Behaviour of Structural Sections," by S. Kaba and S. Mahin - July 1983 (PB84 192 012)A06
- UCB/EERC-83/19 "Effects of Bond Deterioration on Hysteretic Behavior of Reinforced Concrete Joints," by F.C. Filippou, E.P. Popov and V.V. Bertero - Aug. 1983 (PB84 192 020)A10
- UCB/EERC-83/20 "Analytical and Experimental Correlation of Large-Panel Precast Building System Performance," by M.G. Oliva, R.W. Clough, M. Velkov, P. Gavrilovic and J. Petrovski - Nov. 1983
- UCB/EERC-83/21 "Mechanical Characteristics of Materials Used in a 1/5 Scale Model of a 7-Story Reinforced Concrete Test Structure," by V.V. Bertero, A.E. Aktan, H.G. Harris and A.A. Chowdhury - Sept. 1983 (PB84 193 697)A05
- UCB/EERC-83/22 "Hybrid Modelling of Soil-Structure Interaction in Layered Media," by T.-J. Tzong and J. Penzien - Oct. 1983 (PB84 192 178)A08
- UCB/EERC-83/23 "Local Bond Stress-Slip Relationships of Deformed Bars under Generalized Excitations," by R. Eligehausen, E.P. Popov and V.V. Bertero - Oct. 1983 (PB84 192 848)A09
- UCB/EERC-83/24 "Design Considerations for Shear Links in Eccentrically Braced Frames," by J.O. Malley and E.P. Popov - Nov. 1983 (PB84 192 186)A07
- UCB/EERC-84/01 "Pseudodynamic Test Method for Seismic Performance Evaluation: Theory and Implementation," by P.-S. B. Shing and S.A. Mahin - Jan. 1984 (PB84 190 644)A08
- UCB/EERC-84/02 "Dynamic Response Behavior of Xiang Hong Dian Dam," by R.W. Clough, K.-T. Chang, H.-Q. Chen, R.M. Stephen, G.-L. Wang and Y. Ghanaat - April 1984 (PB84 209 402)A08
- UCB/EERC-84/03 "Refined Modelling of Reinforced Concrete Columns for Seismic Analysis," by S.A. Kaba and S.A. Mahin - April 1984 (PB84 234 384)A06
- UCB/EERC-84/04 "A New Floor Response Spectrum Method for Seismic Analysis of Multiply Supported Secondary Systems," by A. Asfura and A. Der Kiureghian - June 1984 (PB84 239 417)A06
- UCB/EERC-84/05 "Earthquake Simulation Tests and Associated Studies of a 1/5th-scale Model of a 7-Story R/C Frame-Wall Test Structure," by V.V. Bertero, A.E. Aktan, F.A. Charney and R. Sause - June 1984 (PB84 239 409)A09
- UCB/EERC-84/06 "R/C Structural Walls: Seismic Design for Shear," by A.E. Aktan and V.V. Bertero
- UCB/EERC-84/07 "Behavior of Interior and Exterior Flat-Plate Connections subjected to Inelastic Load Reversals," by H.L. Zee and J.P. Moehle - August 1984 (PB86 117 629/AS) A07
- UCB/EERC-84/08 "Experimental Study of the Seismic Response of a Two-story Flat-Plate Structure," by J. P. Moehle and J.W. Diebold - August 1984 (PB86 122 553/AS) A12
- UCB/EERC-84/09 "Phenomenological Modeling of Steel Braces under Cyclic Loading," by K. Ikeda, S.A. Mahin and S.N. Dermizakis - May 1984 (PB86 132 198/AS) A08
- UCB/EERC-84/10 "Earthquake Analysis and Response of Concrete Gravity Dams," by G. Fenves and A.K. Chopra - Aug. 1984 (PB85 193 902/AS)A11
- UCB/EERC-84/11 "EAGD-84: A Computer Program for Earthquake Analysis of Concrete Gravity Dams," by G. Fenves and A.K. Chopra - Aug. 1984 (PB85 193 613/AS)A05
- UCB/EERC-84/12 "A Refined Physical Theory Model for Predicting the Seismic Behavior of Braced Steel Frames," by K. Ikeda and S.A. Mahin - July 1984 (PB85 191 450/AS)A09
- UCB/EERC-84/13 "Earthquake Engineering Research at Berkeley - 1984" - Aug. 1984 (PB85 197 341/AS)A10
- UCB/EERC-84/14 "Moduli and Damping Factors for Dynamic Analyses of Cohesionless Soils," by H.B. Seed, R.T. Wong, I.M. Idriss and K. Tokimatsu - Sept. 1984 (PB85 191 468/AS)A04
- UCB/EERC-84/15 "The Influence of SPT Procedures in Soil Liquefaction Resistance Evaluations," by H.B. Seed, K. Tokimatsu, L.F. Harder and R.M. Chung - Oct. 1984 (PB85 191 732/AS)A04
- UCB/EERC-84/16 "Simplified Procedures for the Evaluation of Settlements in Sands Due to Earthquake Shaking," by K. Tokimatsu and H.B. Seed - Oct. 1984 (PB85 197 887/AS)A03
- UCB/EERC-84/17 "Evaluation of Energy Absorption Characteristics of Bridge under Seismic Conditions," by R.A. Imbsen and J. Penzien - Nov. 1984
- UCB/EERC-84/18 "Structure-Foundation Interactions under Dynamic Loads," by W.D. Liu and J. Penzien - Nov. 1984
- UCB/EERC-84/19 "Seismic Modelling of Deep Foundations," by C.-H. Chen and J. Penzien - Nov. 1984
- UCB/EERC-84/20 "Dynamic Response Behavior of Quan Shui Dam," by R.W. Clough, K.-T. Chang, H.-Q. Chen, R.M. Stephen, Y. Ghanaat and J.-H. Qi - Nov. 1984 (PB86 115177/AS) A07

- UCB/EERC-85/01 "Simplified Methods of Analysis for Earthquake Resistant Design of Buildings," by E.F. Cruz and A.K. Chopra - Feb. 1985 (PB86 112299/AS) A12
- UCB/EERC-85/02 "Estimation of Seismic Wave Coherency and Rupture Velocity using the SMART 1 Strong-Motion Array Recordings," by N.A. Abrahamson - March 1985
- UCB/EERC-85/03 "Dynamic Properties of a Thirty Story Condominium Tower Building," by R.M. Stephen, E.L. Wilson and N. Stander - April 1985 (PB86 118965/AS) A06
- UCB/EERC-85/04 "Development of Substructuring Techniques for On-Line Computer Controlled Seismic Performance Testing," by S. Dermitzakis and S. Mahin - February 1985 (PB86 132941/AS) A08
- UCB/EERC-85/05 "A Simple Model for Reinforcing Bar Anchorages under Cyclic Excitations," by F.C. Filippou - March 1985 (PB86 112919/AS) A05
- UCB/EERC-85/06 "Racking Behavior of Wood-Framed Gypsum Panels under Dynamic Load," by M.G. Oliva - June 1985
- UCB/EERC-85/07 "Earthquake Analysis and Response of Concrete Arch Dams," by K.-L. Fok and A.K. Chopra - June 1985 (PB86 139672/AS) A10
- UCB/EERC-85/08 "Effect of Inelastic Behavior on the Analysis and Design of Earthquake Resistant Structures," by J.P. Lin and S.A. Mahin - June 1985 (PB86 135340/AS) A08
- UCB/EERC-85/09 "Earthquake Simulator Testing of a Base-Isolated Bridge Deck," by J.M. Kelly, I.G. Buckle and H.-C. Tsai - January 1986
- UCB/EERC-85/10 "Simplified Analysis for Earthquake Resistant Design of Concrete Gravity Dams," by G. Fenves and A.K. Chopra - September 1985

